**Coventry University**

**DOCTOR OF PHILOSOPHY**

**From two Algebraic Bethe Ansätze to the dynamics of Dicke-Jaynes-Cummings-Gaudin quantum integrable models through eigenvalue-based determinants**

Tschirhart, Hugo

*Award date:*
2017

*Awarding institution:*
Coventry University
Université de Lorraine

[Link to publication](Link to publication)

# From two Algebraic Bethe Ansätze to the dynamics of Dicke-Jaynes-Cummings-Gaudin quantum integrable models through eigenvalue-based determinants

By

**Hugo Tschirhart**

**May 2017**

**Coventry University**

**UNIVERSITÉ DE LORRAINE**

# Certificate of Ethical Approval

Applicant:

Hugo Tschirhart

Project Title:

From two Algebraic Bethe Ansätze to the dynamics of Dicke-Jaynes-Cummings-Gaudin quantum integrable models through eigenvalue-based determinants

This is to certify that the above named applicant has completed the Coventry University Ethical Approval process and their project has been confirmed and approved as Low Risk

Date of approval:

25 May 2017

Project Reference Number:

P57968

**Please add a copy of this section within the first few pages of your thesis, after your title page. Refer to 'Thesis Information Guidance' for more information.**

## Section 3 Submission Declaration

|  | Yes | No |
|---|---|---|
| Have materials contained in your thesis/submission been used for any other submission for an academic award? | ☐ | ☒ |
| If you have answered Yes to above please state award and awarding body and list the material: | | |
| I am aware of no health reasons that will prevent me from undertaking and completing assessment and will undertake to notifying my Director of Studies and PGRSU - Registry as soon as any change in these circumstances occurs. | ☒ | ☐ |
| **Ethical Declaration:**<br>I declare that my research has full University Ethical approval and evidence of this has been included within my thesis/submission.  Please also insert ethics reference number below<br><br>Project Reference: **P57968** | ☒ | ☐ |

# From two Algebraic Bethe Ansätze to the dynamics of Dicke-Jaynes-Cummings-Gaudin quantum integrable models through eigenvalue-based determinants

**Hugo Tschirhart**

UNIVERSITÉ DE LORRAINE

Coventry University

Qui dit quoi ? Que dans un monde où tout le monde croit devoir s'exprimer, il n'y a plus d'illumination possible. Rien ne peut être éclairé dans la luminance totale. Il faut beaucoup de silence pour entendre une note. Il faut beaucoup de nuit pour qu'un éclair puisse jaillir, pour qu'une couleur neuve soit perçue, soit reçue.

Si j'en avais le pouvoir, j'émettrais aujourd'hui un trou noir. Quelque chose comme un cône d'extinction forant au ventre l'épaisseur du jour. Pour rouvrir l'espace. Ce qui me terrifie, ce n'est pas ce chaos de clartés qui brouille la ville comme une avalanche de soleils. C'est qu'il n'y ait plus nulle part une seule ombre. Tout est férocement surexposé.

Mais rien n'est posé. Ni tranché.

— Alain Damasio, *So phare away*

*To those who inspired it*
*and will not read it*

# Acknowledgements/Remerciements

For the acknowledgements, I have decided to write in English the parts relative to people not speaking French and in French for the ones who do because this section is not only dedicated to scientists or people able to read English. I also want to precise that there is no special order in the acknowledgements.

Pour la partie remerciements, j'ai décidé de rédiger en anglais les parties concernant des personnes ne parlant pas français et en français pour les autres car cette section ne concerne pas uniquement des scientifiques ou des personnes sachant lire l'anglais. Je précise qu'il n'y a pas d'ordre spécial dans les remerciements.

I want to begin by thanking all the people I will forget to mention here, together they may deserve a non-negligible part of my acknowledgements./ J'aimerais commencer par remercier toutes les personnes que je vais oublier de mentionner, prises ensemble il se peut qu'elles méritent une part non négligeable de mes remerciements.

Je remercie ma famille, mes parents et ma soeur dont les aléas de la thèse ont fait que nous avons passé plus de temps ensemble que ce que je n'aurais pu le penser au début. Ces moments ont été importants pour moi dans le déroulement de ces trois années. J'ai aussi une pensée spéciale pour ma grand-mère. Et enfin, mes tantes, mes cousines, mes oncles et mes cousins dont je me dis à peu près tous les mois qu'il faudrait que je prenne le temps de leur rendre visite plus souvent.

Je remercie Alexandre et Thierry pour tous les moments qu'ils ont pu m'accorder durant ces trois années. Alexandre pour m'avoir fait confiance depuis le master, son enthousiasme à trouver de nouvelles nouvelles idées et à pousser plus loin celles que l'on avait déjà a vraiment été très encourageant. Thierry pour s'être assuré que tout se passe pour le mieux pour mes séjours à Coventry, son humour et m'avoir permis d'enseigner avec lui.

Je remercie tous les membres du Groupe de Physique Statistique dont Dragi pour les conseils réguliers qu'il a pu me donner, Jérôme pour être le premier à m'avoir dit qu'il était temps de penser à l'après-thèse et m'avoir transmis des offres de post-doctorat, Bertrand qui s'est débrouillé pour m'obtenir un financement de thèse et Christophe pour avoir accepté de faire partie de mon jury alors que cela implique de venir en Angleterre en plein mois de juillet. Je remercie maintenant, le 7ème étage, le 4ème étage, le 5ème étage, le 3ème étage et le 2ème étage du bâtiment du second cycle de la facultés des sciences et technologies.

Je remercie tous les non-permanents qui ont fait partie de mon quotidien que ce soit à la fac ou en formation, que je connais depuis plus ou moins longtemps, et que je me sens obligé de nommer car il est probable que ce document tombe entre leurs mains: Sarah, Vincent,

## Acknowledgements

# Abstract

The work presented in this thesis was inspired by precedent results on the Gaudin models (which are integrable) for spins-$\frac{1}{2}$ only which, by a change of variables in the algebraic Bethe equations, manage to considerably simplify the numerical treatment of such models.

This numerical optimisation is carried out by the construction of determinants, only depending on the previously mentioned variables, for every scalar products appearing in the expression of the mean value of an observable of interest at a given time.

By showing it is possible to use the Quantum Inverse Scattering Method (QISM), even when the vacuum state is not eigenstate of the transfer matrix, the previous results concerning spins-$\frac{1}{2}$ only are generalised to models including an additional spin-boson interaction.

De facto, this generalisation opened different possible paths of research.

First of all, we show that it is possible to further generalise the use of determinants for spin models describing the interaction of one spin of arbitrary norm with many spins-$\frac{1}{2}$. We give the method leading to the explicit construction of determinants' expressions.

Moreover, we can extend this work to other Gaudin models where the vacuum state is not an eigenstate of the transfer matrix. We did this work for spins-$\frac{1}{2}$ interacting with an arbitrarily oriented magnetic field.

Finally, a numerical treatment of systems describing the interaction of many spins-$\frac{1}{2}$ with a single bosonic mode is presented. We study the time evolution of bosonic occupation and of local magnetisation for two different Hamiltonians, the Tavis-Cummings Hamiltonian and a central spin Hamiltonian. We learn that the dynamics of these systems, relaxing from an initial state to a stationary state, leads to a superradiant-like state for certain initial states.

# Résumé

Le travail présenté dans cette thèse est inspiré de précédents résultats sur les les modèles de Gaudin ne contenant que des spins-$\frac{1}{2}$ (ces modèles sont intégrables) qui, par un changement de variable dans les équations de Bethe algébriques, parviennent à simplifier le traitement numérique de ces modèles.

Cette optimisation numérique s'effectue par l'intermédiaire d'une construction en déterminant, ne dépendant que des variables précédemment mentionnées, pour chaque produit scalaire intervenant dans l'expression de la moyenne d'une observable à un temps donné.

En montrant qu'il est possible d'utiliser la méthode du Quantum Inverse Scattering Method (QISM), même dans un cas où l'état du vide n'est pas état propre de la matrice de transfert, les résultats précédents concernant uniquement des spins-$\frac{1}{2}$ sont généralisés à des modèles contenant en plus une interaction spin-boson.

De fait, cette généralisation a ouvert plusieurs voies de recherche possibles.

Premièrement, il est montré qu'il est possible de continuer à généraliser l'utilisation de déterminants pour des modèles de spins décrivant l'interaction d'un spin de norme arbitraire avec des spins-$\frac{1}{2}$. La méthode permettant d'obtenir la construction des expressions explicites de ces déterminants est donnée.

On peut également pousser la généralisation à d'autres modèles de Gaudin dont l'état du vide n'est pas état propre de la matrice de transfert. C'est ce que nous avons fait pour des spins-$\frac{1}{2}$ en interaction avec un champ magnétique dont l'orientation est arbitraire.

Enfin, un traitement numérique de ces systèmes de spins-$\frac{1}{2}$ interagissant avec un mode bosonique est présenté. L'évolution temporelle de l'occupation bosonique et de l'aimantation locale des spins est ainsi étudiée selon deux Hamiltoniens différents, l'Hamiltonien de Tavis-Cummings et un Hamiltonien type spin central. Cette étude nous apprend que la dynamique de ces systèmes, qui relaxent d'un état initial vers un état stationnaire, conduit à un état superradiant lorsque l'état initial choisi y est favorable.

# Contents

# Contents

# List of Figures

# Introduction

## General Context

Contrarily to its classical counterpart [1], the notion of quantum integrability strives to find an unifying definition [2]. Researchers have tried different approaches to this problem [3, 4, 5, 6]. For instance, from a very mathematical point of view using Galois theory [7] or with more physical interpretation as in [8], where it is explained that a system is integrable if the scattering it supports is non-diffractive. Nevertheless, an often mentioned asset of the integrable models is their propensity to be exactly solvable. Interestingly enough, one of the attempts of [1] to define the quantum integrability relies on this "exact-solvability".

The regain of interest for integrable models is due to technical advances enabling experimental physicists to build low dimensional quantum systems described by integrable models. Thus, groups of scientists have been able to set up experiments to study excitons and polaritons in quantum wells [9, 10, 11] and semi-conductors quantum dots [12, 13, 14, 15, 16, 17, 18]. Additionally, a lot of experiments aim to observe the superradiant phase transition in Dicke-like models [19] using a Bose-Einstein condensate in optical cavities [20, 21, 22, 23, 24, 25, 26, 27, 28]. All these new experimental accomplishments call for numerical simulations in order to reach a better understanding of such integrable models. One of the purposes of this thesis is to present numerical tools to enhance the numerical treatment of a family of integrable models: the Gaudin models [29].

Another asset of Gaudin models is that all Hamiltonians, built as a combination of the conserved quantities, belonging to the class of Gaudin Hamiltonians share the same basis of eigenstates. Consequently, a given result can apply to many situations describing, for instance, either the pairing Richardson-Gaudin Hamiltonian [30, 31, 32, 33], the BCS Hamitonian [34, 35] or central spin Hamiltonians [36, 37, 38, 39, 40].

One of the interests of the family of Gaudin models we will focus on, is that they are also able to describe the Tavis-Cummings (TC) model [41, 42]. Since our work enables us to describe the TC models, allowing the description of the previously mentioned superradiant phase, we introduce with more details this phenomenon. The superradiance in quantum mechanics occurs when an ensemble of N emitters, like excited atoms, interact with a "common radiation field" [19]. If the wavelength of the radiation turns out to be much bigger than the separation

of the ensemble of the emitters, then all emitters interact with the radiation in a collective and coherent way. In the early 50's, Robert. H. Dicke suggested a model to describe two level systems ("molecules") interacting with a "common radiation field". He stated that the gas of radiating molecules should be treated as a single quantum system [19]. The Tavis-Cummings model to which we will refer can be understood as the Dicke model in the Rotating Wave Approximation (RWA), thus it can be used to describe cavity quantum electrodynamic (QED) [41, 42]. The following inhomogeneous version of the Tavis-Cummings Hamiltonian:

$$H_{TC} = \omega b^\dagger b + \sum_{j=1}^{N} \epsilon_j S_j^z + V \sum_{j=1}^{N} (b^\dagger S_j^- + S_j^+ b), \tag{1}$$

is therefore one of the many Hamiltonians which belong to the general class of spin-boson Gaudin integrable quantum models. Characterised by a (Zeeman) gap which is here chosen distinct for each of the $N$ spins present, it allows, through a common coupling strength $V$, the flipping (up or down) of each individual spin by an absorption or an emission of a single boson at energy $\omega$.

This superradiant phase is still the focus of many studies. For example, in [43] the question of whether the superradiant transition is a quantum phase transition is answered for Dicke and Tavis-Cummings models, in [44] it is shown that the dephasing of the individual atoms destroys the phase transition, in [45] the phase diagram for ultracold fermions in a transversely pumped cavity is given and in [46] extreme parameters values are chosen (the frequency of the two level systems is very small compared to the bosonic frequency and the coupling is very strong) to study a system's behaviour beyond the RWA.

## Tightened Context and Outline

The work presented in this thesis is rooted in the work of Michel Gaudin which introduced the Generalised Gaudin Algebra (GGA) relying on the classical Yang-Baxter equation [29]. The GGA being based on solutions to this equation, it ensures the integrability of Gaudin models. The chapter 1 introduces this specific algebra.

As mentioned in the previous section, one of the purposes of the present work is to optimise the numerical treatment of Gaudin models to efficiently access the dynamics of these systems. To do so we follow the time evolution of the mean value of observables of interest (denoted $\hat{O}$) from an initial state $|\psi_0\rangle$ which is not eigenstate of any Hamiltonian $H$ who itself belongs to the class of Gaudin Hamiltonians. The very general formula giving this evolution at a time $t$ is:

$$\langle \hat{O} \rangle (t) = \sum_{n,m} \langle \psi_0 | \, n \rangle \langle m | \, \psi_0 \rangle \, e^{i(E_n - E_m)t} \langle n | \hat{O} | m \rangle. \qquad (2)$$

The states $|n\rangle$ and $|m\rangle$ being eigenstates of $H$ with respective eigenvalues $E_n$ and $E_m$, the diagonalisation of $H$ is needed to access the time evolution of a given system. In order to use the properties of integrability of Gaudin models, and to avoid a direct diagonalisation of $H$, we use in this thesis the Quantum Inverse Scattering Method (QISM) construction [47] and the resulting Algebraic Bethe Ansatz (ABA). This step constitutes the first simplification: instead of carrying out an usual diagonalisation, which involves the computation of inverse of matrices that may lead to singularities and thus to numerical instability, it requires to solve a set of coupled non-linear equations (the Bethe equations). Additionally, the number of variables is given by the size of the system whereas a direct diagonalisation requires a number of inputs of the size of the Hilbert space. The explicit expressions of the set of Bethe equations is given in chapter 1 and detailed explanations on how to obtain these equations is presented in Appendix A.2.

We can find further simplifications in the work of Slavnov [48]. Indeed, he rewrote the expressions of scalar products and form factors (the matrix elements of an operator associated to an observable) as functions of the solutions of the Bethe equations, called the rapidities $\lambda_i$. The Slavnov formulas turn out to be determinant expressions. This is in itself a simplification because it exists many efficient way to compute a determinant numerically.

The work presented in this thesis is aligned with the idea of finding determinant expressions to optimise the numerical treatment of integrable models but contrarily to Slavnov determinants, the expressions we derive are expressed as functions of other variables (than the $\lambda_i$) thanks to the transformation presented in [49, 50] and in this thesis. This change of variables and the resulting equations are also detailed in chapter 1.

However, the determinant expressions presented in chapter 1 are valid only for a specific realisation of GGA, when the systems we consider only contain interacting spin-$\frac{1}{2}$. The different steps to obtain these determinant expressions in the context of spin-$\frac{1}{2}$ are presented in chapter 1.

The chapter 2 details every step needed to generalise the work done for the spin-$\frac{1}{2}$ realisation only. In the section (2.1) of this chapter, new determinant expressions are given when one spin of arbitrary norm is interacting with many spins-$\frac{1}{2}$. The section (2.2) is dedicated to a another realisation of the GGA: when the collection of spins-$\frac{1}{2}$ is interacting with a single bosonic mode. It is the introduction of this single bosonic mode that enables the Gaudin models to describe new dynamics, like the Tavis-Cummings case. In section (2.2), the change of variables, the new resulting equations, the explicit determinant expressions for the scalar

products and the form factors are shown for this spin-$\frac{1}{2}$-boson realisation.

The chapter 3 describes the algorithmic aspect of the numerical work on solving the Bethe equations (once the change of variables has been carried out). Besides, the structure of the algorithm, we justify the need of making specific approximations to solve the set of Bethe equations and discuss the consistency of these approximations.

In chapter 4, some examples of the asymptotic behaviour of observables of interest is presented. These results have been obtained using the algorithm presented in chapter 3 as well as the determinant expressions introduced in this thesis. In section 4.3 we also compare our asymptotic results to the ones of the Generalised Gibbs Ensemble (GGE) [51]. The latter theory aiming to describe integrable models in their thermodynamic limit, we compare its predictions to the asymptotic behaviour of the Gaudin models.

In chapter 5, the real time dynamics (of observables considered in chapter 4) are presented. To complete our understanding of the behaviour of spin-$\frac{1}{2}$-boson systems, we compare dynamics ruled by two different Hamiltonians, the Tavis-Cummings Hamiltonian and a "central-spin" Hamiltonian.

# 1 ABA and Gaudin spin models

In the first section of this chapter, we will introduce the Generalised Gaudin Algebra without specifying any particular realisation (giving no explicit expression of the operators defining the algebra, but focusing on the relations between them). In addition, we will present the Algebraic Bethe Ansatz (ABA) in the same formalism which enables us to define the Bethe equations. In the second section, we will show how to rewrite these equations in a set of quadratic ones. The last part of this chapter presents one of the possible realisation of the Generalised Gaudin Algebra describing spins-$\frac{1}{2}$ only. In this context the re-parametrisation of the Bethe equations into quadratic ones will be shown. Knowing the solutions of these new equations allows one to build new determinant expressions of the scalar products and of the form factors (matrix elements of operators under consideration) as functions of the new found variables $\Lambda(\epsilon_i)$ which are solutions of the quadratic Bethe equations.

## 1.1 Algebraic Bethe Ansatz for the rational generalised Gaudin algebra

Let us first introduce the Generalised Gaudin Algebra (GGA) defined by the operators $S^x(u), S^y(u), S^z(u)$ satisfying the commutation relations [29, 52]:

$$
\begin{aligned}
\left[S^x(u), S^y(v)\right] &= i(Y(u,v)S^z(u) - X(u,v)S^z(v)), \\
\left[S^y(u), S^z(v)\right] &= i(Z(u,v)S^x(u) - Y(u,v)S^x(v)), \\
\left[S^z(u), S^x(v)\right] &= i(X(u,v)S^y(u) - Z(u,v)S^y(v)), \\
\left[S^\kappa(u), S^\kappa(v)\right] &= 0, \quad \kappa = x, y, z,
\end{aligned}
\tag{1.1}
$$

where $u, v \in \mathbb{C}$ and $X, Y, Z$ are antisymmetric functions. $S^x(u), S^y(u), S^z(u)$ form a Lie Algebra.

Consistency of the Lie Algebra, imposed by the Jacobi identities, can only be achieved when the functions $X, Y, Z$ fulfil the classical Yang-Baxter equation (see Appendix A.1):

$$X(u,v)Y(v,w) + Y(w,u)Z(u,v) + Z(v,w)X(w,u) = 0. \tag{1.2}$$

We can introduce the operators $S^{\pm}(u) \equiv S^x(u) \pm iS^y(u)$ which fulfil the commutation relations:

$$
\begin{aligned}
\left[S^{\pm}(u), S^{\pm}(v)\right] &= \pm(X(u,v) - Y(u,v))\left[S^z(u) + S^z(v))\right], \\
\left[S^+(u), S^-(v)\right] &= (X(u,v) + Y(u,v))\left[S^z(u) - S^z(v))\right], \\
\left[S^z(u), S^{\pm}(v)\right] &= \pm\frac{1}{2}[(X(u,v) + Y(u,v))S^{\pm}(u) - (X(u,v) - Y(u,v))S^{\mp}(u) \\
&\quad -2Z(u,v)S^{\pm}(u)].
\end{aligned}
\tag{1.3}
$$

In this work, we exclusively deal with one type of solutions to this equation, namely the rational (XXX) Gaudin algebra defined for $u \neq v$ by

$$X(u,v) = Y(u,v) = Z(u,v) = \frac{\gamma}{u-v}, \ \gamma \in \mathbb{C}. \tag{1.4}$$

For the remainder of this thesis, we will choose $\gamma = 1$. The previous commutation relations (1.3) become:

$$
\begin{aligned}
\left[S^{\pm}(u), S^{\pm}(v)\right] &= 0, \\
\left[S^+(u), S^-(v)\right] &= 2X(u,v)\left[S^z(u) - S^z(v)\right], \\
\left[S^z(u), S^{\pm}(v)\right] &= \pm X(u,v)\left(S^{\pm}(u) - S^{\pm}(v)\right).
\end{aligned}
\tag{1.5}
$$

Thanks to the raising and lowering Gaudin operators, we define $S^2(u)$ as:

$$S^2(u) \equiv \frac{1}{2}\left(S^+(u)S^-(u) + S^-(u)S^+(u) + 2S^z(u)S^z(u)\right), \tag{1.6}$$

for which $\left[S^2(u), S^2(v)\right] = 0$, for arbitrary complex parameters $u \neq v$. Here $S^+(u)$ can be seen as an operator which acts on a state and creates a quasi-particle fully parametrised by a single complex variable $u \in \mathbb{C}$. The particle-pseudovacuum $|0\rangle$ is defined as a lowest weight vector for which $S^-(u)|0\rangle = 0$, $\forall\ u \in \mathbb{C}$.

For a given number of particle-like excitations $M$, which is conserved for XXX models, the Quantum Inverse Scattering Method (QISM) [47] and the resulting ABA allow one to find the eigenstates common to every $S^2(u)$, called the Bethe state, by using the following generic construction:

$$|\lambda_1 \dots \lambda_M\rangle \equiv \prod_{i=1}^{M} S^+(\lambda_i)|0\rangle. \tag{1.7}$$

If the pseudovacuum $|0\rangle$ is also an eigenstate of $S^2(u)$ and $S^z(u)$ such as

$$
\begin{aligned}
S^2(u)|0\rangle &= \ell(u)|0\rangle \\
S^z(u)|0\rangle &= \ell^z(u)|0\rangle,
\end{aligned}
\tag{1.8}
$$

the action of the $S^2(u)$ operator on a state of the form (1.7) can be obtained explicitly (see Appendix A.2) from the XXX commutation rules (1.3) as

$$S^2(u)|\lambda_1 \dots \lambda_M\rangle = \left(\prod_{i=1}^{M} S^+(\lambda_i)\right)S^2(u)|0\rangle + \left[S^2(u),\left(\prod_{i=1}^{M} S^+(\lambda_i)\right)\right]|0\rangle$$

$$= E(\{\lambda\}, u)|\lambda_1 \dots \lambda_M\rangle + \sum_{k=1}^{M} G_k(\{\lambda\}, u)|\lambda_1 \dots, \lambda_k \to u, \dots \lambda_M\rangle, \tag{1.9}$$

where we write $\{\lambda\}$ for the set of all the rapidities $\lambda_i$ and where

$$E(\{\lambda\}, u) \quad = \quad \ell(u) + \sum_{i=1}^{M} \left( -2\ell^z(u)X(u, \lambda_i) + \sum_{j \neq i}^{M} X(u, \lambda_i)X(u, \lambda_j) \right), \tag{1.10}$$

and

$$
\begin{aligned}
G_k(\{\lambda\}, u) \quad &= \quad 2X(u, \lambda_k)\left[\ell^z(\lambda_k) + \sum_{j \neq k} X(\lambda_j, \lambda_k)\right] \\
&= \quad \frac{2}{u - \lambda_k}\left[\ell^z(\lambda_k) + \sum_{j \neq k}\frac{1}{\lambda_j - \lambda_k}\right].
\end{aligned} \tag{1.11}
$$

States of the form (1.7) therefore become common eigenstates of $S^2(u) \; \forall \; u \in \mathbb{C} \setminus \{\lambda\}$ provided the $M$ rapidities $\lambda_k$ are solution of a set of coupled non-linear algebraic equations: the Bethe equations. For rational models (1.4), these equations are found by cancelling every $G_k(\{\lambda\}, u)$ in eq. (1.9) and gathering all terms in the brackets except $\frac{1}{\lambda_j - \lambda_k}$ in a function $F(\lambda_i)$, which must vanish with $-\frac{1}{\lambda_j - \lambda_k}$. Therefore, in general, the Bethe equations can be written as:

$$F(\lambda_k) = \ell^z(\lambda_k) = \sum_{j=1(\neq k)}^{M} \frac{1}{\lambda_k - \lambda_j}. \tag{1.12}$$

In that case (1.20) becomes:

$$
\begin{aligned}
S^z(\lambda_k)|0\rangle &= \sum_{j=1(\neq k)}^{M} \frac{1}{\lambda_k - \lambda_j} |0\rangle \\
S^2(\lambda_k)|0\rangle &= \frac{1}{2}\left(S^+(\lambda_k)S^-(\lambda_k) + S^-(\lambda_k)S^+(\lambda_k) + 2\left(S^z(\lambda_k)\right)^2\right)|0\rangle \\
&= \frac{1}{2}\left(2S^+(\lambda_k)S^-(\lambda_k) - \left[S^+(\lambda_k), S^-(\lambda_k)\right] + 2\left(S^z(\lambda_k)\right)^2\right)|0\rangle \\
&= \left(-\lim_{\epsilon \to 0} X(\lambda_k, \lambda_k + \epsilon)\left(S^z(\lambda_k) - S^z(\lambda_k + \epsilon)\right) + \left(\sum_{j=1(\neq k)}^{M} \frac{1}{\lambda_k - \lambda_j}\right)^2\right)|0\rangle \\
&= \left(-\frac{\partial S^z(\lambda_k)}{\partial \lambda_k} + \left(\sum_{j=1(\neq k)}^{M} \frac{1}{\lambda_k - \lambda_j}\right)^2\right)|0\rangle \\
&= \left(\sum_{j=1(\neq k)}^{M} \frac{1}{\left(\lambda_k - \lambda_j\right)^2} + \left(\sum_{j=1(\neq k)}^{M} \frac{1}{\lambda_k - \lambda_j}\right)^2\right)|0\rangle.
\end{aligned}
\tag{1.13}
$$

The explicit expressions for the Bethe equations and the other quantities presented in this chapter will be given in next chapter for systems containing spin-$\frac{1}{2}$.

## 1.2  Quadratic Bethe equations

Numerically, solving the Bethe equations (1.12) involves some difficulties due to the divergences that happen when two rapidities $\lambda_i$ coincide. Willing to rewrite the previous equations into quadratic ones to prevent the divergences from occurring, we introduce the variables :

$$
\Lambda(\epsilon_i) = \sum_{j=1}^{M} \frac{1}{\epsilon_i - \lambda_j}
\tag{1.14}
$$

which come from the polynomial $Q(\epsilon_i) = \prod_{j=1}^{M}\left(\epsilon_i - \lambda_j\right)$ whose $M$ roots correspond to the values of $\lambda_j$. Indeed, we have $\frac{Q'(\epsilon_i)}{Q(\epsilon_i)} = \Lambda(\epsilon_i)$ . To find quadratic Bethe equations, a relation between $F(\lambda_i)$ and $\Lambda^2(\epsilon_i)$ had to be found, we used to following one:

$$
\begin{aligned}
\Lambda^2(\epsilon_i) + \Lambda'(\epsilon_i) &= \sum_{j=1}^{M}\sum_{k=1}^{M}\frac{1}{(\epsilon_i - \lambda_k)(\epsilon_i - \lambda_j)} - \sum_{j=1}^{M}\frac{1}{(\epsilon_i - \lambda_j)^2} \\
&= \sum_{k=1}^{M}\sum_{j\neq k}^{M}\frac{1}{(\epsilon_i - \lambda_k)(\epsilon_i - \lambda_j)} \\
&= \sum_{j=1}^{M}\sum_{k\neq j}^{M}\frac{1}{(\lambda_j - \lambda_k)}\left(\frac{1}{\epsilon_i - \lambda_j} - \frac{1}{\epsilon_i - \lambda_k}\right) \\
&= \sum_{j=1}^{M}\sum_{k\neq j}^{M}\frac{2}{(\lambda_j - \lambda_k)(\epsilon_i - \lambda_j)} \\
&= \sum_{j=1}^{M}\frac{2F(\lambda_j)}{(\epsilon_i - \lambda_j)}.
\end{aligned}
\tag{1.15}
$$

The Bethe equations with $F(u) = -\sum_{i=1}^{N}\frac{A_i}{\epsilon_i - u} + \frac{B}{2g}u + \frac{C}{2g}$ can be equivalently written as pure quadratic equations [49, 50]. Specifying an expression for $F$ restricts the possible realisations for the Generalised Gaudin Algebra, the parameters $A_i, B$ or $C$ still have to be adjusted to define precisely a wanted algebra. For instance, if the $A_i$ are non-zero, it means our algebra rules a system containing spins of norm $A_i$. A variety of XXX models do fall in that category including the spin-only realisations which are reviewed in this chapter and the spin-boson realisations specifically studied in the next chapter. By using the definition (1.14) and (1.15) we have:

$$
\begin{aligned}
\Lambda^2(\epsilon_i) &= -\Lambda'(\epsilon_i) + \sum_{j=1}^{M}\frac{2}{\epsilon_i - \lambda_j}\left(-\sum_{k=1}^{N}\frac{A_i}{\epsilon_k - \lambda_j} + \frac{B}{2g}\lambda_j + \frac{C}{2g}\right) \\
&= -\Lambda'(\epsilon_i) - 2A_i\left(\sum_{j=1}^{M}\frac{2}{(\epsilon_i - \lambda_j)^2} + \sum_{j=1}^{M}\sum_{k\neq i}^{N}\frac{1}{(\epsilon_i - \lambda_j)(\epsilon_k - \lambda_j)}\right) + \frac{B}{g}\sum_{j=1}^{M}\left(1 - \frac{\epsilon_i}{\epsilon_i - \lambda_j}\right) + \frac{C}{g}\Lambda(\epsilon_i) \\
&= (2A_i - 1)\Lambda'(\epsilon_i) - 2A_i\sum_{j=1}^{M}\sum_{k\neq i}^{N}\frac{1}{\epsilon_k - \epsilon_i}\left(\frac{1}{\epsilon_i - \lambda_j} - \frac{1}{\epsilon_k - \lambda_j}\right) + \frac{B\epsilon_i + C}{g}\Lambda(\epsilon_i) + \frac{BM}{g} \\
&= (2A_i - 1)\Lambda'(\epsilon_i) - 2A_i\sum_{k\neq i}^{N}\frac{\Lambda(\epsilon_i) - \Lambda(\epsilon_k)}{\epsilon_k - \epsilon_i} + \frac{B\epsilon_i + C}{g}\Lambda(\epsilon_i) - \frac{B}{g}M.
\end{aligned}
\tag{1.16}
$$

In the specific case of interest here ($A_i = \frac{1}{2}$ for spins-$\frac{1}{2}$) the quadratic Bethe equations can be written as:

$$\Lambda^2(\epsilon_i) + \frac{B}{g}M - \frac{B\epsilon_i + C}{g}\Lambda(\epsilon_i) - \sum_{j \neq i}^N \frac{\Lambda(\epsilon_j) - \Lambda(\epsilon_i)}{\epsilon_j - \epsilon_i} = 0. \tag{1.17}$$

In this section, we have shown how to rewrite the traditional Bethe equations into quadratic equations thanks to new variables $\Lambda(\epsilon_i)$ provided we are working with spins-$\frac{1}{2}$. The case for $A_i \neq \frac{1}{2}$ will be discussed in section 3.1. In the next section, we choose a particular realisation of our algebra, spin-$\frac{1}{2}$ only models, and show how to exploit the solutions of the quadratic equations which is the main motivation of the theoretical work.

## 1.3  Spin-models

In this section, the quadratic Bethe equations are given, for a spin-$\frac{1}{2}$ only realisation. Once the solutions of these quadratic equations are known, one needs to introduce two representations of the same eigenstate to be able to exploit these solutions. Indeed, we explain in the second section that the two representations of an eigenstate enable one to find determinant expressions for quantities of interest.

### 1.3.1  "Particle" and "hole" representations

In the previous section, only the commutation relations of $S^\pm(u)$ are presented but not their explicit expressions which define the realisation of our algebra. The operators that define how to create or annihilate a particle-like excitation and the one that measure the orientation of the spins along the $\hat{z}$-axis are the followings :

$$S^+(u) = \sum_{i=1}^N \frac{S_i^+}{u - \epsilon_i}, \ S^-(u) = \sum_{i=1}^N \frac{S_i^-}{u - \epsilon_i}, \ S^z(u) = \frac{1}{g} - \sum_{i=1}^N \frac{S_i^z}{u - \epsilon_i}, \tag{1.18}$$

with $g$ and $\epsilon_i$ for $i \in \{1 \dots N\}$ arbitrary real parameters. The Hilbert space of a system of $N$ spins-$\frac{1}{2}$ is the tensor product of $N$ subspace of dimension 2 ($\mathbb{C}^2$) and is therefore of dimension $2^N$. The operators $S_i^+, S_i^-$ and $S_i^z$ are the usual spin-$\frac{1}{2}$ operators whose commutations relations are:

$$
\begin{aligned}
\left[S_i^\pm, S_j^\pm\right] &= 0, \\
\left[S_i^+, S_j^-\right] &= 2m_z \delta_{ij}, \\
\left[S_i^z, S_j^\pm\right] &= \pm \delta_{ij} S^\pm,
\end{aligned}
\tag{1.19}
$$

with $m_z = \pm\frac{1}{2}$ regarding the orientation of the spin $i$.

Using the derivation explained in section 1.2 and detailed in the Appendix A.2, we can find the traditional Bethe equations. In this case the vacuum is the state $|\downarrow \dots \downarrow\rangle$ for which all spins are in the "down" state. As before the vacuum is eigenstate of $S^z(u)$ and $S^2(u)$, indeed:

$$
\begin{aligned}
S^z(u)|0\rangle &= \ell^z(u)|0\rangle \\
&= \left( \frac{1}{g} - \sum_{i=1}^N \frac{S_i^z}{u - \epsilon_i} \right) |\downarrow \dots \downarrow\rangle \\
&= \left( \frac{1}{g} + \frac{1}{2} \sum_{i=1}^N \frac{1}{u - \epsilon_i} \right) |\downarrow \dots \downarrow\rangle,
\end{aligned}
\tag{1.20}
$$

$$
\begin{aligned}
S^2(u)|0\rangle &= \ell(u)|0\rangle \\
&= \frac{1}{2} \left( S^+(u)S^-(u) + S^-(u)S^+(u) + 2S^z(u)S^z(u) \right) |\downarrow \dots \downarrow\rangle.
\end{aligned}
\tag{1.21}
$$

$S^+(u)S^-(u)$ do not participate to the eigenvalue whereas $S^-(u)S^+(u)$ only participates when it acts on the same spin, so we have:

$$\ell(u)|0\rangle \;=\; \left(\left(\frac{1}{g}-\sum_{i=1}^{N}\frac{S_i^z}{u-\epsilon_i}\right)^2+\frac{1}{2}\sum_{i=1}^{N}\frac{S_i^+S_i^-}{(u-\epsilon_i)^2}\right)|\downarrow\ldots\downarrow\rangle$$

$$=\;\left(\frac{1}{g^2}-\frac{2}{g}\sum_{i=1}^{N}\frac{S_i^z}{u-\epsilon_i}+\sum_{i=1}^{N}\sum_{j=1}^{N}\frac{S_i^zS_j^z}{(u-\epsilon_i)(u-\epsilon_j)}+\frac{1}{2}\sum_{i=1}^{N}\frac{S_i^+S_i^-}{(u-\epsilon_i)^2}\right)|\downarrow\ldots\downarrow\rangle$$

$$=\;\left(\frac{1}{g^2}+\frac{1}{g}\sum_{i=1}^{N}\frac{1}{u-\epsilon_i}+\frac{1}{4}\sum_{i=1}^{N}\sum_{j=1}^{N}\frac{1}{(u-\epsilon_i)(u-\epsilon_j)}+\frac{1}{2}\sum_{i=1}^{N}\frac{1}{(u-\epsilon_i)^2}\right)|\downarrow\ldots\downarrow\rangle$$

$$=\;\left(\frac{1}{g^2}+\frac{1}{g}\sum_{i=1}^{N}\frac{1}{u-\epsilon_i}+\frac{1}{4}\sum_{i=1}^{N}\sum_{j\neq i}^{N}\frac{1}{(u-\epsilon_i)(u-\epsilon_j)}+\frac{3}{4}\sum_{i=1}^{N}\frac{1}{(u-\epsilon_i)^2}\right)|\downarrow\ldots\downarrow\rangle.$$

$$(1.22)$$

Thus in this case (1.11) becomes:

$$G_k(\{\lambda\},u)\;=\;2X(u,\lambda_k)\left[\ell^z(\lambda_k)+\sum_{j\neq k}X(\lambda_j,\lambda_k)\right]$$

$$=\;\frac{2}{u-\lambda_k}\left[\frac{1}{g}+\frac{1}{2}\sum_{i=1}^{N}\frac{1}{\lambda_k-\epsilon_i}+\sum_{j\neq k}\frac{1}{\lambda_j-\lambda_k}\right].$$

$$(1.23)$$

For $F_k(\{\lambda\},u)$ to be null, the $\lambda_i$ need to fulfil the set of equations:

$$\frac{1}{g}+\frac{1}{2}\sum_{i=1}^{N}\frac{1}{\lambda_k-\epsilon_i}+\sum_{j\neq k}\frac{1}{\lambda_j-\lambda_k}=0,$$

$$(1.24)$$

which are the Bethe equations. So in the case of a spin-$\frac{1}{2}$ realisation we have $F(\lambda_k)=\frac{1}{g}+\frac{1}{2}\sum_{i=1}^{N}\frac{1}{\lambda_k-\epsilon_i}=\sum_{j\neq k}\frac{g}{\lambda_k-\lambda_j}$ and using (1.17) we can write straightforwardly the quadratic Bethe equations:

$$\left[\Lambda^\lambda(\epsilon_i)\right]^2\;=\;\sum_{j\neq i}^{N}\frac{\Lambda^\lambda(\epsilon_i)-\Lambda^\lambda(\epsilon_j)}{\epsilon_i-\epsilon_j}+\frac{2}{g}\Lambda^\lambda(\epsilon_i)\quad\text{(particles)}.$$

$$(1.25)$$

The exponent $\lambda$ denotes that we work within the "particle" representation whereas the exponent $\mu$ will denote the "hole" representation and no exponent will mean that a result will be valid for both cases. In relation to the previous equations (1.24) the quadratic ones are much easier to solve numerically [53, 54]. However the interest of traditional Bethe equations is that the solutions, the rapidities $\lambda_i$, can be used to build the Slavnov determinants [48] and doing so to enable us to study the dynamics of a given system. From this statement we understand the drawbacks of the quadratic equations. If we want to take advantage of the already existing results relative to the Bethe equations we have to transform the $\Lambda(\epsilon_i)$ back to the usual $\lambda_i$. An important part of this work is to present how to exploit knowledge of the $\Lambda(\epsilon_i)$ without changing them back to $\lambda_i$. In that purpose, every quantity of interest will be expressed in terms of $\Lambda(\epsilon_i)$ starting from the scalar products of two eigenstates of $S^2(u)$ defined in the previous section:

$$
\begin{aligned}
\langle \lambda'_1 \dots \lambda'_{M'} | \lambda_1 \dots \lambda_M \rangle &= \langle \downarrow \dots \downarrow | \left( \prod_{i=1}^{M'} (S^+)^\dagger (\lambda'_i) \right) \left( \prod_{i=1}^{M} S^+ (\lambda_i) \right) | \downarrow \dots \downarrow \rangle \\
&= \langle \downarrow \dots \downarrow | \left( \prod_{i=1}^{M'} S^- (\lambda'_i) \right) \left( \prod_{i=1}^{M} S^+ (\lambda_i) \right) | \downarrow \dots \downarrow \rangle .
\end{aligned}
\tag{1.26}
$$

Within this representation, it is simple to understand that two alternative representations of any given eigenstate can be built: one using particle-like excitations through the repeated action of the raising operator on the particle-vacuum $|\lambda_1 \dots \lambda_M\rangle = \prod_{i=1}^{M} S^+(\lambda_i) |\downarrow \dots \downarrow\rangle$ and the second one obtained using lowering operators acting, hole-like excitations, on the hole-vacuum $|\mu_1 \dots \mu_{N-M}\rangle = \prod_{i=1}^{N-M} S^-(\mu_i) |\uparrow \dots \uparrow\rangle$. Thus the previous scalar product can be written:

$$
\begin{aligned}
\langle \mu_1 \dots \mu_{N-M} | \lambda_1 \dots \lambda_M \rangle &= \langle \uparrow \dots \uparrow | \left( \prod_{i=1}^{N-M} (S^-)^\dagger (\mu_i) \right) \left( \prod_{i=1}^{M} S^+ (\lambda_i) \right) | \downarrow \dots \downarrow \rangle \\
&= \langle \uparrow \dots \uparrow | \left( \prod_{i=1}^{N-M} S^+ (\mu_i) \right) \left( \prod_{i=1}^{M} S^+ (\lambda_i) \right) | \downarrow \dots \downarrow \rangle \\
&= \langle \uparrow \dots \uparrow | \left( \prod_{i=1}^{N} S^+ (\nu_i) \right) | \downarrow \dots \downarrow \rangle ,
\end{aligned}
\tag{1.27}
$$

where $\{\nu_1 \dots \nu_N\} = \{\lambda_1 \dots \lambda_M\} \cup \{\mu_1 \dots \mu_{N-M}\}$. There appears the need of finding the traditional equations and then the quadratic Bethe equations for all $\mu_i$. Since the spin algebra is symmetric in its highest/lowest weight configurations, both formulations of the ABA are formally identical, being simply related by a change of the quantisation axis from $\hat{z} \to -\hat{z}$

which exchanges the roles of $S^+(u)$ and $S^-(u)$ and replaces $S^z(u)$ by $-S^z(u)$. The QISM [47] is identically formulated in both cases since $|\uparrow \dots \uparrow\rangle$ is a valid hole-pseudo-vacuum obeying all three properties:

$$S^+(u)|\uparrow \dots \uparrow\rangle = 0, \quad S^2(u)|\uparrow \dots \uparrow\rangle = \ell_\uparrow(u)|\uparrow \dots \uparrow\rangle, \quad -S^z(u)|\uparrow \dots \uparrow\rangle = \ell_\uparrow^z(u)|\uparrow \dots \uparrow\rangle, \quad (1.28)$$

where $\ell_\uparrow(u)$ and $\ell_\uparrow^z(u)$ are the eigenvalues of $S^2(u)$ and $S^z(u)$ in the hole representation.

One then finds the sets of Bethe equations which, for $(N - M)$ holes, read:

$$-\frac{1}{2}\sum_{k=1}^{N}\frac{1}{\epsilon_k - \mu_j} - \frac{1}{g} \;=\; \sum_{k \neq j}^{N-M}\frac{1}{\mu_j - \mu_k}, \quad \text{(holes)} \tag{1.29}$$

and whose quadratic equations are given by:

$$\left[\Lambda^\mu(\epsilon_i)\right]^2 \;=\; \sum_{j \neq i}^{N}\frac{\Lambda^\mu(\epsilon_i) - \Lambda^\mu(\epsilon_j)}{\epsilon_i - \epsilon_j} - \frac{2}{g}\Lambda^\mu(\epsilon_i). \quad \text{(holes)} \tag{1.30}$$

Solutions to these two sets of equations, (1.25) and (1.30), both define the same ensemble of $M$ particles eigenstates of the transfer matrix $S^2(u)$. The explicit expression of $S^2(u)$, for the realisation (1.18) has a series of $N$ poles at $u = \epsilon_i$ whose residues correspond to the $N$ commuting conserved operators:

$$
\begin{aligned}
\operatorname{Res}\left(S^2(u)\right)_{u\to\epsilon_i} &= \lim_{u\to\epsilon_i}(u-\epsilon_i)\frac{1}{2}\left(S^+(u)S^-(u)+S^-(u)S^+(u)+2S^z(u)S^z(u)\right) \\
&= \lim_{u\to\epsilon_i}(u-\epsilon_i)\frac{1}{2}\left(\sum_{k=1}^{N}\sum_{j=1}^{N}\frac{S_k^+ S_j^-}{(u-\epsilon_k)(u-\epsilon_j)}+\sum_{k=1}^{N}\sum_{j=1}^{N}\frac{S_k^- S_j^+}{(u-\epsilon_k)(u-\epsilon_j)}\right. \\
&\qquad\left. +2\left(\frac{1}{g}-\sum_{k=1}^{N}\frac{S_k^z}{u-\epsilon_k}\right)^2\right) \\
&= \frac{1}{2}\left(\sum_{j=1(\neq i)}^{N}\frac{2S_i^+ S_j^-}{\epsilon_i-\epsilon_j}+\sum_{j=1(\neq i)}^{N}\frac{2S_i^- S_j^+}{\epsilon_i-\epsilon_j}+\sum_{j=1(\neq i)}^{N}\frac{4S_i^z S_j^z}{\epsilon_i-\epsilon_j}+\frac{-4S_i^z}{g}\right), \quad (1.31)
\end{aligned}
$$

which gives us

$$
R_i = -\frac{2S_i^z}{g}+\sum_{j=1(\neq i)}^{N}\frac{2\vec{S}_i\cdot\vec{S}_j}{\epsilon_i-\epsilon_j}\quad\text{with}\quad \vec{S}_i\cdot\vec{S}_j=\frac{1}{2}\left(S_i^+ S_j^-+S_i^- S_j^++2S_i^z S_j^z\right), \tag{1.32}
$$

whose eigenvalues $r_i$ are read off the residues of the $S^2(u)$ eigenvalues (1.10). In both representations (for spins-$\frac{1}{2}$ only) these eigenvalues read:

$$
\begin{aligned}
\operatorname{Res}\left(E(\{\lambda\},u)\right)_{u\to\epsilon_i} &= \lim_{u\to\epsilon_i}(u-\epsilon_i)\left(\ell(u)+\sum_{k=1}^{M}\left(-2\ell^z(u)X(u,\lambda_k)+\sum_{j\neq k}^{M}X(u,\lambda_k)X(u,\lambda_j)\right)\right) \\
&= \lim_{u\to\epsilon_i}(u-\epsilon_i)\left(\ell(u)-2\sum_{k=1}^{M}\frac{1}{u-\lambda_k}\ell^z(u)+\sum_{k=1}^{M}\sum_{j\neq k}^{M}\frac{1}{(u-\lambda_k)(u-\lambda_j)}\right) \\
&= \lim_{u\to\epsilon_i}(u-\epsilon_i)\left(\frac{1}{g^2}+\frac{1}{g}\sum_{k=1}^{N}\frac{1}{u-\epsilon_k}+\frac{1}{4}\sum_{k=1}^{N}\sum_{j\neq k}^{N}\frac{1}{(u-\epsilon_k)(u-\epsilon_j)}+\frac{3}{4}\sum_{k=1}^{N}\frac{1}{(u-\epsilon_k)^2}\right. \\
&\qquad\left. -2\sum_{k=1}^{M}\frac{g}{u-\lambda_k}\left(\frac{1}{g}+\frac{1}{2}\sum_{j=1}^{N}\frac{1}{u-\epsilon_j}\right)+\sum_{k=1}^{M}\sum_{j\neq k}^{M}\frac{1}{(u-\lambda_k)(u-\lambda_j)}\right), \quad (1.33)
\end{aligned}
$$

leading to

$$
\begin{aligned}
r_i^{\lambda} &= -\sum_{j=1}^{M} \frac{1}{\epsilon_i - \lambda_j} + \frac{1}{2} \sum_{j=1(\neq i)}^{N} \frac{1}{\epsilon_i - \epsilon_j} + \frac{1}{g} \\
r_i^{\mu} &= -\sum_{j=1}^{N-M} \frac{1}{\epsilon_i - \mu_j} + \frac{1}{2} \sum_{j=1(\neq i)}^{N} \frac{1}{\epsilon_i - \epsilon_j} - \frac{1}{g},
\end{aligned}
\tag{1.34}
$$

which explicitly depend on the state only through $\Lambda^{\lambda}(\epsilon_i) = \sum_{j=1}^{M} \frac{1}{\epsilon_i - \lambda_j}$ and $\Lambda^{\mu}(\epsilon_i) = \sum_{j=1}^{N-M} \frac{1}{\epsilon_i - \mu_j}$. In addition, since the parameters $\lambda$ and $\mu$ have to be either real or come in complex conjugate pairs, the resulting $\Lambda(\epsilon_i)$ are systematically real for any eigenstate of the system.

The correspondence between the two representations of a given eigenstate is then easily found by picking the solutions which give the same ensemble of eigenvalues $r_k$. Doing so, directly shows that the transformation:

$$
\Lambda^{\mu}(\epsilon_i) = \Lambda^{\lambda}(\epsilon_i) - \frac{2}{g}
\tag{1.35}
$$

allows one to simply go from one representation to the other for an arbitrary eigenstate, as defined by any solution of either form of the Bethe equations (1.29) or, alternatively (1.30).

### 1.3.2 Partition functions, normalisation and form factors

Having access to the two representations of any given eigenstate allows one to rewrite their scalar product (even for two eigenstates found at different values of $g$) like in (1.28):

$$
\begin{aligned}
\langle \mu_1 \ldots \mu_{N-M} \mid \lambda_1 \ldots \lambda_M \rangle &= \langle \uparrow \ldots \uparrow | \left( \prod_{i=1}^{N-M} S^+(\mu_i) \right) \left( \prod_{i=1}^{M} S^+(\lambda_i) \right) | \downarrow \ldots \downarrow \rangle \\
&\equiv \langle \uparrow \ldots \uparrow | \left( \prod_{i=1}^{N} S^+(\nu_i) \right) | \downarrow \ldots \downarrow \rangle,
\end{aligned}
\tag{1.36}
$$

only thanks to the $\Lambda(\epsilon_i)$. To give a better understanding of the task, here is an example of the kind of scalar product we want to express:

$$\langle \uparrow\uparrow\uparrow\uparrow | \left( \prod_{i=1}^{3} S^+(v_i) \right) |\downarrow\downarrow\downarrow\rangle \quad = \frac{1}{(v_1 - \epsilon_1)(v_2 - \epsilon_2)(v_3 - \epsilon_3)} + \frac{1}{(v_1 - \epsilon_1)(v_3 - \epsilon_2)(v_2 - \epsilon_3)}$$
$$+ \frac{1}{(v_2 - \epsilon_1)(v_1 - \epsilon_2)(v_3 - \epsilon_3)} + \frac{1}{(v_2 - \epsilon_1)(v_3 - \epsilon_2)(v_1 - \epsilon_3)}$$
$$+ \frac{1}{(v_3 - \epsilon_1)(v_1 - \epsilon_2)(v_2 - \epsilon_3)} + \frac{1}{(v_3 - \epsilon_1)(v_2 - \epsilon_2)(v_1 - \epsilon_3)}. \quad (1.37)$$

First of all, one can compute the scalar product, called partition function, of a Bethe state (defined by (1.7) using an arbitrary set $\{\lambda_1 \dots \lambda_M\}$) with any eigenstate common to the operators $S_1^z \dots S_N^z$. These eigenstates are the states containing $M$ up-pointing spins labelled by the indices $\{i_1 \dots i_M\}$; the $N - M$ other spins $\{\bar{i}_1 \dots \bar{i}_{N-M}\}$ therefore pointing down. We can alternatively write this state as either a particle or a hole-like construction $\left| \uparrow_{\{i_1 \dots i_M\}} \right\rangle = \left| \downarrow_{\{\bar{i}_1 \dots \bar{i}_{N-M}\}} \right\rangle$. The scalar product of the Bethe state with this particular basis state was shown (an equivalent type of proof will be given in the next chapter) to be given by the determinant of an $M \times M$ matrix [55]:

$$\langle \uparrow_{\{i_1 \dots i_M\}} | \lambda_1 \dots \lambda_M \rangle = \langle \uparrow_{\{i_1 \dots i_M\}} | \prod_{i=1}^{M} S^+(\lambda_i) | \downarrow \dots \downarrow \rangle \quad = \quad \mathrm{Det} J_{M \times M} \quad (1.38)$$

$$J_{ab} \quad = \quad \begin{cases} \sum_{c=1(\neq a)}^{M} \frac{1}{\epsilon_{i_a} - \epsilon_{i_c}} - \Lambda^{\lambda}(\epsilon_{i_a}) & a = b \\ \frac{1}{\epsilon_{i_a} - \epsilon_{i_b}} & a \neq b \end{cases} . \quad (1.39)$$

The proof is using the fact that (1.38) is a rational function of the $\lambda_i$ parameters which obeys a simple recursion relation. An identical construction is possible for hole-like states $\langle \uparrow_{\{i_1 \dots i_M\}} | \mu_1 \dots \mu_{N-M} \rangle = \langle \downarrow_{\{\bar{i}_1 \dots \bar{i}_{N-M}\}} | \prod_{i=1}^{N-M} S^-(\mu_i) | \uparrow \dots \uparrow \rangle$, which, by symmetry, are given by the same form of determinant of an $(N - M) \times (N - M)$ matrix. That matrix is then defined by the $N - M$ values of $\epsilon$ associated with the spins which are pointing down in the bra and the replacement $\Lambda^{\lambda} \to \Lambda^{\mu}$.

The scalar products in (1.36) can therefore be written, for an arbitrary ensemble $\{v_1 \dots v_N\}$, as the determinant of the $N \times N$ version of the matrix defined above:

$$\langle\uparrow\dots\uparrow|\left(\prod_{i=1}^{N}S^{+}(\nu_{i})\right)|\downarrow\dots\downarrow\rangle=\mathrm{Det}J_{N\times N}\quad\forall\,\{\nu_{1}\dots\nu_{N}\}\in\mathbb{C}^{N} \tag{1.40}$$

which is explicitly written in terms of the variables $\Lambda^{\nu}(\epsilon_{i})=\sum_{j=1}^{N}\frac{1}{\epsilon_{i}-\nu_{j}}=\Lambda^{\lambda}(\epsilon_{i})+\Lambda^{\mu}(\epsilon_{i})$:

$$J_{ab}\quad=\quad\begin{cases}\displaystyle\sum_{c=1(\neq a)}^{N}\frac{1}{\epsilon_{a}-\epsilon_{c}}-\Lambda^{\lambda}(\epsilon_{a})-\Lambda^{\mu}(\epsilon_{a}) & a=b\\[2ex]\frac{1}{\epsilon_{a}-\epsilon_{b}} & a\neq b\end{cases}. \tag{1.41}$$

While this expression is valid for the overlaps of arbitrary particle-like and hole-like states, one should keep in mind that a generic particle-state (built out of arbitrary $\{\lambda_{1}\dots\lambda_{M}\}$) cannot necessarily be rewritten as an equivalent hole-like representation. However, for eigenstates of $S^{2}(u)$ (defined by a solution to the Bethe equations) we showed that such a hole-representation not only exists, but is also quite simple to find using eq. (1.35).

Consequently, for a given eigenstate, its particle representation ($|\lambda_{1}\dots\lambda_{M}\rangle$) and hole representation $\left(\left|\mu_{1}\dots\mu_{N-M}\right\rangle\right)$ correspond to the same normalised state $|\lambda_{1}\dots\lambda_{M}\rangle_{n}$ and only differ by a constant pre-factor: $|\lambda_{1}\dots\lambda_{M}\rangle=N_{\lambda}|\lambda_{1}\dots\lambda_{M}\rangle_{n}$ and $\left|\mu_{1}\dots\mu_{N-M}\right\rangle=N_{\mu}|\lambda_{1}\dots\lambda_{M}\rangle_{n}$. The scalar product between both representations of the same state and the projections on an arbitrary eigenstate of $S_{j}^{z}$ with $j\in\{1\dots N\}$ gives us access to the individual normalisation of both representations [53] since they respectively give us the product and ratio of these constants:

$$\begin{aligned}\langle\mu_{1}\dots\mu_{N-M}|\,\lambda_{1}\dots\lambda_{M}\rangle\quad&=\quad\mathrm{Det}K\\[1ex]&=\quad N_{\lambda}N_{\mu}\\[1ex]\frac{\langle\uparrow_{\{i_{1}\dots i_{M}\}}|\lambda_{1}\dots\lambda_{M}\rangle}{\langle\uparrow_{\{i_{1}\dots i_{M}\}}|\mu_{1}\dots\mu_{N-M}\rangle}\quad&=\quad\frac{\mathrm{Det}J_{M\times M}^{\lambda}}{\mathrm{Det}J_{(N-M)\times(N-M)}^{\mu}}\\[2ex]&=\quad\frac{N_{\lambda}}{N_{\mu}}.\end{aligned} \tag{1.42}$$

These two relations are evidently sufficient to compute the squared norm of both representations allowing one to properly normalise the states. While the determinant expressions show

that both $N_\mu$ and $N_\lambda$ have to be real, they can still in principle differ by a sign corresponding to a $\pi$ phase between both representations. The sign of the product $N_\lambda N_\mu$ allows one to simply detect this $\pi$ phase for any given eigenstate and therefore correct this possible phase shift between both representations of the normalised eigenstate.

Form factors, the elements of a matrix associated to an operator, for the various local raising and lowering operators $S_i^\pm$ can also be written easily as a similar determinant. Since these form factors can only be non-zero when they involve two states whose number of excitations differs by one and since the local spin-raising operators are simply the residues of the Gaudin operator $S^+(u)$ (1.18), one simply needs to take the appropriate limit of the previous determinant to find:

$$
\begin{aligned}
&\langle\{\mu_1\dots\mu_{N-M}\}|\,S_k^+\,|\{\lambda_1\dots\lambda_{M-1}\}\rangle \\
&= \lim_{u\to\epsilon_k}(u-\epsilon_k)\,\langle\{\mu_1\dots\mu_{N-M}\}|\,S^+(u)\,|\{\lambda_1\dots\lambda_{M-1}\}\rangle \\
&= \lim_{u\to\epsilon_k}(u-\epsilon_k)\mathrm{Det}J(\{\mu_1\dots\mu_{N-M},u,\lambda_1\dots\lambda_{M-1}\}) = \mathrm{Det}J^{\hat{k}},
\end{aligned}
\tag{1.43}
$$

where $J^{\hat{k}}$ is the $(N-1)\times(N-1)$ matrix equivalent to (1.41) from which line and column $k$ have been removed while, at the same time, the sums in the diagonal elements now exclude $\epsilon_k$:

$$
J^{\hat{k}}_{ab} = \begin{cases} \displaystyle\sum_{c=1(\neq a,k)}^{N}\frac{1}{\epsilon_a-\epsilon_c}-\Lambda^\lambda(\epsilon_a)-\Lambda^\mu(\epsilon_a) & a=b \\[4mm] \frac{1}{\epsilon_a-\epsilon_b} & a\neq b \end{cases} \quad \text{with } (a,b\neq k).
\tag{1.44}
$$

The demonstration leading to find the eigenvalue-based representation of the $S_i^z$ form factor will be kept for next chapter because it is straightforwardly generalisable to spin-only realisations and and because the numerical part of the thesis is using the spin-boson expressions. We simply give here the expression of the diagonal (which is denoted by the $m$) form factor of $S_i^z$ out of the eigenvalues of the conserved quantities (1.34) where $g'=1/g$:

$$
\begin{aligned}
\langle \{\mu(g')\}_m | S_k^z | \{\lambda(g')\}_m \rangle &= -\frac{\partial r_k^m(g')}{\partial g'} \langle \{\mu(g')\}_m \mid \{\lambda(g')\}_m \rangle, \\[2mm]
\frac{\langle \{\mu(g')\}_m | S_k^z | \{\lambda(g')\}_m \rangle}{\langle \{\mu(g')\}_m \mid \{\lambda(g')\}_m \rangle} &= \left[ -2 + 2 \frac{\partial \Lambda_m^\lambda(\epsilon_k)}{\partial g'} \right],
\end{aligned}
\tag{1.45}
$$

with $\{\mu\}$ meaning the ensemble of all the $\mu$. We can notice that the form factor is not any more a determinant but expressed as a function of the derivatives of the $\Lambda(\epsilon_i)$. The $\partial \Lambda^\lambda(\epsilon_i)/\partial g'$ are in fact easy to find by just taking the derivative of the quadratic equations(1.25):

$$
2\Lambda^\lambda(\epsilon_i) \frac{\partial \Lambda^\lambda(\epsilon_i)}{\partial g'} = \sum_{j \neq i} \frac{\frac{\partial \Lambda^\lambda(\epsilon_i)}{\partial g'} - \frac{\partial \Lambda^\lambda(\epsilon_j)}{\partial g'}}{\epsilon_i - \epsilon_j} + 2 \frac{\partial \Lambda^\lambda(\epsilon_i)}{\partial g'} + 2\Lambda^\lambda(\epsilon_i) g'
\tag{1.46}
$$

Within this section on the spin-$\frac{1}{2}$ realisation of the algebra, all results that will be generalised in next chapter are shown. A short conclusion on the interests of these expressions follows these last results.

## 1.4   Conclusions

An important aspect of the determinant expressions is that they allow calculations of scalar products and form factors using exclusively the variables $\Lambda(\epsilon_i)$ which are much simpler to obtain since they obey quadratic Bethe equations. Therefore, the determinant expressions have been instrumental in allowing the fast and efficient numerical calculations necessary to study the fully quantum non-equilibrium dynamics of the central spin model [53, 54] for example. While the determinants are those of larger matrices ($N \times N$) than Slavnov's $M \times M$ determinants [48, 56], they can still provide more efficient numerics than the latter. Indeed, the determinants being expressed in terms of the $\{\Lambda^\lambda(\epsilon_1) \dots \Lambda^\lambda(\epsilon_N)\}$ variables, their use avoids the complicated extraction of the $\{\lambda_1 \dots \lambda_M\}$ variables corresponding to a given $\{\Lambda^\lambda(\epsilon_1) \dots \Lambda^\lambda(\epsilon_N)\}$ set.

Another important aspect to highlight, which has not been mentioned at all, is the applicability to these results for a given Hamiltonian. The transfer matrix $S^2(u)$ commuting with every conserved quantity $R_i$, will also commute with every Hamiltonian $H = \sum_i^N \alpha_i R_i$ ( with the $\alpha_i$ chosen by the user) built as a linear combination of the conserved quantities. That is to say that finding the eigenstates of $S^2(u)$ is equivalent to finding the eigenstates of a Hamiltonian built as explained. It is either a strength or a drawback. A drawback because all the previous

method can not be applied outside the class of Hamiltonians previously defined. A strength because any result found in the frame of the Gaudin models encompasses the whole infinity of Hamiltonians one can build out of the conserved quantities.

# 2 Generalising to other realisations of the algebra

In this chapter, the determinant expression for the partition function is given in two new cases. The first one is when the norm of one of the spins is arbitrarily large. The other one is when the collection of spins-$\frac{1}{2}$ is in interaction with a single bosonic mode. In this case, due to the presence of bosonic operators in $S^+(u)$, finding the determinant can not be done straightforwardly by using the results of last chapter.

## 2.1 One spin of arbitrary norm interacting with $N-1$ spin-$\frac{1}{2}$

### 2.1.1 Partition function with one arbitrarily large spin

This section uses in his great majority the work we published in [57]. Starting from expression (1.36), we define a recursive way to build a similar determinant expression for the case where one of the spins (without loss of generality we systematically choose $S_1$) is raised from a $S = \frac{1}{2}$ to $S = 1$, $S = \frac{3}{2}$ and so on, up to an arbitrary $S = \frac{d}{2}$.

Integrability and the Bethe ansatz solution of this particular system do not rely on the representation of the spin, be it spin $\frac{1}{2}$ or higher. In every case, the eigenstates are still built out of the same operator $S^+(\lambda)$ defined in eq. (1.18) acting on the fully down polarised state, i.e. eigenstates of every $S_i^z$ with the lowest possible (negative) eigenvalues $m_z$. The dual (hole representation) is naturally built using $S^-(\lambda)$ acting on the fully up polarised state. Since the first spin can now accommodate more than a single excitation ($\left(S_1^+\right)^2 = 0$ only for spins 1/2), going from the fully down to the fully up polarised state now requires a total of $\Omega = 2S + (N-1)$ excitations.

It also remains true that inverting the quantisation axis guarantees the existence of a dual Bethe ansatz so that the partition function (see subsection 1.3.2) we are interested in corresponds to the scalar product of an arbitrary off-shell Bethe state. We will write $\Uparrow^S$ and $\Downarrow^S$ a spin of norm $S$ polarised up and down, (1.36) becoming $\langle \Uparrow_1^S \dots \uparrow_N | S^+(v_1) S^+(v_2) \dots S^+(v_\Omega) | \Downarrow_1^S \dots \downarrow_N \rangle$.

As in previous chapter we begin by giving a scalar product in a specific case, here a single spin

1 and a single spin $\frac{1}{2}$:

$$
\begin{aligned}
Z^{S;\left(\frac{1}{2}\right)}_{\{v_1,v_2,v_3\}} &= \langle \Uparrow_1 \uparrow_2 | S^+(v_1) S^+(v_2) S^+(v_3) | \Downarrow_1 \downarrow_2 \rangle \\
&= \frac{1}{(v_1-\epsilon_1)(v_2-\epsilon_1)(v_3-\epsilon_2)} + \frac{1}{(v_1-\epsilon_1)(v_3-\epsilon_1)(v_2-\epsilon_2)} \\
&+ \frac{1}{(v_2-\epsilon_1)(v_1-\epsilon_1)(v_3-\epsilon_2)} + \frac{1}{(v_2-\epsilon_1)(v_3-\epsilon_1)(v_1-\epsilon_2)} \\
&+ \frac{1}{(v_3-\epsilon_1)(v_1-\epsilon_1)(v_2-\epsilon_2)} + \frac{1}{(v_3-\epsilon_1)(v_2-\epsilon_1)(v_1-\epsilon_2)} \\
&= \frac{2}{(v_1-\epsilon_1)(v_2-\epsilon_1)(v_3-\epsilon_2)} + \frac{2}{(v_2-\epsilon_1)(v_3-\epsilon_1)(v_1-\epsilon_2)} \\
&+ \frac{2}{(v_1-\epsilon_1)(v_3-\epsilon_1)(v_2-\epsilon_2)}.
\end{aligned}
\tag{2.1}
$$

From this example we can guess that the matrix of interest will still be built out of the set $\{v_1 \ldots v_\Omega\}$ while, this time, the second "set" actually becomes the multiset $\{\epsilon_1, \epsilon_1 \ldots \epsilon_1, \epsilon_2, \epsilon_3, \epsilon_4 \ldots \epsilon_N\}$ with the first element $\epsilon_1$ repeated $2S$ times. That is to say that $2S$ of the rapidities have to be associated with $\epsilon_1$ and the remaining ones are each associated to one of the other spin's $\epsilon_i$. The resulting product of the terms $\frac{1}{v_i - \epsilon_j}$ is then summed over possible mappings.

In general one has

$$
Z^{S;\left(\frac{1}{2}\right)^{\otimes N-1}}_{\{v_1 \ldots v_\Omega\}} = \sum_{A \in R^{(2S)}} \sum_{B \in B^{(\tilde{A})}} \frac{(2S)!}{\prod_{i=1}^{2S}(A_i - \epsilon_1)} \frac{1}{\prod_{i=1}^{N-1}(B_i - \epsilon_{i+1})}
\tag{2.2}
$$

where $R^{(2S)}$ is the set composed of every subset of $\{v_1 \ldots v_\Omega\}$ with given cardinality $2S$ and $B^{(\tilde{A})} = \{(R\backslash A)\}$ is the set of all $(N-1)$-tuples (permutations) one can build out of the elements of the relative complement $R\backslash A$, therefore excluding any rapidity already present in $A$. Having chosen a given set of $2S$ rapidities to associate with the first spin ($\epsilon_1$), we then sum over all bijections between the $N-1$ remaining rapidities and the $N-1$ inhomogeneity parameters associated with the spins $\frac{1}{2}$. Summing these contributions gives us the desired partition function which also corresponds to the "partially-homogeneous" limit obtained from having $2S + N - 1$ spins-$\frac{1}{2}$ of which the first $2S$ share the same inhomogeneity parameter $\epsilon_1$.

This explicit construction retains the basic features of the partition function for spin-$\frac{1}{2}$ models only obtained without repeated $\epsilon_1$, in that it has exclusively single poles in each of the $v_i$ variables. The residue at any of these poles will reproduce the exact same structure in terms

of the set and multiset from which $\nu_i$ and one instance of $\epsilon_j$ has respectively been removed. Moreover, since each rapidity $\nu_i$ necessarily appears in every term, it is obvious that, in the limit when any $\nu_i \to \infty$, the partition function tends to zero.

### 2.1.2 Set of variables

Considering that, in each of the $\nu_i$ variables, only single poles can appear in the partition function, it can therefore be written in a way which explicitly depends on combinations which reproduce this structure. Starting from the $Q(z) = \prod_{i=1}^{\Omega}(z - \nu_i)$ polynomial, one can build a hierarchy of such rational functions:

$$
\begin{aligned}
\Gamma_0(z) &\equiv -\frac{Q(z)}{Q(z)} = -1 \\
\Gamma_1(z) &\equiv -\frac{Q'(z)}{Q(z)} = -\sum_{i=1}^{\Omega} \frac{1}{z - \nu_i} = -\Lambda(z) \\
\Gamma_2(z) &\equiv -\frac{Q''(z)}{Q(z)} = -\sum_{i_1 \neq i_2}^{\Omega} \frac{1}{(z - \nu_{i_1})(z - \nu_{i_2})} = -\Lambda'(z) - \Lambda(z)^2 \\
\Gamma_3(z) &\equiv -\frac{Q'''(z)}{Q(z)} = -\sum_{i_1 \neq i_2 \neq i_3}^{\Omega} \frac{1}{(z - \nu_{i_1})(z - \nu_{i_2})(z - \nu_{i_3})} = -\Lambda''(z) - 3\Lambda(z)\Lambda'(z) - \Lambda^3(z) \\
&\quad \vdots
\end{aligned}
\tag{2.3}
$$

This set of $\Gamma_i(z)$ functions can therefore be defined recursively by noticing that, taking the derivative of $\Gamma_{n-1}(z)$, one finds:

$$
\frac{\partial}{\partial z}\Gamma_{n-1}(z) = -\frac{Q^{(n)}(z)}{Q(z)} + \frac{Q^{(n-1)}(z)}{Q(z)^2}Q'(z) = \Gamma_n(z) - \Lambda(z)\Gamma_{n-1}(z).
$$

$$
\Gamma_n(z) = \frac{\partial}{\partial z}\Gamma_{n-1}(z) + \Lambda(z)\Gamma_{n-1}(z).
\tag{2.4}
$$

In terms of the set of $\Lambda^{(a)}(z)$ (the $a^{\text{th}}$ derivative of $\Lambda(z)$), one can explicitly verify that the solution to this recurrence is given by:

$$\Gamma_n(z) = \sum_{\{k_0, k_1 \dots k_n\}} C^n_{\{k_0, k_1 \dots k_n\}} \left[ \prod_{a=0}^{n} \left( \Lambda^{(a)}(z) \right)^{k_a} \right], \tag{2.5}$$

with

$$C^n_{\{k_0, k_1 \dots k_n\}} = \frac{n!}{\prod_{a=0}^{n} \left[ \left[ (a+1)! \right]^{k_a} k_a! \right]} \delta_{[\sum_{a=0}^{n}(a+1)k_a], n} \cdot \tag{2.6}$$

Supposing the form valid for $n-1$, we find that recursion (2.4) will then be verified since:

$$\frac{\partial}{\partial z} \Gamma_{n-1}(z) + \Lambda(z) \Gamma_{n-1}(z) = \frac{\partial \left( \sum_{\{k_0, k_1 \dots k_{n-1}\}} C^{n-1}_{\{k_0, k_1 \dots k_{n-1}\}} \left[ \prod_{a=0}^{n-1} \left( \Lambda^{(a)}(z) \right)^{k_a} \right] \right)}{\partial z}$$

$$+ \Lambda^{(0)}(z) \left( \sum_{\{k_0, k_1 \dots k_{n-1}\}} C^{n-1}_{\{k_0, k_1 \dots k_{n-1}\}} \left[ \prod_{a=0}^{n-1} \left( \Lambda^{(a)}(z) \right)^{k_a} \right] \right)$$

$$= \sum_{b=0}^{n-1} \sum_{\{k_0, k_1 \dots k_{n-1}\}} k_b C^{n-1}_{\{k_0, k_1 \dots k_{n-1}\}} \left[ \prod_{a=0 (\neq b \neq b+1)}^{n-1} \left( \Lambda^{(a)}(z) \right)^{k_a} \right] \left( \Lambda^{(b)}(z) \right)^{k_b - 1} \left( \Lambda^{(b+1)}(z) \right)^{k_{b+1} + 1}$$

$$+ \left( \sum_{\{k_0, k_1 \dots k_{n-1}\}} C^{n-1}_{\{k_0, k_1 \dots k_{n-1}\}} \left[ \left( \Lambda^{(0)}(z) \right)^{k_0 + 1} \prod_{a=1}^{n-1} \left( \Lambda^{(a)}(z) \right)^{k_a} \right] \right), \tag{2.7}$$

which, regrouping the terms with a given set of powers $(k_0, k_1 \dots k_n)$, can be rewritten as:

$$\frac{\partial}{\partial z} \Gamma_{n-1}(z) + \Lambda(z) \Gamma_{n-1}(z) = \sum_{\{k_0, k_1 \dots k_n\}} \tilde{C}^n_{\{k_0, k_1 \dots k_n\}} \prod_{a=0}^{n} \left( \Lambda^{(a)}(z) \right)^{k_a} \tag{2.8}$$

with coefficients

$$\tilde{C}^n_{\{k_0, k_1 \dots k_n\}} = C^{n-1}_{\{k_0, k_1 \dots k_{n-1}\}} + \sum_{b=0}^{n-1} k_b C^{n-1}_{\{k_0, k_1 \dots k_b + 1, k_{b+1} - 1 \dots k_n\}}. \tag{2.9}$$

It is then simple to verify that this last relation is indeed verified by the coefficients proposed in (2.6) since every term respects the $\sum_{a=0}^{n}(a+1)k_a = n$ condition so that the right hand side can be written as:

$$C^{n-1}_{\{k_0,k_1...k_{n-1}\}} + \sum_{b=0}^{n-1} k_b C^{n-1}_{\{k_0,k_1...k_b+1,k_{b+1}-1...k_{n-1}\}}$$

$$= \left[ \frac{(n-1)!\,(1!)^{k_0}}{\prod_{a=0}^{n-1}\left[[(a+1)!]^{k_a}\,k_a!\right]} + \sum_{b=0}^{n-1} k_b \frac{(b+2)!\,k_{b+1}}{(b+1)!\,k_b} \frac{(n-1)!}{\prod_{a=0}^{n-1}\left[[(a+1)!]^{k_a}\,k_a!\right]} \right] \delta_{\left[\sum_{a=0}^{n-1}(a+1)k_a\right],\,n-1}$$

$$= \left[ \frac{(n-1)!\left[(0+1)k_0 + \sum_{b=0}^{n-1}(b+2)\,k_{b+1}\right]}{\prod_{a=0}^{n-1}\left[[(a+1)!]^{k_a}\,k_a!\right]} \right] \delta_{\left[\sum_{a=0}^{n-1}(a+1)k_a\right],\,n-1}$$

$$= \left[ \frac{(n-1)!\left[\sum_{b=0}^{n}(b+1)\,k_b\right]}{\prod_{a=0}^{n-1}\left[[(a+1)!]^{k_a}\,k_a!\right]} \right] \delta_{\left[\sum_{a=0}^{n-1}(a+1)k_a\right],\,n-1} = \left[ \frac{(n)!\,\delta_{\left[\sum_{a=0}^{n}(a+1)k_a\right],\,n}}{\prod_{a=0}^{n}\left[[(a+1)!]^{k_a}\,k_a!\right]} \right] = C^{n}_{\{k_0,k_1...k_n\}}.$$

$$(2.10)$$

Verifying the validity of (2.6) for $n = 1$ is simple since only $k_0 = 1$ with $k_{i\neq 0} = 0$ respects the condition imposed by the Kronecker delta, namely that $\sum_{a=0}^{n}(a+1)k_a = n$. This verification therefore completes the proof.

For the system of interest here, we will build the partition function explicitly in terms of the variables $\{\Gamma_1(\epsilon_1)\dots\Gamma_{2S}(\epsilon_1),\Gamma_1(\epsilon_2),\Gamma_1(\epsilon_3)\dots\Gamma_1(\epsilon_N)\}$, which as we have shown can themselves be simply built out of $\{\Lambda(\epsilon_1)\dots\Lambda^{(2S)}(\epsilon_1),\ \Lambda(\epsilon_2),\Lambda(\epsilon_3)\dots\Lambda(\epsilon_N)\}$, i.e. on every $\Lambda(\epsilon_i)$ and on the $2S$ first derivatives of $\Lambda(z)$ evaluated at $\epsilon_1$. These are precisely the variables in terms of which the set of quadratic Bethe equations is built and which allow one to build a simpler numerical approach to the problem of finding eigenstates of the system.

### 2.1.3 Higher spin partition function

As we mentioned before, the explicit expression for the partition function given in (2.2) is a rational function which contains only single poles for each of the rapidities $v_i$ and is fully symmetric under exchange of any two of these parameters.

It obeys a set of recursive relations linking the partition functions for a variety of systems. Explicitly regrouping the terms where $v_i$ (any of them, by symmetry) is paired to $\epsilon_1$, one can write it as a sum over the similar partition functions one obtains when the first spin goes from $S \to S - \frac{1}{2}$, after excluding rapidity $v_i$:

$$Z^{S;\left(\frac{1}{2}\right)^{\otimes N-1}}_{\{v_1...v_\Omega\}} = \sum_{i=1}^{\Omega} \frac{2S}{v_i - \epsilon_1} Z^{S-\frac{1}{2};\left(\frac{1}{2}\right)^{\otimes N-1}}_{\{v_1...v_{i-1},v_{i+1}...v_\Omega\}}. \tag{2.11}$$

Identically, one can also write it in terms of the partition functions obtained by excluding any one of the spins $\frac{1}{2}$ (say spin $j$):

$$Z^{S;\left(\frac{1}{2}\right)^{\otimes N-1}}_{\{v_1...v_\Omega\}} = \sum_{i=1}^{\Omega} \frac{1}{v_i - \epsilon_j} Z^{S;\left(\frac{1}{2}\right)^{\otimes N-2}_j}_{\{v_1...v_{i-1},v_{i+1}...v_\Omega\}}. \tag{2.12}$$

As we also pointed out, the construction is such that $\lim_{v_i \to \infty} Z^{S\left(\frac{1}{2}\right)^{\otimes N-1}}_{\{v_1...v_\Omega\}} = 0$, for any of the rapidities.

These properties can be used to set up a recursive proof for any proposed form, whose starting point will be the previously found representation (1.41) for a collection of $N$ spins $\frac{1}{2}$. However, since it will become the starting point of the recursive proof this work is built on, we point out immediately that an alternative determinant representation can be built by simply changing the signs of every off-diagonal element. Indeed, since transposition leaves a determinant invariant, in this particular case where off-diagonal elements are related by $\tilde{J}_{ij} = -\tilde{J}_{ji}$, one can also write:

$$\langle \uparrow\uparrow \dots \uparrow| \prod_{i=1}^{N} S^+(v_i) |\downarrow\downarrow \dots \downarrow\rangle = \det J_{N\times N} \tag{2.13}$$

with

$$J_{ij} = \begin{cases} \sum_{k\neq i}^{N} \frac{1}{\epsilon_i - \epsilon_k} - \sum_{k=1}^{N} \frac{1}{\epsilon_i - v_k} & i = j \\ \frac{1}{\epsilon_j - \epsilon_i} & i \neq j \end{cases}. \tag{2.14}$$

To prove the equality of two rational functions (in this case containing only single poles), one simply needs to show that they share the same poles, the same residues at these poles and the same limit at infinity. Thus, any proposed representation for the partition functions can be shown to be valid by simply verifying that these conditions are met for the proposed representation.

Three necessary and sufficient conditions therefore need to be fulfilled in order to validate an expression for the partition function obtained after raising the first spin from $S - \frac{1}{2}$ to $S$ while adding a new rapidity $v_\Omega$.

First, from (2.11), the residue of this partition function at $\nu_\Omega = \epsilon_1$ has to be given by

$$\text{Res}_{\nu_\Omega = \epsilon_1} Z^{S;\left(\frac{1}{2}\right)^{\otimes N-1}}_{\{\nu_1 \dots \nu_\Omega\}} = 2S \, Z^{S-\frac{1}{2};\left(\frac{1}{2}\right)^{\otimes N-1}}_{\{\nu_1 \dots \nu_{\Omega-1}\}} \, , \tag{2.15}$$

which considering the explicit symmetry under exchange of any two rapidities would also be valid for the poles at an arbitrary $\nu_i = \epsilon_1$. This symmetry is guaranteed since the proposed determinant representation will be expressed exclusively in terms of the $\Gamma$ variables, themselves symmetrical under such an exchange.

Secondly, from (2.12), one needs the residue at $\nu_{\Omega+1} = \epsilon_N$ to be given by the determinant obtained after removing the last spin:

$$\text{Res}_{\nu_{\Omega+1} = \epsilon_N} Z^{S;\left(\frac{1}{2}\right)^{\otimes N-1}}_{\{\nu_1 \dots \nu_{\Omega+1}\}} = Z^{S;\left(\frac{1}{2}\right)^{\otimes N-2}_{\hat{N}}}_{\{\nu_1 \dots \nu_\Omega\}} \, , \tag{2.16}$$

again a fact which remains valid for the residue at $\nu_i = \epsilon_N$ for any of the rapidities. Provided the proposed form is explicitly symmetric under the exchange of any two of the spins-$\frac{1}{2}$, this last condition also immediately leads to a similar result for the residues at each $\nu_i = \epsilon_j$ for any $i \in \{1, \dots \Omega\}$ and $j \in \{2, 3 \dots N\}$.

Any representation which verifies these conditions will therefore have the correct poles and residues and its validity will then only require that the limit at any $\nu_i \to \infty$ be 0. Since our determinant representation will be expressed in terms of the $\Gamma$ variables, it is not only symmetric under exchange of two rapidities but it is also obviously non-diverging for any $\nu_i \to \infty$. These facts imply that, once every pole and residue have been checked to be the right ones, the only possible difference between the known expression and the proposed one could be the addition of a simple constant. It will therefore be sufficient to check that, when every rapidity is taken to infinity, the limit does indeed go to zero.

The proposed form will consequently be equal to wanted determinant expression provided we verify the three conditions described in this section: residues at $\epsilon_1$, residues at $\epsilon_{i \neq 1}$ and the limit at $\infty$.

### 2.1.4 Determinant representation

In the same spirit as the partition function for a collection of spins $\frac{1}{2}$, we construct a $N \times N$ determinant representation such that for every $\nu_i$, the poles at $\nu_i = \epsilon_j$ exclusively appear on line $j$ of the matrix. Moreover, we posit that the diagonal element $J^S_{11}$ contains every allowed $\Gamma_n(\epsilon_1)$ ($n \in \{0, 1 \dots 2S\}$) while off-diagonal elements in the first line do not contain the last one: $\Gamma_{2S}(\epsilon_1)$. The same remains true on the other lines corresponding to a spin-$\frac{1}{2}$ and we therefore have a generic form:

$$
\begin{aligned}
J_{11}^S &= (2S)! \sum_{n=0}^{2S} {}^S C_{11}^n \Gamma_n(\epsilon_1) \\[2mm]
J_{1j}^S &= (2S)! \sum_{n=0}^{2S-1} {}^S C_{1j}^n \Gamma_n(\epsilon_1) && \forall\, j \neq 1 \\[2mm]
J_{ii}^S &= {}^S C_{ii}^0 + {}^S C_{ii}^1 \Gamma_1(\epsilon_i) && \forall\, i \neq 1 \\[2mm]
J_{ij}^S &= {}^S C_{ij}^0 && \forall\, i \neq 1\,,\ j \neq 1,\ j \neq i.
\end{aligned}
\tag{2.17}
$$

Exchanging both the rows and the columns associated with any two spins $j$, $j'$ leaves a determinant invariant. Consequently, this makes, as we required, the expression explicitly symmetric under the exchange of two spins. Once again, being built out of the symmetric variables $\Gamma_n(\epsilon_j)$ it is also symmetric under the exchange of any two rapidities $v_j, v_{j'}$, making both fundamental assumptions of the preceding section valid.

As we will demonstrate, the following set of coefficients ${}^S C_{ij}^a$ gives a correct representation of the partition function $Z_{\{v_1...v_\Omega\}}^{S;\left(\frac{1}{2}\right)^{\otimes N-1}} = \det_{N \times N} J^S$ where

$$
J_{ij}^S = \begin{cases}
(2S)! \displaystyle\sum_{n=0}^{2S} \left[ \sum_{E \in S^{(2S-n)}} \frac{1}{\prod_{k=1}^{2S-n}(\epsilon_1 - E_k)} \right] \Gamma_n(\epsilon_1) & i = j = 1 \\[4mm]
-(2S)! \displaystyle\sum_{n=0}^{2S-1} \left[ \sum_{p=n}^{2S-1} \sum_{E \in S_j^{(p-n)}} \frac{2S-p}{(\epsilon_1 - \epsilon_j)^{2S-p}} \frac{1}{\prod_{k=1}^{p-n}(\epsilon_1 - E_k)} \right] \Gamma_n(\epsilon_1) & i = 1 \neq j \\[4mm]
\left[ \dfrac{2S}{\epsilon_i - \epsilon_1} + \displaystyle\sum_{k \neq i \neq 1}^{N} \frac{1}{\epsilon_i - \epsilon_k} \right] + \Gamma_1(\epsilon_i) & i = j \neq 1 \\[4mm]
\dfrac{1}{\epsilon_j - \epsilon_i} & i \neq j \neq 1
\end{cases}
,
\tag{2.18}
$$

with $S^{(n)}$ the ensemble of multisets built by picking $n$ elements in $\{\epsilon_2, \dots \epsilon_N\}$, while $S_j^{(n)}$ is the ensemble of multisets built by picking $n$ elements in $\{\epsilon_2, \dots \epsilon_{j-1}, \epsilon_{j+1} \dots \epsilon_N\}$ (excluding $\epsilon_j$).

That is to say that on the first line, $C_{11}^n$ is, for any order $n$, given by the sum over every possible choice, with repetitions allowed, of $n$ elements out of $\{\epsilon_2, \dots \epsilon_N\}$. The off-diagonal elements coefficients are built in the same fashion, except that in column $j$, $\epsilon_j$ has to be picked at least once and the terms are weighted by $2S - p$, the number of times $\epsilon_j$ actually appears.

For example, when combining a spin $\frac{3}{2}$ and two spins $\frac{1}{2}$, one would find the following set of coefficients:

$$
\begin{aligned}
{}^{\frac{3}{2}}C_{11}^0 &= \frac{1}{(\epsilon_1-\epsilon_2)^3} + \frac{1}{(\epsilon_1-\epsilon_3)^3} + \frac{1}{(\epsilon_1-\epsilon_2)^2(\epsilon_1-\epsilon_3)} + \frac{1}{(\epsilon_1-\epsilon_2)(\epsilon_1-\epsilon_3)^2} \\
{}^{\frac{3}{2}}C_{11}^1 &= \frac{1}{(\epsilon_1-\epsilon_2)^2} + \frac{1}{(\epsilon_1-\epsilon_3)^2} + \frac{1}{(\epsilon_1-\epsilon_2)(\epsilon_1-\epsilon_3)} \\
{}^{\frac{3}{2}}C_{11}^2 &= \frac{1}{(\epsilon_1-\epsilon_2)} + \frac{1}{(\epsilon_1-\epsilon_3)} \\
{}^{\frac{3}{2}}C_{11}^3 &= 1 \\
{}^{\frac{3}{2}}C_{12}^0 &= \frac{1}{(\epsilon_2-\epsilon_1)}\left( \frac{3}{(\epsilon_1-\epsilon_2)^2} + \frac{1}{(\epsilon_1-\epsilon_3)^2} + \frac{2}{(\epsilon_1-\epsilon_2)(\epsilon_1-\epsilon_3)} \right) \\
{}^{\frac{3}{2}}C_{12}^1 &= \frac{1}{(\epsilon_2-\epsilon_1)}\left( \frac{2}{(\epsilon_1-\epsilon_2)} + \frac{1}{(\epsilon_1-\epsilon_3)} \right) \\
{}^{\frac{3}{2}}C_{12}^2 &= \frac{1}{(\epsilon_2-\epsilon_1)} \\
{}^{\frac{3}{2}}C_{22}^0 &= \frac{3}{(\epsilon_2-\epsilon_1)} + \frac{1}{(\epsilon_2-\epsilon_3)} \\
{}^{\frac{3}{2}}C_{22}^1 &= 1 \\
{}^{\frac{3}{2}}C_{ij}^0 &= \frac{1}{(\epsilon_j-\epsilon_i)},
\end{aligned}
\tag{2.19}
$$

where one can write the coefficients of the third column by exchanging the role of $\epsilon_2$ with $\epsilon_3$.

It is a simple enough task to verify the residue at $\epsilon_1$ since these poles exclusively appear on the first line of the matrix, from which every term in the determinant can only contain a single one of the first line's element . The residue of the determinant is therefore given as a determinant as well, built form the residues of the matrix elements of the first line while the other matrix elements are found by computing the $v_\Omega \to \epsilon_1$ limit. Knowing that:

$$
\begin{aligned}
\lim_{v_\Omega \to \epsilon_1} \Gamma_n^{\{v_1...v_\Omega\}}(\epsilon_j) &= \Gamma_n^{\{v_1...v_{\Omega-1}\}}(\epsilon_j) + \frac{1}{\epsilon_1-\epsilon_j}\Gamma_{n-1}^{\{v_1...v_{\Omega-1}\}}(\epsilon_j) \quad \forall j \neq 1, \\
\mathrm{Res}_{v_\Omega=\epsilon_1}\Gamma_n^{\{v_1...v_\Omega\}}(\epsilon_1) &= \Gamma_{n-1}^{\{v_1...v_{\Omega-1}\}}(\epsilon_1),
\end{aligned}
\tag{2.20}
$$

we find:

$$
\mathrm{Res}_{v_\Omega=\epsilon_1} \det_{N\times N} J^S = \det_{N\times N} \tilde{J}^{S-\frac{1}{2}},
\tag{2.21}
$$

where $\tilde{J}^{S-\frac{1}{2}}$ is easily shown to correspond to the $J^{S-\frac{1}{2}}$ defined in (2.18) for a spin $S-\frac{1}{2}$:

$$
\begin{aligned}
\tilde{J}_{11}^{S-\frac{1}{2}} &= (2S)! \sum_{n=1}^{2S} {}^{S}C_{11}^{n} \Gamma_{n-1}^{\{v_1 \ldots v_{\Omega-1}\}}(\epsilon_1) \\
&= 2S(2S-1)! \sum_{n=0}^{2S-1} {}^{S}C_{11}^{n+1} \Gamma_{n}^{\{v_1 \ldots v_{\Omega-1}\}}(\epsilon_1) = 2S J_{11}^{S-\frac{1}{2}} \\
\tilde{J}_{1j}^{S-\frac{1}{2}} &= (2S)! \sum_{n=1}^{2S-1} {}^{S}C_{1j}^{n} \Gamma_{n-1}^{\{v_1 \ldots v_{\Omega-1}\}}(\epsilon_1) \\
&= 2S(2S-1)! \sum_{n=0}^{2S-2} {}^{S}C_{1j}^{n+1} \Gamma_{n}^{\{v_1 \ldots v_{\Omega-1}\}}(\epsilon_1) = 2S J_{1j}^{S-\frac{1}{2}} \quad \forall\, j \neq 1 \\
\tilde{J}_{ii}^{S-\frac{1}{2}} &= {}^{S}C_{ii}^{0} - \frac{1}{\epsilon_i - \epsilon_1} + \Gamma_{1}^{\{v_1 \ldots v_{\Omega-1}\}}(\epsilon_i) = J_{ii}^{S-\frac{1}{2}} \qquad\qquad \forall\, i \neq 1 \\
\tilde{J}_{ij}^{S-\frac{1}{2}} &= {}^{S}C_{ij}^{0} = J_{ij}^{S-\frac{1}{2}} \qquad\qquad\qquad\qquad\qquad \forall\, i \neq 1\,,\, j \neq i,
\end{aligned}
$$

$$(2.22)$$

since

$$
\begin{aligned}
{}^{S-\frac{1}{2}}C_{11}^{n} &= \left[ \sum_{E \in S^{(2S-1-n)}} \frac{1}{\prod_{k=1}^{2S-1-n}(\epsilon_1 - E_k)} \right] = {}^{S}C_{11}^{n+1} \\
{}^{S-\frac{1}{2}}C_{1j}^{n} &= -\left[ \sum_{p=n}^{(2S-1)-1} \sum_{E \in S_j^{(p-n)}} \frac{2S-1-p}{(\epsilon_1 - \epsilon_j)^{2S-1-p}} \frac{1}{\prod_{k=1}^{p-n}(\epsilon_1 - E_k)} \right] \\
&= -\left[ \sum_{p'=n+1}^{2S-1} \sum_{E \in S_j^{(p'-n-1)}} \frac{2S-p'}{(\epsilon_1 - \epsilon_j)^{2S-p'}} \frac{1}{\prod_{k=1}^{p'-n-1}(\epsilon_1 - E_k)} \right] = {}^{S}C_{1j}^{n+1} \quad \forall j \neq 1 \\
{}^{S-\frac{1}{2}}C_{ii}^{0} &= \left[ \frac{2S-1}{\epsilon_i - \epsilon_1} + \sum_{k \neq i \neq 1}^{N} \frac{1}{\epsilon_i - \epsilon_k} \right] = {}^{S}C_{ii}^{0} - \frac{1}{\epsilon_i - \epsilon_1} \quad \forall i \neq 1
\end{aligned}
$$

$$(2.23)$$

This shows that the first recursive condition concerning the value of the residues at $v_i = \epsilon_1$ is met by the determinant of matrix (2.18).

With the same logic, using

$$
\lim_{v_\Omega \to \epsilon_N} \Gamma_n^{\{v_1 \ldots v_\Omega\}}(\epsilon_j) = \Gamma_n^{\{v_1 \ldots v_{\Omega-1}\}}(\epsilon_j) + \frac{1}{\epsilon_N - \epsilon_j} \Gamma_{n-1}^{\{v_1 \ldots v_{\Omega-1}\}}(\epsilon_j) \,\, \forall j \neq N
$$

$$
\mathrm{Res}_{v_\Omega = \epsilon_N} \Gamma_n^{\{v_1 \ldots v_\Omega\}}(\epsilon_N) = \Gamma_{n-1}^{\{v_1 \ldots v_{\Omega-1}\}}(\epsilon_N), \tag{2.24}
$$

we find

$$\mathrm{Res}_{\nu_{\Omega}=\epsilon_N} \det J^S = \det \tilde{J}^{\hat{N}},$$
(2.25)

with

$$\tilde{J}_{NN}^{\hat{N}} = 1$$

$$\tilde{J}_{Nj}^{\hat{N}} = 0 \qquad \forall \quad j \neq N$$

$$\tilde{J}_{ii}^{\hat{N}} = {}^S C_{ii}^0 - \frac{1}{\epsilon_i - \epsilon_N} + \Gamma_1^{\{\nu_1 \ldots \nu_{\Omega-1}\}}(\epsilon_i) = J_{ii}^{\hat{N}} \qquad \forall \quad i \neq 1 \neq N$$

$$\tilde{J}_{ij}^{\hat{N}} = {}^S C_{ij}^0 = J_{ij}^{\hat{N}} \qquad \forall \quad i \neq 1 \neq N \, , \, j \neq i$$

$$\tilde{J}_{1j}^{\hat{N}} = (2S)! \left( {}^S C_{1j}^{2S-1} \Gamma_{2S-1}^{\{\nu_1 \ldots \nu_{\Omega-1}\}}(\epsilon_1) \right.$$

$$+ \sum_{n=0}^{2S-2} \left[ \frac{{}^S C_{1j}^{n+1}}{\epsilon_N - \epsilon_1} + {}^S C_{1j}^n \right] \Gamma_n^{\{\nu_1 \ldots \nu_{\Omega-1}\}}(\epsilon_1) \right) = J_{1j}^{\hat{N}} \qquad \forall \quad j \neq 1$$

$$\tilde{J}_{11}^{\hat{N}} = (2S)! \left( {}^S C_{11}^{2S} \Gamma_{2S}^{\{\nu_1 \ldots \nu_{\Omega-1}\}}(\epsilon_1) \right.$$

$$+ \sum_{n=0}^{2S-1} \left[ \frac{{}^S C_{11}^{n+1}}{\epsilon_N - \epsilon_1} + {}^S C_{11}^n \right] \Gamma_n^{\{\nu_1 \ldots \nu_{\Omega-1}\}}(\epsilon_1) \right) = J_{11}^{\hat{N}},$$
(2.26)

where $J^{\hat{N}}$ is the $(N-1) \times (N-1)$ matrix which corresponds to the matrix one would obtain from (2.18) for a system made out of a spin $S$ and a collection of $N-2$ spins $\frac{1}{2}$ labelled from 2 to $N-1$. Since line $N$ is turned into $(0\ 0\ \ldots\ 0\ 1)$, the resulting determinant giving the residue is then the one of the $(N-1) \times (N-1)$ matrix $J^{\hat{N}}$. Indeed, using the notation ${}^{S;\hat{N}} C_{ij}^n$ for the coefficients appearing in $J^{\hat{N}}$, we do have :

$$
\begin{aligned}
{}^{S;\hat{N}}C_{ii}^0 &= \left[\frac{2S}{\epsilon_i-\epsilon_1} + \sum_{k\neq i\neq 1}^{N-1}\frac{1}{\epsilon_i-\epsilon_k}\right] \\
&= \left[\frac{2S}{\epsilon_i-\epsilon_1} + \sum_{k\neq i\neq 1}^{N}\frac{1}{\epsilon_i-\epsilon_k}\right] - \frac{1}{\epsilon_i-\epsilon_N} = {}^S C_{ii}^0 - \frac{1}{\epsilon_i-\epsilon_N} \quad \forall i \neq 1, N \qquad (2.27) \\
{}^{S;\hat{N}}C_{1j}^n &= \left[\sum_{E\in S_{\hat{N}}^{(2S-n)}}\frac{1}{\prod_{k=1}^{2S-n}(\epsilon_1-E_k)}\right] \\
&= \sum_{E\in S^{(2S-n)}}\frac{1}{\prod_{k=1}^{2S-n}(\epsilon_1-E_k)} - \frac{1}{(\epsilon_1-\epsilon_N)}\left(\sum_{E\in S^{(2S-n-1)}}\frac{1}{\prod_{k=1}^{2S-n-1}(\epsilon_1-E_k)}\right) \\
&= {}^S C_{1j}^n + \frac{1}{\epsilon_N-\epsilon_1}{}^S C_{1j}^{n+1}. \qquad (2.28)
\end{aligned}
$$

The sum over $S_{\hat{N}}^{(2S-n)}$ (which excludes $\epsilon_N$) has been rewritten as the sum over $S^{(2S-n)}$ (now including $\epsilon_N$) from which we remove every term which contains at least one instance of $\epsilon_N$, terms which are built from multiplying $\frac{1}{(\epsilon_1-\epsilon_N)}$ by the terms of cardinality $n-1$. The only exceptions to this last rule are for the coefficients ${}^{S;\hat{N}}C_{11}^{2S} = 1 = {}^S C_{11}^{2S}$ and ${}^{S;\hat{N}}C_{1j(\neq 1,N)}^{2S-1} = \frac{1}{\epsilon_j-\epsilon_1} = {}^S C_{1j(\neq 1,N)}^{2S-1}$ showing the complete equivalence of the determinants of $\tilde{J}^{\hat{N}}$ and $J^{\hat{N}}$.

Having shown that every residue at $\epsilon_1$ of the determinant of $J^S$ gives back the similar determinant of a matrix $J^{S-\frac{1}{2}}$ (multiplied by $2S$) and that residues at a different $\epsilon_j$ gives the determinant of the matrix $J^{\hat{j}}$ with spin $j$ removed, we know that to complete the proof we now simply need to show that the limit when every $\nu_i \to \infty$ of the proposed determinant, called $J_{ij}^{lim}$, is going to zero. Within the determinant, the different terms in $\Gamma_{n>0}(\epsilon_i)$ cancel in this limit, so that only the determinant of the matrix containing the constant coefficients remains:

$$
J_{ij}^{lim} = \begin{cases}
(2S)! \displaystyle\sum_{E\in S^{(2S)}}\frac{1}{\prod_{k=1}^{2S}(\epsilon_1-E_k)} & i = j = 1 \\[2ex]
-(2S)! \displaystyle\sum_{n=0}^{2S-1}\sum_{E\in S_j^{(n)}}\frac{2S-n}{(\epsilon_1-\epsilon_j)^{2S-n}}\frac{1}{\prod_{k=1}^{n}(\epsilon_1-E_k)} & i = 1 \neq j \\[2ex]
\dfrac{2S}{\epsilon_i-\epsilon_1} + \displaystyle\sum_{k\neq i\neq 1}^{N}\frac{1}{\epsilon_i-\epsilon_k} & i = j \neq 1 \\[2ex]
\dfrac{1}{\epsilon_j-\epsilon_i} & i \neq j \neq 1
\end{cases} . \qquad (2.29)
$$

By adding all the matrix elements $J_{i,(j\neq 1)}^{lim}$ of a given line to the first column, the determinant

remains unchanged while the elements of the first column become:

$$J_{i1}^{lim} = \begin{cases} \left( \displaystyle\sum_{E \in S^{(2S)}} \frac{(2S)!}{\prod_{k=1}^{2S}(\epsilon_1 - E_k)} - \sum_{j=2}^{N} \sum_{n=0}^{2S-1} \sum_{E \in S_j^{(n)}} \frac{2S-n}{(\epsilon_1 - \epsilon_j)^{2S-n}} \frac{(2S)!}{\prod_{k=1}^{n}(\epsilon_1 - E_k)} \right) & i = 1 \\[3mm] \frac{1-2S}{\epsilon_1 - \epsilon_i} & i \neq 1 \end{cases} \qquad (2.30)$$

We consider a given element of $\displaystyle\sum_{E \in S^{(2S)}} \frac{1}{\prod_{k=1}^{2S}(\epsilon_1 - E_k)}$ for which each factor of the type $\frac{1}{(\epsilon_1 - \epsilon_i)}$ appears with a given power between $0$ and $2S$ and can be written as $\displaystyle\prod_{i=2}^{N} \frac{1}{(\epsilon_1 - \epsilon_i)^{x_i}}$ with $0 \leq x_i \leq 2S$. In $\displaystyle\sum_{j=2}^{N} \sum_{n=0}^{2S-1} \sum_{E \in S_j^{(n)}} \frac{2S-n}{(\epsilon_1 - \epsilon_j)^{2S-n}} \frac{1}{\prod_{k=1}^{n}(\epsilon_1 - E_k)}$, $\displaystyle\prod_{i=2}^{N} \frac{1}{(\epsilon_1 - \epsilon_i)^{x_i}}$ appears $x_i$ times because of this factor: $\frac{2S-n}{(\epsilon_1 - \epsilon_j)^{2S-n}}$. By completing the sum over $j$ and knowing that $\displaystyle\sum_{i=2}^{N} x_i = 2S$, each of the $\displaystyle\prod_{i=2}^{N} \frac{1}{(\epsilon_1 - \epsilon_i)^{x_i}}$ appears $1 - 2S$ times in $J_{11}$. Therefore, all the matrix elements in the first column became :

$$J_{i1}^{lim} = \begin{cases} (2S)! \left( \displaystyle\sum_{E \in S^{(2S)}} \frac{1-2S}{\prod_{k=1}^{2S}(\epsilon_1 - E_k)} \right) & i = 1 \\[3mm] \frac{1-2S}{\epsilon_1 - \epsilon_i} & i \neq 1 \end{cases} , \qquad (2.31)$$

while the other columns have been left untouched. Comparing these new elements with the previous ones from equation (2.29):

$$J_{i1}^{lim} = \begin{cases} (2S)! \left( \displaystyle\sum_{E \in S^{(2S)}} \frac{1}{\prod_{k=1}^{2S}(\epsilon_1 - E_k)} \right) & i = 1 \\[3mm] \frac{1}{\epsilon_1 - \epsilon_i} & i \neq 1 \end{cases} , \qquad (2.32)$$

we are left with $\det J^{lim} = (1 - 2S) \det J^{lim}$. This unambiguously implies that $\det J^{lim} = 0$.

Provided the proposed expression is valid for a collection of $N$ (and $N-1$) spins $\frac{1}{2}$, we showed that $Z^{S=1}$ is then indeed given by $\det J^{S=1}$. Recursively we therefore proved the validity of $Z^{S=3/2} = \det J^{S=3/2}$ and so on, for an arbitrary value of $S$.

For $S = 1/2$, eq. (2.18) is given explicitly by:

$$
\begin{aligned}
J_{ii} &= \sum_{n=0}^{1} \left[ \sum_{E \in S^{(1-n)}} \frac{1}{\prod_{k=1}^{1-n}(\epsilon_i - E_k)} \right] \Gamma_n(\epsilon_i) \ \ \forall i \\
J_{ij} &= \sum_{n=0}^{1-1} \left[ \sum_{p=n}^{1-1} \sum_{E \in S_j^{(p-n)}} \frac{1-p}{(\epsilon_i - \epsilon_j)^{1-p}} \frac{1}{\prod_{k=1}^{p-n}(\epsilon_1 - E_k)} \right] \Gamma_n(\epsilon_1) \ \ \forall i \neq j \\
&= \frac{1}{(\epsilon_i - \epsilon_j)}
\end{aligned}
\tag{2.33}
$$

which is indeed equal to eq. (2.14), therefore completing the proof. This proof also completes the part of this present work on spin only models for which we have shown that the partition function could be written in a determinant expression only depending of the $\Lambda(\epsilon_i)$. In the next section we will now incorporate a bosonic mode interacting with our collection of spins-$\frac{1}{2}$.

## 2.2 Spin-boson models

While they simply form a different realisation of the same algebra, models containing a bosonic mode differ fundamentally by no longer being bounded from above and below, since they now support an arbitrary number of excitations $M \in \mathbb{N}_0$. These results have been published in [58].

In this section, such a generalisation is presented in a way which is as similar as it can be to the approach used for spins-1/2. It is first shown how to build an alternative hole-like Bethe ansatz for spin-boson models and, then, demonstrated how the domain wall boundary partition functions can be rewritten as eigenvalue-based determinants. The application of these two results to the calculation of various form factors is then presented in the last subsection.

### 2.2.1 Spin-boson realisations

In generalising the previous results to models which include a bosonic mode, we explicitly restrict ourselves to the particular realisation which combines a single bosonic degree of freedom and $N$ spins-1/2. It explicitly reads:

$$
S^+(u) = b^\dagger + \sum_{j=1}^{N} \frac{V}{u - \epsilon_j} S_j^+ \ , \ S^-(u) = b + \sum_{j=1}^{N} \frac{V}{u - \epsilon_j} S_j^- \ , \ S^z(u) = \frac{\omega - u}{2V} - \sum_{j=1}^{N} \frac{V}{u - \epsilon_j} S_j^z, \tag{2.34}
$$

with $b^\dagger$, $b$ obeying canonical bosonic commutation rules. The conserved charges, found by looking at the residues of $S^2(u)$, are then given by [59]:

$$R_i = (\epsilon_i - \omega) S_i^z + V \left( b^\dagger S_i^- + b S_i^+ \right) + \sum_{j \neq i}^{N} \frac{2V^2}{\epsilon_i - \epsilon_j} \vec{S}_i \cdot \vec{S}_j, \tag{2.35}$$

in terms of which, the full generating function is given by

$$S^2(u) = \sum_{i=1}^{N} \frac{R_i}{u - \epsilon_i} + \left[ b^\dagger b + \sum_{i=1}^{N} S_i^z \right] + \frac{1}{2} + \left( \frac{\omega - u}{2V} \right)^2 + \frac{3}{4} \sum_{i=1}^{N} \frac{V^2}{(u - \epsilon_i)^2}, \tag{2.36}$$

where the $\frac{3}{4}$ factors are simply the Casimir invariant of each local spin-$\frac{1}{2}$.

A typical application of the QISM on this system [52] would be carried out by using the particle-like construction creating excitations above a pseudo-vacuum defined by a fully down-polarised spin sector and an empty bosonic mode. It leads to eigenstates of the form:

$$|\lambda_1 \dots \lambda_M\rangle = \prod_{i=1}^{M} S^+(\lambda_i) |0; \downarrow, \dots \downarrow\rangle. \tag{2.37}$$

This vacuum $|0; \downarrow, \dots \downarrow\rangle$ is indeed an eigenstate of both $S^2(u)$ and $S^z(u)$ and is annihilated by any $S^-(u)$. Thus, it allows the direct use of the construction described in section 1.1. The resulting ABA shows that the previous state becomes an eigenstate of $S^2(u)$ whenever $\{\lambda_1 \dots \lambda_M\}$ is a solution of the algebraic system of Bethe equations:

$$\frac{\omega - \lambda_i}{2V^2} + \frac{1}{2} \sum_{k=1}^{N} \frac{1}{\lambda_i - \epsilon_k} = \sum_{j \neq i}^{M} \frac{1}{\lambda_i - \lambda_j}. \tag{2.38}$$

The eigenvalues of the conserved charges (2.35) are then respectively given by:

$$r_i = \frac{V^2}{2} \left( \sum_{j \neq i}^{N} \frac{1}{\epsilon_i - \epsilon_j} \right) - \frac{\epsilon_i - \omega}{2} - V^2 \sum_{j=1}^{M} \frac{1}{\epsilon_i - \lambda_j}. \tag{2.39}$$

Since they have a fixed number $M$ of particle excitations these states are not only eigenstates of every $R_i$ but are, as well, eigenstates of the "number" operator $b^\dagger b + \sum_{i=1}^{N} S_i^z$ with eigenvalue $M - N/2$. According to (2.36) they are therefore eigenstates of $S^2(u)$, $u \neq \epsilon_j \ \forall u \in \mathbb{C}$ and $\forall \ j$ with eigenvalue $\sum_{i=1}^{N} \frac{r_i}{u - \epsilon_i} + M - \frac{N}{2} + \frac{1}{2} + \left( \frac{\omega - u}{2V} \right)^2 + \frac{3}{4} \sum_{i=1}^{N} \frac{V^2}{(u - \epsilon_i)^2}$.

This realisation allows an equivalent description in terms of eigenvalue-based quadratic Bethe equations [49] given, this time, by:

$$[\Lambda(\epsilon_i)]^2 = \sum_{j \neq i}^{N} \frac{\Lambda(\epsilon_i) - \Lambda(\epsilon_j)}{\epsilon_i - \epsilon_j} - \frac{\epsilon_i - \omega}{V^2} \Lambda(\epsilon_i) + \frac{M}{V^2}, \tag{2.40}$$

with $\Lambda(\epsilon_i) = \sum_{j=1}^{M} \frac{1}{\epsilon_i - \lambda_j}$ still.

Central to the constructions presented before for spin-only models is the inherent symmetry between maximal and minimal weight states which allowed one to define an equivalent hole-like Bethe ansatz. However, for these spin-boson models, the unboundedness of the bosonic part gives rise to a problem in defining the alternative hole-pseudovacuum. Still, simple considerations about the total number of quasi-particles $M$, which is a conserved quantity in XXX (and XXZ) models, allow one to suppose that a possible hole-vacuum state could be chosen as $|M; \uparrow \uparrow \dots \uparrow\rangle$. Indeed, acting on this state with $N$ lowering operators $\prod_{i=1}^{N} S^-(\mu_i) |M; \uparrow \uparrow \dots \uparrow\rangle$ produces a state which spans the same subspace of the full Hilbert space as $\prod_{i=1}^{M} S^+(\lambda_i) |0; \downarrow \downarrow \dots \downarrow\rangle$. Both states are indeed linear superposition of tensor-product states containing any number of bosonic excitations $N_b \in [0, M]$ and any subset of $M - N_b$ spins (picked out of the $N$ available ones) pointing up. However, it remains to be shown that $\prod_{i=1}^{N} S^-(\mu_i) |M; \uparrow \uparrow \dots \uparrow\rangle$ can provide an alternative representation of the eigenstates of the system.

Working with a typical QISM construction for these models, one would explicitly calculate $S^2(u) \left[ \prod_{i=1}^{N} S^-(\mu_i) \right] |M; \uparrow \uparrow \dots \uparrow\rangle = \left[ \prod_{i=1}^{N} S^-(\mu_i) \right] S^2(u) |M; \uparrow \uparrow \dots \uparrow\rangle + [S^2(u), \prod_{i=1}^{N} S^-(\mu_i)] |M; \uparrow \uparrow \dots \uparrow\rangle$ and look for the set of equations for $\{\mu_1 \dots \mu_N\}$ whose solutions reduce to $S^2(u) \left[ \prod_{i=1}^{N} S^-(\mu_i) \right] |M; \uparrow \uparrow \dots \uparrow\rangle = E(u) \left[ \prod_{i=1}^{N} S^-(\mu_i) \right] |M; \uparrow \uparrow \dots \uparrow\rangle$. By being an eigenstate of $S^2(u)$, a proper pseudo-vacuum would make the term $\left[ \prod_{i=1}^{N} S^-(\mu_i) \right] S^2(u) |M; \uparrow \uparrow \dots \uparrow\rangle$ trivially proportional to the original ansatz $\left[ \prod_{i=1}^{N} S^-(\mu_i) \right] |M; \uparrow \uparrow \dots \uparrow\rangle$. However, in the case at hand here, this potential "hole-

vacuum" is not an eigenstate of $S^2(u)$:

$$
\begin{aligned}
S^2(u)|M;\uparrow\ldots\uparrow\rangle &= \left[S_z^2(u) + \frac{1}{2}S^+(u)S^-(u) + \frac{1}{2}S^-(u)S^+(u)\right]|M;\uparrow\ldots\uparrow\rangle \\
&= \left[S_z^2(u) + \frac{1}{2}\left[S^+(u),S^-(u)\right] + S^-(u)S^+(u)\right]|M;\uparrow\ldots\uparrow\rangle \\
&= \ell(u)|M;\uparrow\ldots\uparrow\rangle + \sqrt{M+1}\,S^-(u)|M+1;\uparrow\ldots\uparrow\rangle .
\end{aligned}
$$

$$(2.41)$$

since $|M;\uparrow\ldots\uparrow\rangle$ is an eigenstate of $S_z^2(u) + \frac{1}{2}\left[S^+(u),S^-(u)\right]$ whose eigenvalue we write $\ell(u)$. The second term can be written in that way since $S^+(u)$ only affects the bosonic part because every spin in the vacuum state is already pointing up. The fact that we do not have here a "proper" hole-vacuum turns this reversed problem into one which could be approached using Sklyanin's separation of variables [60] and the resulting Functional Bethe Ansatz (FBA) [61]. We show however that, although it is slightly more complex, one can still follow closely the QISM approach to formulate an alternative algebraic Bethe ansatz.

The standard application of the generating function $S^2(u)$ on the hole-like ansatz $|\mu\rangle \equiv \prod_{i=1}^{N} S^-(\mu_i)|M;\uparrow\ldots\uparrow\rangle$ would result in the generic form:

$$
\begin{aligned}
S^2(u) &= \tilde{E}(u,\{\mu_1\ldots\mu_n\})|\mu\rangle + \sum_{k=1}^{N} F_k(u,\{\mu_1\ldots\mu_n\})|\mu\rangle_{\mu_k\to u} + \\
&\quad \sqrt{M+1}\left(\prod_{i=1}^{N} S^-(\mu_i)\right)S^-(u)|M+1;\uparrow\ldots\uparrow\rangle .
\end{aligned}
$$

$$(2.42)$$

It turns out, and that is easily verified numerically for small systems, that the last two terms one might naively consider to be the unwanted terms, cannot be cancelled out for arbitrary $u \in \mathbb{C}$. When used in conjunction with a proper pseudo-vacuum, the QISM does lead to a simple structure where both the correct eigenvalue and the unwanted terms naturally appear. Here, due the "faulty" vacuum in use, $\tilde{E}(u,\{\mu_1\ldots\mu_n\})$ is not the actual eigenvalue of $S^2(u)$. The unwanted terms which can be cancelled must contain a $u$-dependent piece $\Delta E(u,\{\mu_1\ldots\mu_n\})|\mu\rangle$ taken from the term $\tilde{E}(u,\{\mu_1\ldots\mu_n\})|\mu\rangle$ and the actual eigenvalue then becomes $\tilde{E}(u,\{\mu_1\ldots\mu_n\}) - \Delta E(u,\{\mu_1\ldots\mu_n\})$. Having no a priori knowledge of the function $\Delta E(u,\{\mu_1\ldots\mu_n\})$, one should use for a given $u$ in order to build the correct unwanted term: $\Delta E(u,\{\mu_1\ldots\mu_n\})|\mu\rangle + \sum_{k=1}^{N} F_k(u,\{\mu_1\ldots\mu_n\})|\mu\rangle_{\mu_k\to u} + \sqrt{M+1}\left(\prod_{i=1}^{N} S^-(\mu_i)\right)S^-(u)|M+1;\uparrow\ldots\uparrow\rangle$. Using the previous expression, the traditional approach used in section 1.3 fails to simply provide

the desired solution.

However, since, according to eq. (2.36), finding the common eigenstates of $S^2(u) \ \forall \ u \in \mathbb{C}$ is formally equivalent to finding the common eigenstates of the $N$ conserved charges $R_k$, we choose to work directly with the latter. It remains simple to then go back to the spectrum of $S^2(u)$ since its whole analytic structure is known. We therefore simply look at the residues (at $u \to \epsilon_k$) of the $S^2(u)$ operator's application on $\prod_{i=1}^{N} S^-(\mu_i) |M; \uparrow \dots \uparrow\rangle$ to write:

$$
\begin{aligned}
R_k |\mu\rangle &= \lim_{u \to \epsilon_k} (u - \epsilon_k) S^2(u) |\mu\rangle \\
&= V^2 \left[ \frac{1}{2} \sum_{j \neq k} \frac{1}{\epsilon_k - \epsilon_j} - \frac{\omega - \epsilon_k}{2V^2} - \sum_{j=1}^{N} \frac{1}{\epsilon_k - \mu_j} \right] |\mu\rangle \\
&\quad + V^2 \left[ \sum_{j=1}^{N} \frac{B_j}{\epsilon_k - \mu_j} \left( \prod_{i \neq j}^{N} S^-(\mu_i) \right) \right] S_k^- |M; \uparrow \dots \uparrow\rangle \\
&\quad + V\sqrt{M+1} \left( \prod_{i=1}^{N} S^-(\mu_i) \right) S_k^- |M+1; \uparrow \dots \uparrow\rangle
\end{aligned}
\tag{2.43}
$$

with

$$
B_j = \left( -\frac{\omega - \mu_j}{V} + \sum_{i=1}^{N} \frac{V}{\mu_j - \epsilon_i} + \sum_{i \neq j} \frac{2V}{(\mu_i - \mu_j)} \right).
\tag{2.44}
$$

Working directly with the conserved charges, $R_k$ now results in a form which provides clear separation of the wanted and unwanted terms. Indeed, the first term in (2.43) will ultimately become $r_k |\mu_1 \dots \mu_N\rangle$ while the two last ones are the actual unwanted terms whose global cancellation will turn the generic ansatz into a proper eigenstate of the ensemble of $R_k$ (and therefore of $S^2(u)$) with eigenvalues $r_k$.

The Gaudin lowering operator $S^-(u)$, given in (2.34), can act either on the bosonic or on the spin subspace. Assuming for now that the number of excitations is $M \geq N-1$, one of the contributions to the unwanted terms will come from the joint action of the bosonic part of every $S^-(\mu_i)$. This reduces both kets contributing to the unwanted terms down to $S_k^- |M-(N-1); \uparrow \dots \uparrow\rangle$. Cancelling the total coefficient in front of this particular state:

$$
V^2 \left[ \sum_{j=1}^{N} \frac{B_j}{\epsilon_k - \mu_j} \frac{\sqrt{M!}}{\sqrt{(M+1-N)!}} \right] + V\sqrt{M+1} \frac{\sqrt{(M+1)!}}{\sqrt{(M+1-N)!}}
\tag{2.45}
$$

is achieved when:

$$\sum_{j=1}^{N} \frac{B_j}{\epsilon_k - \mu_j} + \frac{M+1}{V} = 0. \tag{2.46}$$

To form an eigenstate, the cancellation would need to occur for all possible $k \in [1, N]$ which results in a linear system of equations:

$$\begin{pmatrix} 1/(\epsilon_1 - \mu_1) & 1/(\epsilon_1 - \mu_2) & \dots & 1/(\epsilon_1 - \mu_N) \\ \vdots & \vdots & \dots & \vdots \\ 1/(\epsilon_N - \mu_1) & 1/(\epsilon_N - \mu_2) & \dots & 1/(\epsilon_N - \mu_N) \end{pmatrix} \begin{pmatrix} B_1 \\ \vdots \\ B_N \end{pmatrix} = \begin{pmatrix} -\frac{M+1}{V} \\ \vdots \\ -\frac{M+1}{V} \end{pmatrix}, \tag{2.47}$$

which is easily solved by recognising the Cauchy matrix. Indeed, its well-known inverse leads to the solution:

$$B_j \equiv \frac{-\omega + \mu_j}{V} + \sum_{i=1}^{N} \frac{V}{\mu_j - \epsilon_i} + \sum_{i \neq j}^{N} \frac{2V}{\mu_i - \mu_j} = -\frac{(M+1)}{V} \frac{\prod_{k=1}^{N}(\epsilon_k - \mu_j)}{\prod_{a \neq j}^{N}(\mu_a - \mu_j)}. \tag{2.48}$$

Of course this, in principle, simply cancels one subset of coefficients. One still needs to prove that solutions to these equations will cancel every coefficient in the unwanted terms.

A generic coefficient results from having the product of Gaudin lowering operators acting on both the bosonic and the spin part. Looking at a given ket, for which the subset of $r + 1 = N - M + m$ spins labelled $\{i_1 \dots i_r, k\}$ points down (the corresponding number of bosons remaining being $m$), the coefficient in front of this basis vector $\left| m; \downarrow_{\{i_1 \dots i_r, k\}} \right\rangle$ is given by

$$C^r_{\{i_1 \dots i_r, k\}} \quad = \quad \frac{\sqrt{M!}}{\sqrt{m!}} V^{r+2} \left( \sum_{j=1}^{N} \frac{B_j}{\epsilon_k - \mu_j} \left[ \sum_{A_{\hat{j}} \in S^r_{\hat{j}}} \frac{1}{\prod_{k=1}^{r}(a_k - \epsilon_{i_k})} \right] \right.$$
$$\left. + \frac{(M+1)}{V} \left[ \sum_{A \in S^r} \frac{1}{\prod_{k=1}^{r}(\alpha_k - \epsilon_{i_k})} \right] \right) \tag{2.49}$$

where $S^r_{\hat{j}}$ is the set of all $r$-tuples built out of $r$ non-repeated elements of $\{\mu_1, \dots \mu_{j-1}, \mu_{j+1} \dots \mu_N\}$ and $S^r$ is the similar set of all $r$-tuples one can build out of the elements of $\{\mu_1, \dots \mu_N\}$. The n-th element of $A_{\hat{j}} = (a_1, \dots a_r)$ is then any one of the available parameters $\mu$ (excluding $\mu_j$) while the n-th element of $A = (\alpha_1, \dots \alpha_r)$ can be any one of the $N$ parameters $\mu$ (this time including $\mu_j$).

To turn both brackets into a factor common to every term of the sum over $j$, the first one can be rewritten by extending the sum over elements of $S^r_{\hat{j}}$ to one over every element of $S^r$. One then needs to subtract the newly introduced contributions: those which belong to the relative complement $S^r \setminus S^r_{\hat{j}}$, i.e. $r$-tuples which do contain $\mu_j$. The previous expression then becomes

$$C^r_{\{i_1 \dots i_r, k\}} \quad = \quad \frac{V^{r+2}\sqrt{M!}}{\sqrt{m!}} \left( \left( \sum_{j=1}^{N} \frac{B_j}{\epsilon_k - \mu_j} + \frac{(M+1)}{V} \right) \left[ \sum_{A \in S^r} \frac{1}{\prod_{k=1}^{r}(a_k - \epsilon_{i_k})} \right] \right.$$
$$\left. - \sum_{j=1}^{N} \frac{B_j}{\epsilon_k - \mu_j} \left[ \sum_{A \in S^r \setminus S^r_{\hat{j}}} \frac{1}{\prod_{k=1}^{r}(a_k - \epsilon_{i_k})} \right] \right). \tag{2.50}$$

The first term is cancelled by the solutions (2.48) discussed previously, i.e.: $B_j = -\frac{(M+1)}{V} \frac{\prod_{k=1}^{N}(\epsilon_k - \mu_j)}{\prod_{a \neq j}^{N}(\mu_a - \mu_j)}$ and we are left with:

$$C^r_{\{i_1 \dots i_r, k\}} \propto \sum_{j=1}^{N} \frac{B_j}{\epsilon_k - \mu_j} \sum_{A \in S^r \setminus S^r_{\hat{j}}} \frac{1}{\prod_{k=1}^{r}(a_k - \epsilon_{i_k})}. \tag{2.51}$$

Since every element $A$ in the sum now contains, with certainty, a term $a_{k'} = \mu_j$ (with $k'$ denoting the position where $\mu_j$ appears in $A$), we can rewrite the sum as:

$$C^r_{\{i_1...i_r,k\}} \propto \sum_{k'=1}^{r} \sum_{j=1}^{N} \frac{B_j}{(\epsilon_k - \mu_j)(\mu_j - \epsilon_{k'})} \sum_{A \in S^{r-1}_{\hat{j}}} \frac{1}{\prod_{k=1}^{r-1}(a_k - \epsilon_{i_k})}, \tag{2.52}$$

where $\epsilon_{i_k}$ is now understood as the elements of $(\epsilon_{i_1} \ldots \epsilon_{i_{k'-1}} \epsilon_{i_{k'+1}} \ldots \epsilon_{i_r})$ therefore excluding $\epsilon_{i_{k'}}$.

One can keep the process going by including back $\mu_j$ in the last sum to now make it go over every element of $S^{r-1}$ while removing $\sum_{A \in S^{r-1} \setminus S^{r-1}_{\hat{j}}}$:

$$
\begin{aligned}
C^r_{\{i_1...i_r,k\}} \quad \propto \quad & \sum_{k'=1}^{r} \sum_{j=1}^{N} \frac{B_j}{(\epsilon_k - \mu_j)(\mu_j - \epsilon_{k'})} \sum_{A \in S^{r-1}} \frac{1}{\prod_{k=1}^{r-1}(a_k - \epsilon_{i_k})} \\
& - \sum_{k'=1}^{r} \sum_{j=1}^{N} \frac{B_j}{(\epsilon_k - \mu_j)(\mu_j - \epsilon_{k'})} \sum_{A \in S^{r-1} \setminus S^{r-1}_{\hat{j}}} \frac{1}{\prod_{k=1}^{r-1}(a_k - \epsilon_{i_k})}, \\
= \quad & \sum_{k'=1}^{r} K_{k'} \left[ \sum_{j=1}^{N} \frac{B_j}{(\epsilon_k - \mu_j)(\mu_j - \epsilon_{k'})} \right] \\
& - \sum_{k'' \neq k'} \sum_{k'=1}^{r} \sum_{j=1}^{N} \frac{B_j}{(\epsilon_k - \mu_j)(\mu_j - \epsilon_{k'})(\mu_j - \epsilon_{k''})} \sum_{A \in S^{r-2}_{\hat{j}}} \frac{1}{\prod_{k=1}^{r-2}(a_k - \epsilon_{i_k})}
\end{aligned}
\tag{2.53}
$$

where the set of $\epsilon_{i_k}$ now excludes both $\epsilon_{i_{k'}}$ and $\epsilon_{i_{k''}}$, and we defined the constant $K_{k'} = \sum_{A \in S^{r-1}} \frac{1}{\prod_{k=1}^{r-1}(a_k - \epsilon_{i_k})}$. Doing this iteratively until the $r$ spins have their $\epsilon_{i_k}$ coupled with $\mu_j$, one easily sees that the whole expression becomes a sum of terms of the form:

$$\sum_{j=1}^{N} \frac{B_j}{\prod_{k=1}^{n}(\epsilon_{i_k} - \mu_j)}, \tag{2.54}$$

with $n \geq 2$, which we can show are all identically zero. Indeed, replacing $B_j$ by the solution mentioned before (2.48), we find:

$$\sum_{j=1}^{N} \frac{B_j}{\prod_{k=1}^{n}(\epsilon_{i_k} - \mu_j)} = -\frac{(M+1)}{V} \sum_{j=1}^{N} \frac{\prod_{k=1}^{N}(\epsilon_k - \mu_j)}{\prod_{a \neq j}^{N}(\mu_a - \mu_j) \prod_{k=1}^{n}(\epsilon_{i_k} - \mu_j)} \tag{2.55}$$

and choosing one $\epsilon_{i_{k'}}$ to play a particular role it can also be written as:

$$\sum_{j=1}^{N} \frac{B_j}{\prod_{k=1}^{n}(\epsilon_{i_k} - \mu_j)} = -\frac{(M+1)}{V} \sum_{j=1}^{N} \frac{\frac{\prod_{k=1}^{N}(\epsilon_k - \mu_j)}{\prod_{k \neq k'}^{n}(\epsilon_{i_k} - \mu_j)}}{\epsilon_{i_{k'}} - \mu_j} \frac{1}{\prod_{a \neq j}^{N}(\mu_a - \mu_j)}. \tag{2.56}$$

Considering that a generic polynomial $L(z)$ of maximal order $N-1$ can always be expanded on the basis of Lagrange polynomials (using the $N$ points $\{\mu_1 \dots \mu_N\}$) as:

$$L(z) = \ell(z) \sum_{j=1}^{N} \frac{L(\mu_j)}{z - \mu_j} \frac{1}{\prod_{k \neq j}(\mu_j - \mu_k)}, \tag{2.57}$$

with $\ell(z) = \prod_{k=1}^{N}(z - \mu_k)$ and the $\mu_i$ the zeros of the polynomial $L$, we define the $(N - n + 1)$-order polynomial $A(z) = \frac{\prod_{k=1}^{N}(\epsilon_k - z)}{\prod_{k \neq k'}^{n}(\epsilon_{i_k} - z)}$. Its order will always be low enough (for $n \geq 2$) for it to have an exact expansion in the $N$-points Lagrange basis: $\frac{A(z)}{\ell(z)} = \sum_{j=1}^{N} \frac{A(\mu_j)}{z - \mu_j} \frac{1}{\prod_{k \neq j}(\mu_j - \mu_k)}$. We can therefore recognise in (2.56) the expression for $\frac{A(z)}{\ell(z)}$ at $z = \epsilon_{i_{k'}}$. This allows us to evaluate the preceding sum as:

$$\sum_{j=1}^{N} \frac{B_j}{\prod_{k=1}^{n}(\epsilon_{i_k} - \mu_j)} \propto \sum_{j=1}^{N} \frac{A(\mu_j)}{\epsilon_{i_{k'}} - \mu_j} \frac{1}{\prod_{k \neq j}(\mu_j - \mu_k)} = \frac{A(\epsilon_{i_{k'}})}{\ell(\epsilon_{i_{k'}})} = 0. \tag{2.58}$$

Indeed, the polynomial $A(z)$ has zeros at every $\epsilon_k$ except at the $n-1$ elements of the set $\{\epsilon_{i_1}, \dots \epsilon_{i_{k'-1}}, \epsilon_{i_{k'+1}} \dots \epsilon_{i_n}\}$. Therefore $z = \epsilon_{i_{k'}}$ remains a zero of the polynomial $A(z)$ proving that the sum (2.56) systematically cancels when $\{\mu_1 \dots \mu_N\}$ is a solution of eqs. (2.48).

Thus, it has been shown that, for a system containing $N$ spins-1/2 and a single bosonic mode, a state built as:

$$\left| \{\mu_1 \ldots \mu_N\} \right\rangle = \prod_{i=1}^{N} \mathrm{S}^-(\mu_i) \left| M; \uparrow \ldots \uparrow \right\rangle \tag{2.59}$$

becomes an eigenstate of the $N$ conserved charges $R_k$ defined in (2.35) with corresponding eigenvalues (see eq. (2.43)):

$$r_k = V^2 \left[ \frac{1}{2} \sum_{j \neq k} \frac{1}{\epsilon_k - \epsilon_j} - \frac{\omega - \epsilon_k}{2V^2} - \sum_{j=1}^{N} \frac{1}{\epsilon_k - \mu_j} \right], \tag{2.60}$$

whenever $\{\mu_1 \ldots \mu_N\}$ is solution of the $N$ algebraic Bethe equations (2.48):

$$\frac{-\omega + \mu_j}{V} + \sum_{i=1}^{N} \frac{V}{\mu_j - \epsilon_i} + \sum_{i \neq j}^{N} \frac{2V}{\mu_i - \mu_j} = -\frac{(M+1)}{V} \frac{\prod_{k=1}^{N}(\epsilon_k - \mu_j)}{\prod_{a \neq j}^{N}(\mu_a - \mu_j)}. \tag{2.61}$$

For any of these states, the corresponding eigenvalue of the full generating function $\mathrm{S}^2(u)$ is then simply obtained by reconstructing the appropriate linear combination given in (2.36) leading to:

$$\mathrm{S}^2(u) \left| \{\mu_1 \ldots \mu_N\} \right\rangle =$$
$$\left[ \sum_{k=1}^{N} \frac{r_k}{u - \epsilon_k} + M - \frac{N}{2} + \frac{1}{2} + \left( \frac{\omega - u}{2V} \right)^2 + \frac{3}{4} \sum_{k=1}^{N} \frac{V^2}{(u - \epsilon_k)^2} \right] \left| \{\mu_1 \ldots \mu_N\} \right\rangle, \tag{2.62}$$

with the eigenvalues $r_k$ given in eq. (2.60).

Having shown that one can indeed build a valid hole-like representation of eigenstates, we now simply need to find the correspondence between both representations of a given eigenstate.

As for spin-only models, this can be done by equating both sets of eigenvalues $r_k$, respectively found in eqs. (2.39) and (2.60):

$$-\frac{\omega - \epsilon_k}{2} - V^2 \sum_{j=1}^{N} \frac{1}{\epsilon_k - \mu_j} = -\frac{\epsilon_k - \omega}{2} - V^2 \sum_{j=1}^{M} \frac{1}{\epsilon_k - \lambda_j},$$
$$\Lambda^\lambda(\epsilon_k) = \Lambda^\mu(\epsilon_k) + \frac{\omega - \epsilon_k}{V^2}, \tag{2.63}$$

giving us the explicit way to transform one representation into the other. A direct substitution of this transformation in the quadratic Bethe equations (2.40) consequently gives us the equivalent equations for the hole-like representation:

$$\left[\Lambda^\mu(\epsilon_i)\right]^2 = \sum_{j \neq i} \frac{\Lambda^\mu(\epsilon_i) - \Lambda^\mu(\epsilon_j)}{\epsilon_i - \epsilon_j} + \frac{\epsilon_i - \omega}{V^2} \Lambda^\mu(\epsilon_i) + \frac{M - N + 1}{V^2}. \tag{2.64}$$

Although our main interest for finding such a representation was the construction of eigenvalue-based determinant expressions for scalar products and form factors, even by itself, the hole-representation can be useful. Indeed, such a parametrisation of the eigenstates always involves exactly $N$ rapidities $\mu_i$ which have to be solution of a system of $N$ equations. The traditional particle-representation is, on the other hand, defined by $M$ parameters $\lambda_i$, a number which can grow arbitrarily large due to the unboundedness of the bosonic operators. This alternative representation therefore still allows us to express any eigenstate containing $M > N$ particle-like excitations in a more compact form systematically writeable in terms of only $N$ complex parameters.

### 2.2.2 Partition function

As was possible for spin-only models, we want to be able to access physical quantities in terms of simple expressions involving exclusively the $\Lambda(\epsilon_i)$ variables. In this section we will start by deriving a determinant expression for domain wall boundary partition functions from which expressions for the scalar products and form factors will, in the end, be derived.

Therefore, we want to prove that the scalar product of a generic Bethe-like state (2.37) with an arbitrary common eigenstate of $b^\dagger b$ and the ensemble of $S_i^z$:

$$\left|M;\uparrow_{\{i_1\dots i_m\}}\right\rangle \equiv (b^+)^M \prod_{j=1}^{m} S_{i_j}^+ |0,\downarrow\dots\downarrow\rangle \tag{2.65}$$

with $M, m \in \mathbb{N}$ and $m \leq N$, is writable as the determinant of an $m \times m$ matrix:

$$\langle M;\uparrow_{\{i_1\dots i_m\}} |\lambda_1\dots\lambda_{M+m}\rangle = \sqrt{M!}V^m \mathrm{Det}J$$

$$J_{ab} = \begin{cases} \displaystyle\sum_{c=1(\neq a)}^{m} \frac{1}{\epsilon_{i_a} - \epsilon_{i_c}} - \Lambda(\epsilon_{i_a}) & a = b \\ \dfrac{1}{\epsilon_{i_a}-\epsilon_{i_b}} & a \neq b \end{cases}, \tag{2.66}$$

which differs significantly from the more traditional Izergin determinant [62] by using the variables $\Lambda(\epsilon_{i_a})$ which are explicitly symmetric constructions in terms of the rapidities $\{\lambda_1\dots\lambda_M\}$.

In order to show this, one can start from the explicit construction of the state $|\lambda_1\dots\lambda_{M+m}\rangle$ (eq. (2.37)), which leads to the formal expression:

$$\langle M;\uparrow_{\{i_1\dots i_m\}} |\lambda_1\dots\lambda_{M+m}\rangle = \sqrt{M!}\, V^m \sum_{\{P_k\}}\sum_{\{P\}} \prod_{i\neq\{k_1\dots k_M\}}^{M+m} \frac{1}{\lambda_i - \epsilon_{P_i}}. \tag{2.67}$$

Here $\{P\}$ is the ensemble of possible permutations of the indices $\{i_1\dots i_{M+m}\}$ and $P_i$ denotes the $i^{\text{th}}$ element of the given permutation. In the same way we define $\{P_k\}$ as the ensemble of possible subsets $\{k_1\dots k_M\}$ one can build out of $\{1\dots M+m\}$; this subset labels the rapidities used to create the $M$ bosons. In other words, we create the state $\left|M;\uparrow_{\{i_1\dots i_m\}}\right\rangle$ starting from the particle vacuum $|0;\downarrow\dots\downarrow\rangle$ by using any subset of $M$ rapidities to create bosons. The remaining unused rapidities can be associated in any possible bijection with $\{i_1\dots i_m\}$ so that each rapidity is used individually to excite any one of the local spins we need to flip up.

By isolating in (2.67) the terms which depend on $\lambda_{M+m}$, one finds that the overlaps obey the simple recursion relation:

$$\langle M; \uparrow_{\{i_1 \dots i_m\}} | \lambda_1 \dots \lambda_{M+m} \rangle = \langle M; \uparrow_{\{i_1 \dots i_m\}} | b^\dagger | \lambda_1 \dots \lambda_{M+m-1} \rangle$$

$$+ \sum_{j=1}^{m} \frac{V}{\lambda_{M+m} - \epsilon_{i_j}} \langle M; \uparrow_{\{i_1 \dots \hat{i}_j \dots i_m\}} | \lambda_1 \dots \lambda_{M+m-1} \rangle,$$

$$(2.68)$$

where $\left| M; \uparrow_{\{i_1 \dots \hat{i}_j \dots i_m\}} \right\rangle$ is the state with $M + m - 1$ excitations, for which $\epsilon_{i_j}$ has been removed from the ensemble $\{i_1 \dots i_m\}$ and therefore points down.

We now want to show that the proposed determinant representation (2.66) obeys the same recursion relation. Since they are obviously rational functions of every $\lambda_i$ variable, it is then sufficient to show that, when written as determinants, the left and right hand sides of the recursion (2.68) have the same poles (at $\lambda_{M+m} = \epsilon_{i_j}$), the same residues $\langle M; \uparrow_{\{i_1 \dots \hat{i}_j \dots i_m\}} | \lambda_1 \dots \lambda_{M+m-1} \rangle$ at these poles and the same limit when $\lambda_{M+m} \to \infty$.

The determinant in (2.66) clearly only has single poles at $\lambda_{M+m} = \epsilon_{i_j}$ which come only from the diagonal element $J_{jj}$ since only it contains, through $-\Lambda(\epsilon_{i_j})$, the term $\frac{1}{\lambda_{M+m} - \epsilon_{i_j}}$. The residue is then simply given by the determinant of the minor obtained after removing line and column $j$ and taking the $\lambda_{M+m} \to \epsilon_{i_j}$ limit:

$$\lim_{\lambda_{M+m} \to \epsilon_{i_j}} (\lambda_{M+m} - \epsilon_{i_j}) \sqrt{M!} \, V^m \mathrm{Det} J = \sqrt{M!} \, V^m \mathrm{Det} J^{\hat{j}} \qquad (2.69)$$

with

$$J^{\hat{j}}_{a,b} = \begin{cases} \displaystyle\sum_{c=1 (\neq a)}^{m} \frac{1}{\epsilon_{i_a} - \epsilon_{i_c}} - \sum_{k=1}^{M+m-1} \frac{1}{\epsilon_{i_a} - \lambda_k} - \frac{1}{\epsilon_{i_a} - \epsilon_{i_j}} & a = b \; (a, b \neq j) \\[2ex] \frac{1}{\epsilon_{i_a} - \epsilon_{i_b}} & a \neq b \; (a, b \neq j) \end{cases} . \qquad (2.70)$$

The diagonal elements of this matrix evidently reduce to $\displaystyle\sum_{c \neq a \; (a, c \neq j)}^{m} \frac{1}{\epsilon_{i_a} - \epsilon_{i_c}} - \sum_{\alpha=1}^{M+m-1} \frac{1}{\epsilon_{i_a} - \lambda_\alpha}$ and therefore the limit (2.69) does indeed correspond to the determinant representation (2.66) of $V \langle M; \uparrow_{\{i_1 \dots \hat{i}_j \dots i_m\}} | \lambda_1 \dots \lambda_{M+m-1} \rangle$, as it should in order to obey the recursion relation (2.68). Since every rapidity $\lambda_j$ plays an identical role, choosing $\lambda_{M+m}$ enables us , without loss of generality, to state that the determinant representations have poles and residues at those poles

which are indeed the same on both sides of the recursive equation (2.68).

Moreover, the $\lambda_{M+m} \to \infty$ limit of the determinant (2.66) is easily found since the corresponding terms $\frac{1}{\lambda_{M+m}-\epsilon_{i_a}}$ in every $\Lambda(\epsilon_{i_a})$ then simply go to zero. Therefore, $\lim_{\lambda_{M+m}\to\infty} \langle M; \uparrow_{\{i_1\ldots i_m\}} | \lambda_1\ldots\lambda_{M+m}\rangle$ reduces to the determinant expression (2.66) one would find for $\sqrt{M}\langle M-1; \uparrow_{\{i_1\ldots i_m\}} | \lambda_1\ldots\lambda_{M+m-1}\rangle$. Acting on the bra with the bosonic operator, the limit of the right hand side of (2.68) trivially gives $\langle M; \uparrow_{\{i_1\ldots i_m\}} | b^\dagger | \lambda_1\ldots\lambda_{M+m-1}\rangle = \sqrt{M}\langle M-1; \uparrow_{\{i_1\ldots i_m\}} | \lambda_1\ldots\lambda_{M+m-1}\rangle$ which does indeed correspond to the left hand side limit we just discussed. Consequently, if the determinant representation (2.66) is supposed valid, the left hand side and right hand side of the recursion relation (2.68) are both rational functions of $\{\lambda_1\ldots\lambda_{M+m}\}$ and since they have the same poles, the same residues and the same limit as $\lambda_i \to \infty$, they are equal.

For $M+1$ rapidities and a single flipped spin $i_1$, the explicit expansion given in (2.67) gives the scalar product $\langle M, \uparrow_{\{i_1\}} | \lambda_1\ldots\lambda_{M+1}\rangle = \sqrt{M!}\sum_{j=1}^{M+1} \frac{V}{\lambda_j-\epsilon_{i_1}}$ which is indeed equivalent to the $1 \times 1$ version of the above determinant $\sqrt{M!}\,(-\Lambda_{i_1}) = -\sqrt{M!}\sum_{j=1}^{M+1} \frac{V}{\epsilon_{i_1}-\lambda_j}$. Since neither the order of the rapidities $\lambda_i$ nor of the $\epsilon_{i_j}$ matters, this equality concludes the recursive proof. Being valid for $M+1$ rapidities, the determinant expression can be recursively built for $M+2$ rapidities and two flipped spins and so on, proving the validity of (2.66).

### 2.2.3 Form factors

We showed, in the previous subsection, that the partition function can be written as the determinant of an $N \times N$ matrix which only depends on the eigenvalues of the conserved charges. In the current section, we now demonstrate that generic scalar products as well as form factors can also be written in terms of those partition functions, therefore giving us access to simple expressions for these quantities, again written explicitly in terms of the same variables.

**Normalisations**

Let us first deal with the issue of the normalisation of eigenstates. As was the case for spin-only models (see section 1.3.2), both representations of the same eigenstate will only differ by a constant:

$$|\{\lambda_1\ldots\lambda_M\}\rangle = N_\lambda |\{\lambda_1\ldots\lambda_M\}\rangle_{\mathrm{n}}$$
$$|\{\mu_1\ldots\mu_N\}\rangle = N_\mu |\{\lambda_1\ldots\lambda_M\}\rangle_{\mathrm{n}}, \tag{2.71}$$

where $|\{\lambda_1\ldots\lambda_M\}\rangle_{\mathrm{n}}$ is the properly normalised eigenstate in question. Using the transfor-

mation (2.63) relating both representations, one can write the overlap (given by eq. (2.66)) as:

$$
\begin{aligned}
\langle \{\mu_1 \ldots \mu_N\} \mid \{\lambda_1 \ldots \lambda_M\}\rangle &= \langle M; \uparrow \ldots \uparrow | \prod_{i=1}^{N} S^+(\mu_i) \prod_{j=1}^{M} S^+(\lambda_j) |0; \downarrow \ldots \downarrow\rangle \\
&= N_\lambda N_\mu = \sqrt{M!}\, V^N \mathrm{Det} J
\end{aligned}
\tag{2.72}
$$

with

$$
J_{ab} = \begin{cases} \displaystyle\sum_{c=1(\neq a)}^{N} \frac{1}{\epsilon_a - \epsilon_c} - 2\Lambda^\lambda(\epsilon_a) + \frac{\omega - \epsilon_a}{V^2} & a = b \\[2ex] \frac{1}{\epsilon_a - \epsilon_b} & a \neq b \end{cases}.
\tag{2.73}
$$

Interestingly, this corresponds to the determinant of the Jacobian matrix $J_{ij} = \frac{\partial F_j}{\partial \Lambda(\epsilon_i)}$ of the set of quadratic Bethe equations (2.40):

$$
F_j = -\left[\Lambda(\epsilon_j)\right]^2 + \sum_{i \neq j}^{M} \frac{\Lambda(\epsilon_j) - \Lambda(\epsilon_i)}{\epsilon_j - \epsilon_i} - \frac{\epsilon_j - \omega}{V^2}\Lambda(\epsilon_j) + \frac{M}{V^2} = 0.
\tag{2.74}
$$

This is, of course, highly reminiscent of the Gaudin-Korepin determinant [63] which gives the norm $\langle \lambda_1 \ldots \lambda_M \mid \lambda_1 \ldots \lambda_M \rangle$ as the $M \times M$ determinant of the Jacobian matrix of the rapidites-based Bethe equations this time taking derivatives with respect to $\lambda_i$.

Secondly, as for spin-only models, the ratio $N_\lambda / N_\mu$ can be obtained by projecting both representations onto a reference state: a single arbitrary eigenstate common to $\{S_1^z \ldots S_N^z\}$ and $b^\dagger b$ (within the appropriate total excitation number subspace). The simplest choice could be to use $|M; \downarrow \ldots \downarrow\rangle$ as this reference state, since its scalar product with the particle-representation $\langle M; \downarrow \ldots \downarrow | \{\lambda_1 \ldots \lambda_M\}\rangle$ is trivially given by $\sqrt{M!}$; the coefficient involved coming only from the repeated action of the bosonic parts of the $S^+(\lambda_i)$ operators. On the other hand, the second scalar product $\langle M; \downarrow \ldots \downarrow \mid \{\mu_1 \ldots \mu_N\}\rangle$ would then involve only the $N$ spins parts of every $S^-(\mu_i)$ and would therefore be given by a $N \times N$ determinant.

Since the numerical calculation of the determinant of a $N \times N$ matrix requires $N^3$ operations, it would therefore be more efficient to normalise by calculating the ratio using projections on a reference state which contains $M$ (or $N/2$ when $M > N/2$) excitations in the spin sector. This would indeed minimise the total number of operations involved in computing both determinants, which would then be given by $M^3 + (N - M)^3$ (or simply $N^3/4$ when $M > N/2$). In large scale calculations, this can become an important factor in the total computation time.

Finally, one should keep in mind that, in certain calculations such as the resolution of the identity: $\sum_n |\psi_n\rangle \langle\psi_n| = \mathbb{1}$, in which eigenstates systematically appear twice, we do not need the individual norms. Indeed, the terms can be properly normalised using only the single $N \times N$ determinant given in (2.72) by using the following constructions: $\frac{|\{\lambda_1...\lambda_M\}\rangle \langle\{\mu_1...\mu_N\}|}{\langle\{\mu_1...\mu_N\}|\{\lambda_1...\lambda_M\}\rangle}$.

**Local raising and lowering operators** $(S_i^+, S_i^-, b^\dagger, b)$

The raising and lowering operators only have non-zero form factors only between two states which contain respectively $M$ and $M \pm 1$ excitations. These can therefore be straightforwardly written as partition functions by using the appropriate representations of both states involved in the calculation:

$$
\begin{aligned}
&\langle\mu_1...\mu_N| S^+(u) |\lambda_1...\lambda_{M-1}\rangle \\
&= \langle M; \uparrow...\uparrow| \left(\prod_{i=1}^{N} S^+(\mu_i)\right) S^+(u) \left(\prod_{j=1}^{M-1} S^+(\lambda_j)\right) |0; \downarrow...\downarrow\rangle, \\
&\langle\lambda_1...\lambda_{M-1}| S^-(u) |\mu_1...\mu_N\rangle \\
&= \langle 0; \downarrow...\downarrow| \left(\prod_{j=1}^{M-1} S^-(\lambda_j)\right) S^-(u) \left(\prod_{i=1}^{N} S^-(\mu_i)\right) |M; \uparrow...\uparrow\rangle.
\end{aligned}
\tag{2.75}
$$

These are given by the $N \times N$ determinant (2.66) built out of the ensemble of "rapidities" $\{\nu_1...\nu_{N+M}\} = \{\mu_1...\mu_{N+M}, u, \lambda_1...\lambda_{M-1}\}$ and give us access directly to any local spin operators by looking at the residues at $u \to \epsilon_i$ knowing that $\lim_{u \to \epsilon_i}(u - \epsilon_k) S^\pm(u) = V S_k^\pm$. Since the pole at $u \to \epsilon_k$ only appears in the diagonal element $J_{kk}$ of the partition function via the term $-\Lambda^\nu(\epsilon_k) = -\sum_{i=1}^{N} \frac{1}{\epsilon_k - \mu_i} - \sum_{i=1}^{M-1} \frac{1}{\epsilon_k - \lambda_i} - \frac{1}{\epsilon_k - u}$, the residue at $u = \epsilon_k$ is given by the minor determinant obtained after removing line and column $k$. Setting $u = \epsilon_k$ in the other diagonal terms lead to $-\frac{1}{\epsilon_a - u}$ cancelling the similar term in the sum $\sum_{c=1(\neq a)}^{N} \frac{1}{\epsilon_a - \epsilon_c}$. We are therefore left with the simple $N-1 \times N-1$ determinant:

$$
\langle\mu_1...\mu_N| S_k^+ |\lambda_1...\lambda_{M-1}\rangle = \sqrt{M!} \, V^{N-1} \text{Det} J^k,
\tag{2.76}
$$

with

$$
J_{a,b}^k = \begin{cases} \displaystyle\sum_{c=1(\neq a,k)}^N \frac{1}{\epsilon_a - \epsilon_c} - \Lambda^\lambda(\epsilon_a) - \Lambda^\mu(\epsilon_a) & a = b \\[2ex] \frac{1}{\epsilon_a - \epsilon_b} & a \neq b \end{cases} \quad \text{with } (a, b \neq k). \tag{2.77}
$$

The $u \to \infty$ limit gives us the bosonic operator form factors since $\lim_{u\to\infty} S^+(u) = b^\dagger$. It is also easily obtained since the limit simply leads to the cancellation of the $\frac{1}{\epsilon_a - u}$ terms in each of the diagonal elements of the matrix. The resulting determinant representation is then given by the $N \times N$ determinant:

$$
\langle \mu_1 \ldots \mu_N | b^\dagger | \lambda_1 \ldots \lambda_{M-1} \rangle = \sqrt{M!}\, V^N \mathrm{Det} J^B,
$$

$$
J_{a,b}^B = \begin{cases} \displaystyle\sum_{c=1(\neq a)}^N \frac{1}{\epsilon_a - \epsilon_c} - \Lambda^\lambda(\epsilon_a) - \Lambda^\mu(\epsilon_a) & a = b \\[2ex] \frac{1}{\epsilon_a - \epsilon_b} & a \neq b \end{cases}. \tag{2.78}
$$

## Local "number" operators $S_i^z$ and $b^\dagger b$

The "number" operators, namely the local $S_i^z$ spin operators and the bosonic occupation operator $b^\dagger b$ do not naturally allow such a simple expression. In this section, we show how one can still derive eigenvalue-based expressions for their form factors. The basic approach used here to derive such expressions is to make use of the known determinant expression (2.66) to evaluate scalar products between an eigenstate $|\{\mu(\omega)\}_m\rangle$ of the system for a given parameter $\omega$ and a second one $|\{\lambda(\omega + d\omega)\}_n\rangle$ evaluated at $\omega + d\omega$. This second eigenstate then corresponds to an infinitesimal deformation of the eigenstate of interest: $|\{\lambda(\omega)\}_n\rangle$ found at $\omega$.

Starting from the explicit expression of the conserved charges of the model (eq. (2.35)), we have $S_k^z = -\frac{\partial R_k(\omega)}{\partial \omega} = \frac{-R_k(\omega + d\omega) + R_k(\omega)}{d\omega}$ and therefore can deduce the spin form factors from the evaluation of:

$$\langle\{\mu(\omega)\}_m\big|S_k^z|\{\lambda(\omega+d\omega)\}_n\rangle = \big[r_k^m(\omega)-r_k^n(\omega+d\omega)\big]\frac{\langle\{\mu(\omega)\}_m\,|\{\lambda(\omega+d\omega)\}_n\rangle}{d\omega}.$$

(2.79)

Using the explicit eigenvalues (2.39) and (2.60), the diagonal form factors which involve the same state in the bra and the ket will then lead to the typical Hellmann-Feynman theorem:

$$\langle\{\mu(\omega)\}_m\big|S_k^z|\{\lambda(\omega)\}_m\rangle = -\frac{\partial r_k^m(\omega)}{\partial\omega}\,\langle\{\mu(\omega)\}_m\,|\,\{\lambda(\omega)\}_m\rangle,$$

$$\frac{\langle\{\mu(\omega)\}_m\big|S_k^z|\{\lambda(\omega)\}_m\rangle}{\langle\{\mu(\omega)\}_m\,|\,\{\lambda(\omega)\}_m\rangle} = \left[-\frac{1}{2}+V^2\frac{\partial\Lambda_m^\lambda(\epsilon_k)}{\partial\omega}\right].$$

(2.80)

while the off-diagonal ones give:

$$\langle\{\mu(\omega)\}_m\big|S_k^z|\{\lambda(\omega)\}_n\rangle = \big[r_k^m(\omega)-r_k^n(\omega)\big]\frac{\langle\{\mu(\omega)\}_m\,|\{\lambda(\omega+d\omega)\}_n\rangle}{d\omega}$$

$$= \left[\epsilon_k-\omega+V^2\Lambda_n^\lambda(\epsilon_k)-V^2\Lambda_m^\mu(\epsilon_k)\right]\frac{\langle\{\mu(\omega)\}_m\,|\{\lambda(\omega+d\omega)\}_n\rangle}{d\omega},\ m\neq n.$$

(2.81)

One notices that a single evaluation of $\frac{\langle\{\mu(\omega)\}_m\,|\{\lambda(\omega+d\omega)\}_n\rangle}{d\omega}$ gives direct access to every one of the $N$ local $S_i^z$ form factors. Since the Gaudin raising operators $S^+(u)$ does not explicitly depend on the parameter $\omega$, the overlap of interest is given once more by the same partition function whose determinant expression (2.66) has been given before. The deformation to $\omega+d\omega$ indeed only appears indirectly through the infinitesimal modification of the $\lambda$ rapidities. This scalar product could, in principle, be numerically evaluated as a single determinant using the eigenvalues defining exactly the states respectively at $\omega$ and $\omega+\Delta\omega$ (with $\Delta\omega$ being small but finite):

$$\lim_{\Delta\omega\to0}\frac{\langle\{\mu(\omega)\}_m\,|\{\lambda(\omega+\Delta\omega)\}_n\rangle}{\Delta\omega} = \sqrt{M!}\,V^N\frac{1}{\Delta\omega}\lim_{\Delta\omega\to0}\mathrm{Det}J$$

(2.82)

with:

$$J_{a,b} = \begin{cases} \displaystyle\sum_{c=1(\neq a)}^{N} \frac{1}{\epsilon_a - \epsilon_c} - \Lambda_n^\lambda(\epsilon_a)\Big|_{\omega+\Delta\omega} - \Lambda_m^\mu(\epsilon_a)\Big|_\omega & a = b \\[2ex] \frac{1}{\epsilon_a - \epsilon_b} & a \neq b \end{cases}. \tag{2.83}$$

Being of order $\Delta\omega$, the resulting determinant would however then be nearly singular, a fact which could lead to important numerical stability issues. However, an exact evaluation remains possible by taking the limit analytically using $\Lambda_n^\lambda(\epsilon_a)\big|_{\omega+\Delta\omega} \approx \Lambda_n^\lambda(\epsilon_a)\big|_\omega + \frac{\partial\Lambda_n^\lambda(\epsilon_a)}{\partial\omega}\Delta\omega$ and the fact that $\langle\psi_m(\omega)\,|\psi_n(\omega)\rangle = 0$ since both eigenstates are distinct and therefore orthogonal. Retaining the linear terms leads to the following sum of $N$ determinants:

$$\lim_{\Delta\omega\to 0} \frac{\langle\{\mu(\omega)\}_m\,|\{\lambda(\omega+\Delta\omega)\}_n\rangle}{\Delta\omega} = \sqrt{M!}\,V^N \sum_{k=1}^{N} \frac{\partial\Lambda_n^\lambda(\epsilon_k)}{\partial\omega}\det\tilde{J}^k, \tag{2.84}$$

which are just the $N-1 \times N-1$ minors obtained from $J$ after removing line and column $k$:

$$\tilde{J}_{ab}^k = \begin{cases} \displaystyle\sum_{c=1(\neq a)}^{N} \frac{1}{\epsilon_a - \epsilon_c} - \Lambda_n^\lambda(\epsilon_a) - \Lambda_m^\mu(\epsilon_a) & a = b \\[2ex] \frac{1}{\epsilon_a - \epsilon_b} & a \neq b \end{cases} \quad \text{with } (a, b \neq k). \tag{2.85}$$

Notice that they differ from the form factors for $S_k^+$ found in eq. (2.77) by the fact that the sum over $\epsilon_c$ still includes the term $c = k$. The expression found here depends not only on the eigenvalues $\Lambda^\lambda(\epsilon_i)$ but also on their derivatives $\frac{\partial\Lambda^\lambda(\epsilon_i)}{\partial\omega}$. Fortunately, they can be directly obtained from the knowledge of the set $\{\Lambda^\lambda(\epsilon_1)\dots\Lambda^\lambda(\epsilon_N)\}$ by simply solving the linear system of equations:

which one finds by taking the $\omega$ derivative of the quadratic Bethe equations (2.40).

From the fact that $\hat{M} = b^\dagger b + \sum_{i=1}^{N} S_i^z$ is also a conserved quantity, with eigenvalue $M - \frac{N}{2}$ for states containing $M$ particle-like excitations, one can directly find a similar expression for the

bosonic occupation form factor:

$$
\langle \{\mu(\omega)\}_m | \, b^\dagger b \, | \{\lambda(\omega)\}_n \rangle \quad = \quad \langle \{\mu(\omega)\}_m | \, M - \frac{N}{2} \, | \{\lambda(\omega)\}_n \rangle
$$

$$
- \sum_{i=1}^{N} \langle \{\mu(\omega)\}_m | \, S_i^z \, | \{\lambda(\omega)\}_n \rangle . \tag{2.86}
$$

Using the previous $S^z$ form factors we have

$$
\frac{\langle \{\mu(\omega)\}_m | \, b^\dagger b \, | \{\lambda(\omega)\}_m \rangle}{\langle \{\mu(\omega)\}_m \, | \, \{\lambda(\omega)\}_m \rangle} \quad = \quad M - \frac{N}{2} + \sum_{i=1}^{N} \frac{\partial r_i^m(\omega)}{\partial \omega} = M - \sum_{i=1}^{N} \left[ \frac{\partial \Lambda_m^\lambda(\epsilon_i)}{\partial \omega} \right],
$$

$$
\tag{2.87}
$$

$$
\langle \{\mu(\omega)\}_m | \, b^\dagger b \, | \{\lambda(\omega)\}_n \rangle \quad = \quad \left( \sum_{i=1}^{N} \left[ r_i^n(\omega) - r_i^m(\omega) \right] \right)
$$

$$
\times \frac{\langle \{\mu(\omega)\}_m \, | \{\lambda(\omega + d\omega)\}_n \rangle}{d\omega}, \quad m \neq n \tag{2.88}
$$

which is once again proportional to the term $\frac{\langle \{\mu(\omega)\}_m \, | \{\lambda(\omega + d\omega)\}_n \rangle}{d\omega}$ and can therefore be explicitly computed as eq. (2.84).

## 2.3 Conclusions

This section has several purposes because it concludes the theoretical part of this work. In a first time, short conclusions about the two generalisations are given and then the utility of the spin-boson realisation for the remainder of the work is discussed.

First of all, the method to have access to the partition function with a spin whose norm is arbitrarily chosen was straightforward because the complexity came from the expressions but not from the method because it is highly relying on the work done for spins-$\frac{1}{2}$ only. The future work is obviously to find the determinant expression for a partition function with more spins with arbitrary norm but the complexity of the expressions prevented us from achieving that for the moment.

However in the second section, it was shown that, despite the lack of symmetry between the "highest" and "lowest" weight state of quantum integrable models derived from a realisation of the rational GGA which contains a bosonic mode, one can still use the QISM. The fact of being able to use the QISM in this case is in itself a result and a similar work can be done to

tackle the lack of symmetry in other realisations. For instance we as well have done the work of applying these steps to a realisation defined by:

$$
\begin{aligned}
S^+(u) &= B_0^+ + \sum_{i=1}^{N} \frac{S_i^+}{u - \epsilon_i} \\
S^-(u) &= B_0^- + \sum_{i=1}^{N} \frac{S_i^-}{u - \epsilon_i} \\
S^z(u) &= -B^z - \sum_{i=1}^{N} \frac{S_i^z}{u - \epsilon_i},
\end{aligned}
\tag{2.89}
$$

with $B_0^+$, $B_0^-$ and $B^z$ the component of a general external magnetic field [64]. This work can be compared to [65] where the triangular boundaries could correspond to the case where $B_0^+ = 0, B_0^- \neq 0$ and $B_0^+ \neq 0, B_0^- = 0$.

Within the spin-boson realisation, the QISM was used to build two distinct algebraic Bethe ansätze and therefore two representations of eigenstates of Gaudin models. These were then used to relate scalar products of states and form factors of local operators to a domain wall boundary partition function which was shown to have a simple expression as the determinant of a matrix whose elements depend only on the eigenvalues of the model's conserved charges.

Another recent contribution [66], using the Richardson-Gaudin pairing model (to study the Read-Green resonance in topological superconductor coupled to a bath), supports our statement on the variety of phenomena which can be modelled by Gaudin models.

The determinant expressions derived within this chapter can have an important positive impact on the computation time required for numerical work on these systems. Indeed, being defined only through these eigenvalues which are solutions of a set of quadratic Bethe equations, they allow one to avoid the explicit finding of the rapidities describing a given state $\{\lambda_1 \dots \lambda_M\}$. This work further establishes our capacity to rebuild many aspects of the algebraic Bethe ansatz using only constructions which are explicitly symmetric in the Bethe rapidities, a useful fact which could possibly generalise to a much broader class of integrable systems.

We now want to highlight some other work that are related to ours. In [67] it is shown how to recover spin-boson algebra from spin conserved quantities by deforming one of them. Relying on this previous way of approaching spin-boson Gaudin models, the papers [68] and [69] extend our work to the XXZ Gaudin models and create an unifying algebra that are able to describe Richardson-Gaudin models or Dicke models.

The problem of finding the Bethe equations with the same number of the creation operators than the number of sites has been studied in the context of Heisenberg XXX with general

boundaries in [70]. The question of being still able to apply the ABA in the context of integrable dissipative exclusion problem which can map onto the open XXZ spin chain solved treated in [71]. Moreover, the problem of cancelling similar supplementary terms as in (2.42) is tackled in other contexts in [72, 73, 74]. Other methods to solve models without proper pseudo-vacuum have been introduced in recent years, for instance the: q-Onsager approach [75], the functional Bethe ansatz [76, 77, 78] or the generalisation of the coordinate Bethe ansatz [79].

In the next chapters, numerics using these determinants expressions will be explained and then shown. In a first time, a chapter will explained how the quadratic Bethe equations were solved numerically, then graphics illustrating the asymptotic dynamics will be presented to conclude with real time dynamics graphics.

# 3 Solving the quadratic Bethe equations numerically

## 3.1   Presentation of the problem

In this chapter, we focus on the numerical techniques one can use to find the eigenstates of $S^2$ by looking for the solutions of the quadratic Bethe equations (2.40). Defining $\Lambda(\epsilon_i) = \frac{\Lambda_i}{V^2}$ these quadratic equations (2.40) become:

$$
[\Lambda_i]^2 \quad = \quad V^2 \sum_{j \neq i}^{N} \frac{\Lambda_i - \Lambda_j}{\epsilon_i - \epsilon_j} - (\epsilon_i - \omega)\Lambda_i + V^2 M, \tag{3.1}
$$

where each side of the equations has been multiplied by $V^4$ to present exactly the ones that were solved numerically. We explained in the previous chapter that the interest of these quadratic Bethe equations is that they contain all the possible information on the variables $\lambda_i$ while being easier to solve. Moreover for a system of N spins-$\frac{1}{2}$ with $M$ excitations (bosonics or spin excitations), one has a total of $N$ $\Lambda_i$ variables instead of $M$ variables. So, not only the quadratic equations are easier to solve, but for a systems containing $M > N$ total excitations, there are also fewer equations than in the traditional set of Bethe equations. Additionally, one of the goals of the thesis is to investigate a system's dynamics and stationary states for different values of $M$ and in particular when $M$ is large regarding $N$. This domain of excitations ($M > N$) is easily reachable because it still corresponds to a systems of $N$ equations. However, we add here a limitation in the number of excitations we can choose that arises with the capacity of a computer. The presence of $\sqrt{M!}$, in the expression of (2.66) for instance, limits $M$ at 170 because 171! is greater than $1.79769e + 308$, which on many computers is the largest floating point number that can be represented in eight bytes.

In the light of everything we have explained before, we are left with $N$ quadratic equations of $N$ variables to solve. In the cases where $A_i \neq \frac{1}{2}$, if we want to derive quadratic equations in a

same way as for (2.40), i.e. from traditional Bethe equations $F(u) = -\sum_{i=1}^{N} \frac{A_i}{\epsilon_i - u} + \frac{B}{2g} u + \frac{C}{2g} = \sum_{j=1(\neq i)}^{M} \frac{g}{\lambda_i - \lambda_j}$, we notice we would obtain more than $N$ variables because of the presence of the $\Lambda^{(n)}(\epsilon_i)$ (the derivatives of the $\Lambda(\epsilon_i)$). For instance, for $A_i = 1$ we would have to work with $2N$ variables, $N$ variables $\Lambda(\epsilon_i)$ and $N$ variables $\Lambda'(\epsilon_i)$. A way of dealing with the equations when the derivatives do not vanish is explained in [49].

## 3.2 The algorithm

The method we chose to solve this system of equations is a multi-linear Newton's method. In this section, we start by briefly explaining the structure of the Newton's algorithm and in a second part we give more details on each step of the algorithm.

The algorithm solves the quadratic equations and gives all the solutions for a chosen coupling, we will call it $V_{final}$. To reach the solution at $V_{final}$, the quadratic equation are solved at $V = 0$ in a first time. We then progressively increase the coupling by increments $\delta V$ until we reach $V_{final}$. To solve the equations at a given $V$, we need a starting point, we will call it a "guess point", that is an approximation of the solutions. The guess point we use at each step is in fact the solutions at the previous step, i.e. the starting point of the algorithm to solve the equations at a given $V$ is the solutions at $V - \delta V$.

For systems containing $N$ spins-$\frac{1}{2}$ and $M_b$ bosons the first step is to generate all the possible solutions at $V = 0$ which will be the initial configurations. The number of total excitations $M$ being conserved, for each initial configuration of spins there is only one corresponding number of bosons leading to $2^N$ different initial configurations. The program we wrote solves the equations for every configuration generated and then saves the $N$ corresponding solutions $\Lambda_i$ in a file.

For each initial configuration we consider the traditional Bethe equations (2.38) where both sides have been multiplied by $2V^2$:

$$\omega - \lambda_i + \sum_{k=1}^{N} \frac{V^2}{\lambda_i - \epsilon_k} = \sum_{j \neq i}^{M} \frac{2V^2}{\lambda_i - \lambda_j}. \tag{3.2}$$

At $V = 0$ it is easy to find the solutions to these equations . Indeed $V = 0$ leads to:

$$a) \; \lambda_i \;\; = \;\; \epsilon_j + \lim_{V \to 0} \frac{V^2}{\epsilon_j - \omega},$$

$$b) \; \lambda_i \;\; = \;\; \omega. \tag{3.3}$$

There are $M$ $\lambda_i$ variables, each of them corresponds to either a bosonic excitation or a spin one. In a) the rapidity $\lambda_i$ comes from an excitation of the $j^{th}$ spin whereas in b) the rapidity comes from a bosonic excitation. These two kinds of excitations corresponds to different terms in the sum that appears in our change of variables $\Lambda_j = \sum_{i=1}^{M} \frac{V^2}{\epsilon_j - \lambda_i}$ from the $\lambda_i$ to the $\Lambda_j$:

$$a) \;\; \frac{V^2}{\epsilon_j - \lambda_i} \;\; = \;\; \omega - \epsilon_j,$$

$$b) \;\; \frac{V^2}{\epsilon_j - \lambda_i} \;\; = \;\; 0. \tag{3.4}$$

As a consequence, at $V = 0$ for a system with $M_b$ bosonic excitations, there will be $M_b$ terms in the sum that will cancels and $M - M_b$ that will be equal to $\omega - \epsilon_j$. As an example, for an initial configuration $|6; \downarrow\uparrow\downarrow\uparrow\rangle$, with $M_b = 6$, $N = 4$ spins-$\frac{1}{2}$ and a total number of excitations $M = 8$, we have at $V = 0$:

$$\Lambda_j \;\; = \;\; \sum_{i=1}^{8} \frac{V^2}{\epsilon_j - \lambda_i} = \omega - \epsilon_2 + \omega - \epsilon_4. \tag{3.5}$$

Numerically, starting from this solution at $V = 0$, we increase $V$ step by step until we reach the coupling of interest. For simplicity we write $\vec{\Lambda} = (\Lambda_1, \ldots, \Lambda_N)$ when a function depends of all the components of $\vec{\Lambda}$. We then define:

$$F_j(\vec{\Lambda}, V) = V^2 \left[ \sum_{i \neq j}^{N} \frac{\Lambda_j - \Lambda_i}{\epsilon_j - \epsilon_i} + M \right] - (\epsilon_j - \omega)\Lambda_j - \left[\Lambda_j\right]^2. \tag{3.6}$$

The procedure we set up is the following: we want the algorithm to find iteratively a better guess point to obtain the solutions at a given $V$, $\Lambda_{i;V}$, knowing $\Lambda_{i;V-\delta V}$, the solution at $V - \delta V$, from a previous step of the program, in other words $\vec{F}(\vec{\Lambda}_{i;V-\delta V}, V - \delta V) = 0$. This previous step enables us to make a guess $\vec{\Lambda}_V^{guess}$ at $V$. Let us assume we already have a $\vec{\Lambda}_V^{guess}$, by applying Newton's algorithm we have the following relation for one of our quadratic equations:

$$F_j(\vec{\Lambda}_V^{guess} + \delta\vec{\Lambda}, V) = F_j(\vec{\Lambda}_V^{guess}, V) + J\delta\vec{\Lambda} = 0, \tag{3.7}$$

where $J$ is the Jacobian matrix whose elements $J_{j;k}$ are:

$$J_{j;k} = \frac{\partial F_j(\vec{\Lambda}_V^{guess}, V)}{\partial \Lambda_k} = V^2 \sum_{i \neq j}^{N} \frac{\frac{\partial \Lambda_j}{\partial \Lambda_k} - \frac{\partial \Lambda_i}{\partial \Lambda_k}}{\epsilon_j - \epsilon_i} - \frac{\partial \Lambda_j}{\partial \Lambda_k}\left(\epsilon_j - \omega + 2\Lambda_j\right), \tag{3.8}$$

leading to:

$$\delta\vec{\Lambda} = -J^{-1}\vec{F}(\vec{\Lambda}_V^{guess}, V). \tag{3.9}$$

Following the principle of a Newton's algorithm, the program will iterate until it finds a $\delta\vec{\Lambda}$ that satisfies equation (3.9) with a precision chosen by the user. Thus, if the program converges to a solution, we obtain a new set of $\Lambda_{i;V}^{guess}$ whose "quality factor" $\left|\vec{F}(\vec{\Lambda}_V^{guess}, V)\right|$ is better than before. This operation is repeated until $\left|\vec{F}(\vec{\Lambda}_V^{guess}, V)\right| < \varepsilon$, where $\varepsilon$ is the chosen precision of the program also defined by the user. Eventually, at the end of this process, we find the solutions for the quadratic equations at a given $V$ and this process will be repeated by increasing $V$ by $\delta V$ until we reach $V_{final}$.

## 3.3 Enhancement of the guess

The condition for our program to converge is that the very first guess, before starting the Newton algorithm, is good enough to be in the basin of attraction of the algorithm. To highly increase the chances that our guess is in the basin of attraction we use a Taylor expansion of $\Lambda_{i;V-\delta V}$ around $V - \delta V$ to a chosen order $n$:

$$\Lambda_{j;V}^{guess} \approx \sum_{i=0}^{n} \frac{\partial^n \Lambda_{i;V-\delta V}}{\partial V^n} \frac{(\delta V)^n}{n!}. \tag{3.10}$$

As a consequence, we need to compute the $\frac{\partial^n \Lambda_{i;V-\delta V}}{\partial V^n}$. To do so we take the derivative of the equality $\vec{F}(\vec{\Lambda}_{i;V-\delta V}, V - \delta V) = 0$ leading to:

$$
\begin{aligned}
\frac{d\vec{F}(\vec{\Lambda}_i, V - \delta V)}{dV} &= \frac{\partial \vec{F}(\vec{\Lambda}_i, V - \delta V)}{\partial V} \frac{dV}{dV} + \frac{\partial \vec{F}(\vec{\Lambda}_i, V - \delta V)}{\partial \vec{\Lambda}_i} \frac{d\vec{\Lambda}_i}{dV} \\
&= \frac{\partial \vec{F}(\vec{\Lambda}_i, V - \delta V)}{\partial V} + \frac{\partial \vec{F}(\vec{\Lambda}_i, V - \delta V)}{\partial \vec{\Lambda}_i} \vec{\Lambda}_i'. \\
&= 0
\end{aligned}
\tag{3.11}
$$

where we have written $\vec{\Lambda}_i = \vec{\Lambda}_{i;V-\delta V}$ for simplicity. In a same manner as before we arrive at:

$$\vec{\Lambda}_i' = -J^{-1} \frac{\partial \vec{F}(\vec{\Lambda}_i, V - \delta V)}{\partial V}. \tag{3.12}$$

We need to compute the next total derivative $\frac{\partial^2 \vec{F}(\vec{\Lambda}_i, V - \delta V)}{\partial (V)^2}$ at $V - \delta V$ and so on. Applying this method $n$ times, we deduce a set of linear equations for the $n^{th}$ derivative dependent on all lower derivatives of $\vec{\Lambda}_i$:

$$J_{ij} \frac{\partial^n \Lambda_i}{\partial V^n} = V^2 \sum_{j \neq i}^{N} \frac{\frac{\partial^n \Lambda_i}{\partial V^n} - \frac{\partial^n \Lambda_j}{\partial V^n}}{\epsilon_i - \epsilon_j} + A_{n;j} = B_{n;j} \left( \left\{ \frac{\partial^k \Lambda_i}{\partial v^k} \right\}_{k=0}^{n-1} \right), \tag{3.13}$$

where we write $v = V^2$ for simplicity. $B_{n;j} \left( \left\{ \frac{\partial^k \Lambda_i}{\partial v^k} \right\}_{k=0}^{n-1} \right)$ means that $B_{n;j}$ depends of all the lower order derivatives $\frac{\partial^k \Lambda_i}{v^k}$ as it can be seen in its explicit expression one can find iteratively (Appendix A.3):

$$
\begin{aligned}
B_{n;j} &= B'_{n-1} + \frac{1}{v}\left(-\frac{\partial^{n-1}\Lambda_j}{\partial v^{n-1}}\left[(\epsilon_j - \omega) + 2\Lambda_j\right] - B_{n-1;j}\right) + 2\frac{\partial \Lambda_j}{\partial v}\frac{\partial^{n-1}\Lambda_j}{\partial v^{n-1}} \\
&= \frac{-n}{v}\left(B_{n-1;j} + \frac{\partial^{n-1}\Lambda_j}{\partial v^{n-1}}\left[(\epsilon_j - \omega) + 2\Lambda_j\right]\right) + \sum_{k=1}^{n-1}\binom{n}{k}\frac{\partial^k \Lambda_j}{\partial v^k}\frac{\partial^{n-k}\Lambda_j}{\partial v^{n-k}}, \\
B_{0;j} &= -\Lambda_j \Lambda_j, \\
A_{n;j} &= -\frac{\partial^n \Lambda_j}{\partial v^n}\left[(\epsilon_j - \omega) + 2\Lambda_j\right].
\end{aligned}
\tag{3.14}
$$

One can notice that the Jacobian is the same matrix regardless $n$ and so it only needs to be inverted once and then (3.13) can be rewritten as:

$$
\frac{\partial^n \Lambda_i}{\partial V^n} = -J^{-1}B_{n;j}\left(\left\{\frac{\partial^n k\Lambda_i}{\partial v^k}\right\}_{k=0}^{n-1}\right).
\tag{3.15}
$$

As explained before, the computation of the derivation to carry out the Taylor expansion enables us to find a good guess $\Lambda_{j;V}^{guess}$ to start the iteration. We can add that all the parameters chosen by the user, namely $\varepsilon$, the value of the jump $\delta V$ between each step and $n$, have to be optimised and in our case it has been done empirically. Indeed, $\varepsilon$ has to be small enough so that the solution at $V - \delta V$ will become a good enough guess at $V$. The jump $\delta V$ also has to be optimised because increasing the coupling by a very small $\delta V$ requires a lot of step to reach $V_{final}$ while choosing a bigger $\delta V$ may draw away the solutions of the equations too far from the guess point. Finally, the higher the number of derivatives $n$ is, the more the convergence of the algorithm is increased but the longer time the algorithm needs to run.

Eventually, we decide to adjust $\delta V$ dynamically, i.e. at each step of the algorithm the coupling is increased by a substantial $\delta V$ and then decreased slowly until the program is able to converge so that the jump $\delta V$ is as big as possible at each step. However, at $V = 0$ the equations are very sensitive because any $\delta V$ substantially changes the equations, so the value of $\delta V$ needs to be very small if we want the solutions at $V = 0$ to remain a good guess. That is why we chose to solve the systems for a very small $V$ so that solutions will be near the ones at $V = 0$ without carry out the step of the successive divisions of a big $\delta V$ to save some computation time. These solutions for a very small coupling will lead us to a first guess which will be the starting point of all remaining steps.

Following the routine we described, we find the solutions of the quadratic Bethe equations at $V_{final}$. As a final remark, all the systems of equations of the form (3.9) have been solved by

using the library *Scipy* of the language *Python.* In a first time, the command *lu factor* is used to carry out a decomposition LU of the Jacobian matrix and then the command *lu solve* to solve the system once it is in the form of a LU-matrix system of equations. Decomposing a matrix into a product of a lower triangular one with a upper triangular makes the numerical treatment of matrices very efficient. This decomposition can be used to compute determinants as well. This is another asset of having determinant expressions for our scalar products.

# 4 Steady State properties: Local magnetisation and bosonic occupation

In this chapter we present numerical results for two different physical quantities in the steady-state obtained after a variety of product-states initial conditions are evolved unitarily. The long-time averaged magnetisation along the z-axis and bosonic occupation are evaluated in the Diagonal Ensemble (DE) (we introduce this ensemble in the next section) by performing the complete sum over the full Hilbert space for small system sizes. These numerically exact results are independent of any particular choice of Hamiltonian and therefore describe general results valid for any member of the class of quantum integrable models built out of the same underlying conserved quantities as explained in 1.4. Nevertheless, we will use the TC Hamiltonian (1), and the physics usually related to it, presented in the introduction as reference to interpret our results since it captures most of the global features.

The collection of results obtained can be qualitatively understood by thinking of it as a "relaxation" process for which at infinitely strong coupling, $V \to \infty$, every initial state will "relax" to a common superradiant state. Numerically, we can try to get close to this superradiant state by considering strong, but finite, couplings. Therefore, all the steady states we present can be understood as an interrupted "relaxation" process towards a superradiant state. Nonetheless, for strong enough couplings the system, in its steady state, will tend to be superradiant whereas for weaker couplings the "relaxation" process is interrupted before the system can show a superradiant-like behaviour.

We call our state superradiant-like when each spin is in a maximally coherent superposition of its $|\uparrow\rangle$ and $|\downarrow\rangle$ states, i.e. they are in-plane polarised. Consequently the bosonic mode is also in a maximally coherent superposition of different occupation number states. Eventually, we can say that a finite value of the coupling between the spins and the bosonic mode then leads to a long-time limit steady state whose properties are qualitatively captured by a simple "dynamical" vision in which the coupling strength $V$ plays the role of a time $t_V$ at which this "relaxation process" towards superradiance is interrupted.

This chapter is divided in three mains parts: section 4.1 explains why it is a good approximation to work in the Diagonal Ensemble , section 4.2 presents the numerical data and a possible

physical interpretation of these results thanks to a recurrent comparison with a reference steady state which exhibits the characteristics of a superradiant-like state (as we have defined it) and lastly, these results are compared to the values of observables one can get within the Generalised Gibbs Ensemble (GGE).

## 4.1 Form Factors

Following the last chapters, the point of using numerics to access quantities such as local magnetisation or bosonic occupation was not to only study the dynamics of our systems but also to make the best possible use of the variables $\Lambda(\epsilon_i)$ (for the first time) in spin-boson systems. The expression of the mean value of an observable $O$ at a given time $t$ is:

$$\langle \hat{O} \rangle (t) = \sum_{n,m} \langle \psi_0 | n \rangle \langle m | \psi_0 \rangle \, e^{i(E_n - E_m)t} \langle n | \hat{O} | m \rangle , \tag{4.1}$$

which is a double sum over the full set of normalised eigenstates $|n\rangle$ of $H$ (with eigenvalue $E_n$). We begin this section with the expressions depending of $\Lambda(\epsilon_i)$ we need in (4.1).

It was shown in subsection 2.2.2 that the projection of a state of the form (2.37) onto a product state containing $M - m$ bosons with the $m$ spins of index $\{i_1 \dots i_m\}$ pointing up while the $N - m$ other spins point down, can be written as an $m \times m$ determinant whose matrix elements depend exclusively on $\Lambda(\epsilon_i)$:

$$\langle M - m; \uparrow_{\{i_1 \dots i_m\}} | \lambda_1 \dots \lambda_M \rangle = \sqrt{(M - m)!} \, V^m \, \mathrm{Det} J$$

$$J_{ab} = \begin{cases} \displaystyle\sum_{c=1(\neq a)}^{m} \frac{1}{\epsilon_{i_a} - \epsilon_{i_c}} - \Lambda(\epsilon_{i_a}) & a = b \\ \frac{1}{\epsilon_{i_a} - \epsilon_{i_b}} & a \neq b \end{cases} . \tag{4.2}$$

This construction enables to express $\langle \psi_0 | n \rangle$ in terms of $\Lambda(\epsilon_i)$. The squared norm $N_\lambda$ of the state $|\lambda_1 \dots \lambda_M\rangle$ was also shown to be computable as a $N \times N$ determinant of the same form.

For any eigenstate, the quantum expectation values of local operators were shown in subsection 2.2.3 to be obtainable from the Hellmann-Feynman theorem, giving the following

expression for the local magnetisation:

$$\frac{\langle \lambda_1 ... \lambda_M | S_k^z | \lambda_1 ... \lambda_M \rangle}{N_\Lambda} \quad = \quad \left[ -\frac{1}{2} + \frac{\partial \Lambda(\epsilon_k)}{\partial \omega} \right], \tag{4.3}$$

while the bosonic occupation follows from $\hat{M} = b^\dagger b + \sum_{i=1}^N S_i^z$ which has a well defined eigenvalue for every such state:

$$\frac{\langle \lambda_1 ... \lambda_M | b^\dagger b | \lambda_1 ... \lambda_M \rangle}{N_\Lambda} \quad = \quad M - \sum_{i=1}^N \left[ \frac{\partial \Lambda(\epsilon_i)}{\partial \omega} \right]. \tag{4.4}$$

Although there is an infinite number of possible Hamiltonians $H = \gamma \hat{M} + \sum_{i=1}^N \alpha_i R_i$ which share the same eigenstates, the full time evolution of a given observable would still depend, through the eigenvalues $E_n = \gamma M + \sum_{i=1}^N \alpha_i r_i$ (with $M$ the eigenvalue of $\hat{M}$ here), on a particular choice of Hamiltonian.

However, the long time average reduces, due the averaging out of any non-zero frequency, to the diagonal contributions for $n = m$:

$$\lim_{t \to \infty} \frac{1}{t} \int_0^t \langle \hat{O} \rangle (t') dt' = \sum_n \langle \psi_0 | n \rangle \langle n | \psi_0 \rangle \langle n | \hat{O} | n \rangle. \tag{4.5}$$

This is what we call, working in the DE. Underlying this assumption is the fact that no systematic degeneracies occur so that $E_n \neq E_m$ for any $n \neq m$. Although technically, for a given system, level crossings will occur so that for certain specific values of $V$ it is possible to find two degenerate states, no systematic degeneracies will occur since sets $\{\Lambda_1 ... \Lambda_N\}$ solution to the quadratic Bethe equation are all distinct.

In this work, for small enough systems the sum over the Hilbert space can be performed in full, but for larger systems it also becomes possible to use Monte Carlo sampling in order to evaluate the involved sums [80, 81, 82, 53, 54].

Provided a sufficiently spread out projection of the initial state over the eigenstates of the Hilbert space, i.e. the Inverse Participation Ratio: $\sum_n |\langle n | \psi_0 \rangle|^4 \ll 1$, and a large enough system to support a near-continuum of frequencies, the oscillating terms in $\langle \hat{O} \rangle (t)$ should rapidly cancel out leading to a steady state whose properties actually correspond to the long term average:

$$\lim_{t\to\infty} \langle \hat{O} \rangle (t) = \lim_{t\to\infty} \frac{1}{t} \int_0^t \langle \hat{O} \rangle (t) dt. \tag{4.6}$$

This evidently excludes systems for which persistent oscillations remain at long times therefore making $\lim_{t\to\infty} \langle \hat{O} \rangle (t)$ no longer properly defined. For finite size systems, the true complete dynamics will retain "weak" fluctuations around the long-time average due to the finite number of frequencies involved. As shown in [83] for the bosonic occupation number, the relaxation towards a steady state, with well-defined asymptotic expectation values, is a completely reasonable assumption in this type of system.

## 4.2 Numerical results

The systems we considered are composed of a collection of $N = 15$ spins-$\frac{1}{2}$ interacting with a bath of bosons. At $t = 0$ the spins are in their initial configuration and the system is given $M$ total excitations. This number of excitations being conserved, the number of bosons in the bath is determined by the number of spins-up (the equivalent of a spin excitation). With the time, the system is evolving under a Hamiltonian which determines the efficiency of the redistribution of its excitations so that the spins tend to polarise in the plane which involves the system in being in a superradiant-like state. However, the integrability limits the freedom of redistribution by imposing conserved quantities associated to each spin. Knowing that we give an infinite time to a chosen Hamiltonian to redistribute the excitations among the system, the question is whether or not an infinite time is enough to overpass the effect of the integrability. For instance, by giving an infinite time to $H_{TC}$ to rule the dynamics of one of our systems up to their steady states, we would expect it to thermalise and to have a superradiant-like steady state.

In this section, we begin, in the first subsection, by giving a complete study of the steady states, obtained for different values of the coupling $V$, resulting of the evolution of one unique initial configuration of spins, one unique value of $M$ and one unique value of $\omega$. A lot of different statements about the impact of every of those parameters on the steady states, wether or not this configuration and the value of these parameters favour a superradiant-like state, will be done. The purpose of the following subsections will be to put to the proof every statement valid for the reference state by comparing it to other cases.

### 4.2.1 Reference state and Coupling constant

This first subsection aims to illustrate this interrupted relaxation picture towards the superradiant-like state. Moreover, it will provide a comparison reference for the remainder of the section.

The example of interest is the steady state of the local magnetisation for a variety of coupling constants when the initial state is chosen to be a typical, i.e. highly entropic, product state. Since the individual gaps are $\epsilon_i = i$, flipping up the even numbered spins, ensures a spreading of the excitations over every available energy scale. Therefore, it should allow a maximally efficient redistribution of the local excess of energy leading to a "thermalised" steady state which has lost as much information as possible about the initial state.



Figure 4.1: Local magnetisation in the steady-state for the initial state: $|17;\uparrow\downarrow\uparrow\downarrow\uparrow\downarrow\uparrow\downarrow\uparrow\uparrow\downarrow\uparrow\rangle$ for a variety of coupling constants $V$. The total number of excitations is $M = 25$ and the bosonic frequency is set to $\omega = 6.95$ in the middle of the energy band.

The dynamics being a process of exchange of excitations, we could have expected that an infinite time would compensate a weak coupling and allows the system to behave as if it has an infinite coupling. For every different value of the couplings $V$, we observe a different magnetisation for the spins, i.e. a different steady state. Consequently, the idea that regardless of the value of $V$ (as long as it is not 0) our system would thermalise to a common state given an infinite time is wrong. Thus, depending on the strength of the coupling, a system driven to the steady steady under $H_{TC}$ will reach or not a superradiant-like state. We define, to simplify our explanation, $V_{sup}$ the coupling needed to reach a superradiant-like steady state, it is the coupling for which the value of the local magnetisation is $\langle S_i^z \rangle < 10^{-2} \forall i$. It is the very existence of the different steady states as functions of $V$ that get closer and closer to be superradiant-like as $V$ increases that supports our idea of thinking in terms of a pseudo-dynamics where $V$ plays the role of a time. This pseudo-dynamics relying on a distinction of the steady states depending on couplings highlights the fact the integrability does limit the redistribution of the local excitations inside the system even when it has an infinite time to do it.

We observe that the spins, in the steady states presented in Fig.4.1, tend to be plane-polarised for the blue curve corresponding to $V = 10$, which sets $V_{sup} \approx 10$ for the reference initial state. For weaker values of $V$, $\langle S_i^z \rangle > 10^{-2}$ for at least two spins (the ones near the edge). Coming from highly entropic initial spin configuration, we expect $V_{sup}$ to be smaller than for any other initial spin configuration. Additionally, we can guess that another aspect that could enhance the efficiency of redistribution of the local spin excitations is precisely having a lot of excitations available. Increasing $M$, the number of total of excitations, is necessarily synonym of increasing the number of bosonic excitations once all the spins are excited. That is why we emit the hypothesis that increasing $M$ may help the system to reach a superradiant-like steady state, in other words, to lower $V_{sup}$ (see subsection 4.2.5) because it has at its disposal more bosons help the redistribution.

One last phenomenon visible in Fig.4.1 we want to comment is the impact for the spins to have their associated energies $\epsilon_i$ near the frequency of the bosonic mode $\omega$. We can clearly notice in Fig.4.1 a phenomenon of resonance. Indeed, the more the associated energy of a spin is close to $\omega$, the weaker coupling it needs to be polarised in the plane. For $\epsilon_7$, we can even assume that any non-zero coupling is enough for it to be polarised in the plane at $t \to \infty$. The phenomenon of resonance associates to resonant energies highly efficient exchange processes. It can be understood for systems that evolve under a TC Hamiltonian. Contrarily, if we choose any $R_i$ (2.35), as Hamiltonian, their is no change in the efficiency of the exchanges between the spins and the bosons regarding their associated energies because only one spin is coupled to the bosons. This supports the consistency of using the TC dynamics as comparison point. Therefore, we can even say that the steady states we are observing are the results of a relaxation from a reference state, with a strong efficiency occurring at the resonance, evolving with $V$. Nevertheless, thinking of this pseudo dynamics of the steady states evolving with $V$ through a TC vision helps to understand the phenomenon of resonance but it should not be mistaken with the real time evolution of a system evolving under the $H_{TC}$ that will be presented in chapter 5.

Thus, we advice the reader to keep in mind that this initial configuration of the reference state, highly entropic in the spin sector with a bosonic mode $\omega$ in the middle of the energy band, favours the capability of the system to reach a superradiant-like steady state.

Let us focus on the steady state of the bosonic occupation. The total number of excitations $M = \langle b^\dagger b \rangle + \langle S_z^{tot} \rangle$ being constant, this quantity will be complementary to the total magnetisation. In Fig.4.2 we can observe from which coupling the mean number of bosons almost stops to change and so from which coupling the system is only reorganising itself in the spin sector, the bosons becoming strictly a medium available for the spins to exchange excitations. We would like to recall here the TC Hamiltonian, $H_{TC} = \omega b^\dagger b + \sum_{j=1}^{N} \epsilon_j S_j^z + V \sum_{j=1}^{N} (b^\dagger S_j^- + S_j^+ b)$ to keep in mind that in this case the spin collection does need the bath to be able to exchange excitations. Indeed, in this reference state we have a system which is almost only reorganising in term of spin excitations from $V \approx 6$ by reading the coupling for which the bosonic occupation $\langle b^\dagger b \rangle = 17.5 \pm 0.02$ (red curve), 17.5 representing a state where the total magnetisation along

Figure 4.2: Bosonic occupation in the steady-state for the initial state: $|17;\uparrow\downarrow\uparrow\downarrow\uparrow\downarrow\uparrow\downarrow\uparrow\downarrow\uparrow\downarrow\uparrow\rangle$ as a function of $V$. The total number of excitations is $M = 25$ and the bosonic frequency is set to $\omega = 6.95$ in the middle of the energy band.

the z axis cancels, i.e. the spins are half excited (dashed black curve). We notice a really weak overshoot occurring from $V = 10$, it contradicts the hypothesis of a monotonic evolution to a fully plane polarised steady state. Moreover, it will force us to verify if the system does correct this overshoot when the coupling is pushed further.

In order to further prove what we claimed in this section regarding the fact that this highly entropic initial state is favouring a superradiant-like steady state, we now look at a radically different initial spin configuration, which this time is explicitly chosen to have low entropy. Having every spin down polarised and pushing moreover the bosonic frequency near the edge of the available spin gaps, we therefore have a configuration which, at low coupling, would be at very high energy in the global TC Hamiltonian spectrum. Close to the edge of the spectrum, the low density of states should prevent efficient relaxation.

We observe in Fig.4.3 that even with a coupling of 12, which is above the reference state's $V_{sup}$, our spins are not yet plane polarised which confirms our assumption that an initial spin configuration highly entropic would give us the smallest $V_{sup}$. Nevertheless, by presenting a plot where the superradiant-like state is not reached, we can wonder if it is possible to asymptotically attain this state. The presence of a substantial overshoot, for the spins whose associated energy is far from $\omega$ and for couplings $V \geqslant 5$, adds additional doubts about whether the system does reach a superradiant-like steady state at $V \to \infty$ with this initial spin configuration and
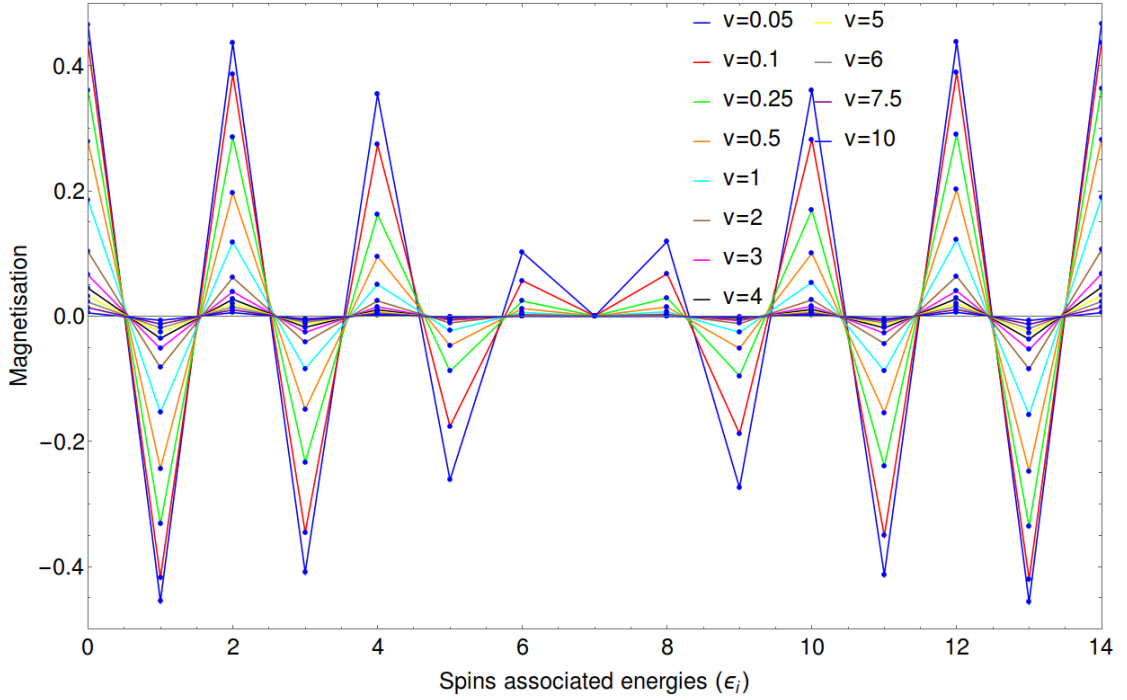
Figure 4.3: Local magnetisation in the steady-state for the initial state: $|25; \downarrow\downarrow\downarrow\downarrow\downarrow\downarrow\downarrow\downarrow\downarrow\downarrow\downarrow\downarrow\downarrow\downarrow\downarrow\downarrow\rangle$ as a function of $V$. The total number of excitations is $M = 25$ and the bosonic frequency is set to $\omega = 13.5$ near the maximum of the energy band.

this value of $\omega$. To comment further, even at $V = 12$ we still see important deviations (for spins with gaps $\epsilon_i$ far from $\omega$) from the state where the spins are fully in-plane polarised. Indeed the low index spins (small gaps) have actually acquired a weak up polarisation, while at this value of the coupling, the highly entropic state did reach an in-plane polarised steady state configuration. Thereby, Fig.4.3 completes Fig.4.2 by showing where the overshoot is occurring locally: it appears far from the resonant spins. Consequently, we show what happen when we push the coupling further to investigate if the system is able to correct this overshoot.

In Fig.4.4 we present plot of $\langle S_i^z \rangle$ for couplings between $V = 0.05$ and $V = 60$. We observe that in such a case, being far (high order in the spin configuration is as far as possible from a superradiant-like spin configuration, by having a total magnetisation the furthest possible from zero) from a supperradiant-like state, still involves a $V_{sup}$ much greater than in the reference state. Moreover, we have to push the number of excitations up to $M = 50$ to be able to observe for $V = 40$ and $V = 60$ a correction for the overshoot previously mentioned. The idea that increasing $M$ is helping the redistribution of the excitations can be confirmed by looking at the spin of index 0 in Fig.4.4 and in Fig.4.3 at $V = 1$, the mean value of the magnetisation is closer to 0 when there is more excitations. This confirms the hypothesis that having a lot of excitations available to carry out the redistribution enhances it. Eventually, in spite of these

Figure 4.4: Local magnetisation in the steady-state for the initial state: $|50; \downarrow\downarrow\downarrow\downarrow\downarrow\downarrow\downarrow\downarrow\downarrow\downarrow\downarrow\downarrow\downarrow\downarrow\rangle$ as a function of $V$. The total number of excitations is $M = 50$ and the bosonic frequency is set to $\omega = 13.5$ near the maximum of the energy band.

unfavourable conditions, the system approaches to the fully plane polarised state for a very strong coupling and we can imagine that it should even reach that state with a coupling even stronger (and with more excitations), unfortunately we were not able to push our numerics for a greater $V$. Nevertheless, this plot supports the idea that the fully plane polarised state should be the final state in every case for a strong enough coupling. These observations also support our vision of a pseudo-dynamics evolving with the coupling because the system has an infinite time to reorganise, so different initial spin configurations should lead to the same steady states, but this is not what we are observing, it is highly coupling dependent. In other words, when the orientation of the spins and $\omega$ are already tuned, the two "weapons" we have to help the system to reach a superradiant-like steady state is to increase $V$ and/or $M$.

We will study with more details the effects that prevent the system from reaching such a state in the next subsections and illustrate, with more examples, the phenomena noticeable in the reference state. We will therefore study how the frequency of the bosonic mode, the initial spin configuration and the total number of excitations will affect this pseudo dynamics and our capability of reaching this final state of reference.

### 4.2.2 Resonance with the bosonic mode $\omega$

We now describe what is happening to the steady state when we explicitly change the value of $\omega$ to confirm the observation made through the reference state that resonant spin get in plane-polarised at weak coupling.

We start the discussion by showing four graphics of the local magnetisation of four different states differing by their value of bosonic frequency $\omega = 13.5, 10.5, 6.95$ and $0.5$. Doing so, we are able to discuss two cases where $\omega$ will be near one extreme value of one $\epsilon_i$ and far from the other extreme value, another case where $\omega$ is the same as in the reference case, in the middle of the value of the $\epsilon_i$ and one intermediate case. The initial spin configurations are fully down polarised states for the four graphics so we will only discuss the effect of the bosonic mode in this subsection.
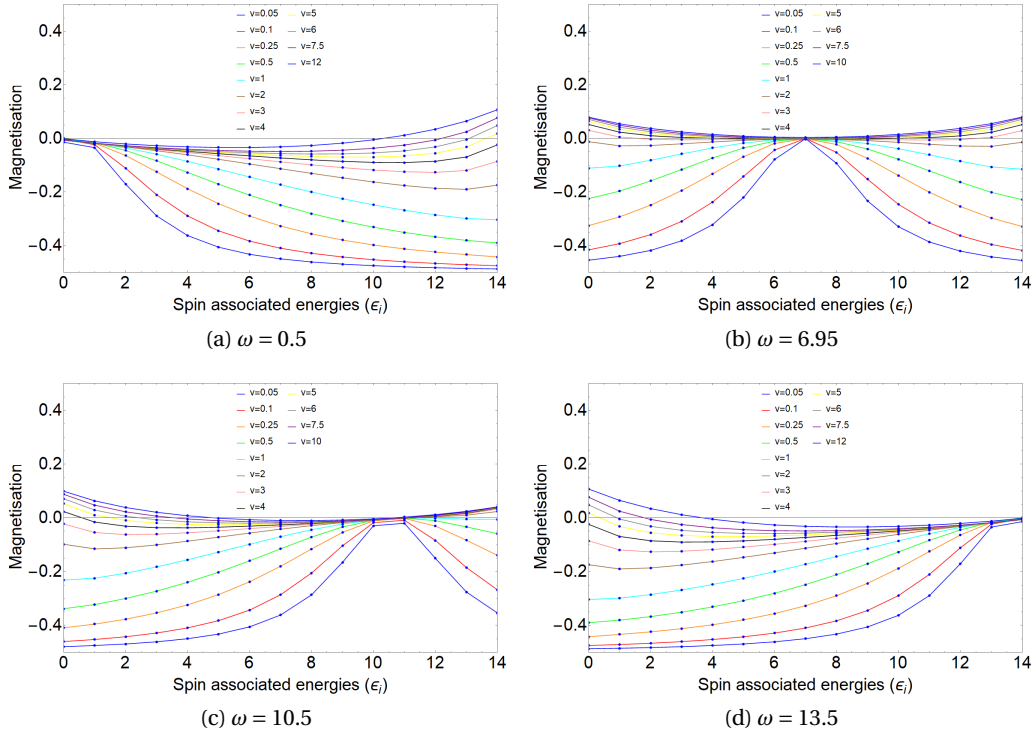


Figure 4.5: Local magnetisation in steady states for the initial state: $|25; \downarrow\downarrow\downarrow\downarrow\downarrow\downarrow\downarrow\downarrow\downarrow\downarrow\downarrow\downarrow\downarrow\downarrow\rangle$ for a variety of coupling constants $V$ and four different bosonic frequencies. The total number of excitations is fixed at $M = 25$.

First of all, in the four group of plots presented the local magnetisation does not fit to our criterion $\langle S_i^z \rangle < 10^{-2} \forall i$, we even have $\langle S_i^z \rangle > 10^{-2} \forall i$. The system is not able to reach a state as plane polarised as the reference state for $V = 10$ (or even $V = 12$), even when $\omega = 6.95$. From that point we confirm that $V_{sup}$ is greater for the fully down polarised initial spin configuration than for the reference initial state. A more detailed discussion about the impact of the initial spin configuration is presented in the next subsection. Through these graphics, we also

confirm that for the spins whose associated $\epsilon_i$ are near $\omega$ the coupling is more effective than far from $\omega$. Indeed the value of the local magnetisation for near-resonant spins is almost equal for a weak coupling, $V = 0.05$ for instance, as for a greater coupling, for instance $V = 10$.

While, in a purely TC like model, this type of resonant behaviour makes perfect sense since since spin-flips whose gap corresponds to the bosonic frequency would be favoured, one needs to keep in mind the fact these results would also apply for a "central spin" Hamiltonian with only the central spin coupled to the bosonic mode. In other words, in the TC case the bath of bosons continuously exchanges excitations with all the spins, it flips them up and receives the excitations when they flip down, these processes being very effective at the resonance. The spins can only communicate and exchange excitations among themselves through the bosonic bath. Whereas in a central spin case, the bosonic bath flips only one spin and has to wait for its de-excitation in the collection of remaining spins to be able to give it another excitation. Thus, the evolution under these two Hamiltonians is substantially different but, because they share the same steady states, in chapter 5 we study the real time dynamics associated to these Hamiltonians to have a better understanding of their differences.

On the other hand, one could expect the local magnetisation to exhibit a monotonic behaviour in $\omega - \epsilon_i$. However, particularly clear for $V = 2$ in panel (b), the non-monotonic behaviour in $\omega - \epsilon_i$ does not find a simple intuitive explanation in the TC model. But, when considering the other underlying conserved charges, the terms $\frac{\vec{S}_i \cdot \vec{S}_j}{\epsilon_i - \epsilon_i}$ make it clear that the distance from the resonance $\omega - \epsilon_i$ is not the only parameter controlling individual spins, but the "position" of their individual gap compared to the other spins' gap will also affect its behaviour.

The fact that any given integrable model in the class studied here can show steady state properties which is not intuitively seen by looking exclusively at its Hamiltonian is one of the main conclusions of this work. Every evolution of the same initial spin configuration with $N$, $M$, $\omega$ and the $\epsilon_i$ equal leads to the same steady state because the conserved quantities are identical in every cases, they play the same role. However, because we are considering different combinations of them, the Hamiltonians, to rule the evolution of a given system, the dynamics will be different.

In Fig.4.6 a plot of the bosonic resonance for the four same states only differing by $\omega$ is presented. The curves for $\omega = 0.5$ and 13.5 (red and dashed black ones) in Fig.4.6 are identical and that indicates a symmetry between these two states in their global behaviour. In these two cases, the roles of the spin of index 0 and of the one of index 14 are exchanged. By comparing these two curves with the two last ones (blue and green), we can notice they cross the line, (undershoot) showing the number of bosons present when the total magnetisation of the system cancels (black line), for a greater $V$. This undershoot in bosons is complementary of the overshoots in magnetisation of Fig.4.5. In the previous section, we saw that an overshoot in magnetisation is occuring before the spins become plane-polarised, so the sooner it is reached the smaller $V_{sup}$ should be. Thus we can conclude that the more $\omega$ differs from the middle of the energy band, the greater $V_{sup}$ is. This conclusion is highly dependent on the
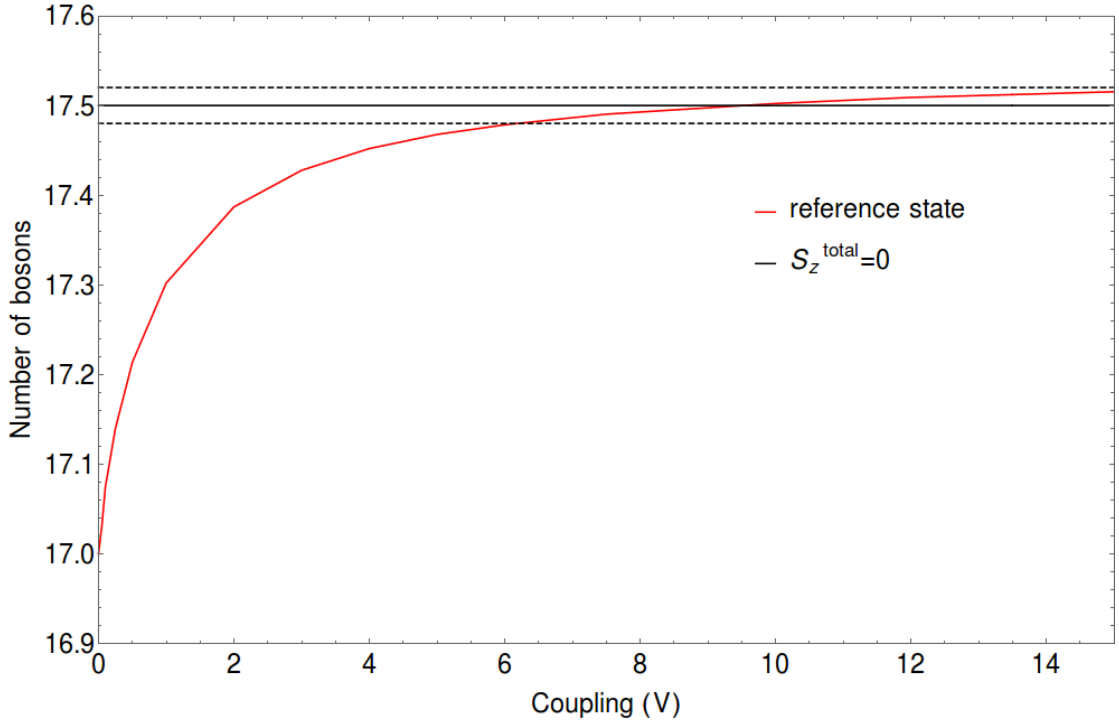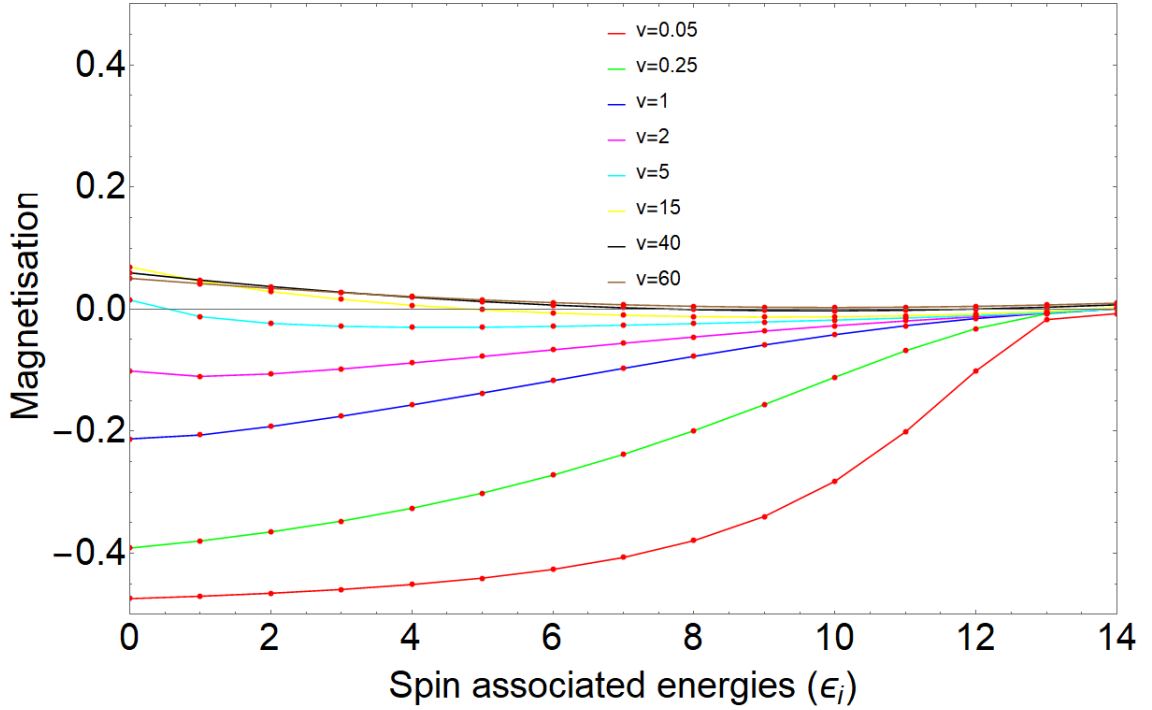
Figure 4.6: Bosonic occupation in steady states for the initial state: $|25; \downarrow\downarrow\downarrow\downarrow\downarrow\downarrow\downarrow\downarrow\downarrow\downarrow\downarrow\downarrow\downarrow\downarrow\downarrow\rangle$ for a variety of coupling constants $V$. The total number of excitations is $M = 25$ and the bosonic frequency are set to $\omega = 0.5, 6.95, 10.5, 13.5$.

definition we have chosen for $V_{sup}$. Indeed, only one spin can prevent a coupling from being defined as $V_{sup}$ by having a non-zero magnetisation. Having $\omega$ in the middle of the energy band lower the maximum difference $\omega - \epsilon_i$ possible and therefore favours the possibility to have a weak $V_{sup}$.

The plots in Fig.4.7, showing the local magnetisation for the same initial spin configuration as in the reference case, illustrate perfectly what we have been able to confirm all along in this subsection. Indeed, only $\omega$ (here it is equal to 0.5) differs from the reference graphic and we can clearly observe the system can not reach the fully plane polarised state for $V = 12$, more particularly for the $\epsilon_i$ far from $\omega$ despite the fact the spins are alternated, in their initial configuration, as for the reference state. Even at those coupling, we still still see a strong memory of the initial which retains the initial spin configuration which is precisely the topic of the next subsection.

### 4.2.3 Initial state

In this section we discuss the importance of the initial spin configuration through the four graphics of Fig.4.8 showing the steady state of the local magnetisation when the initial spin configurations are different.
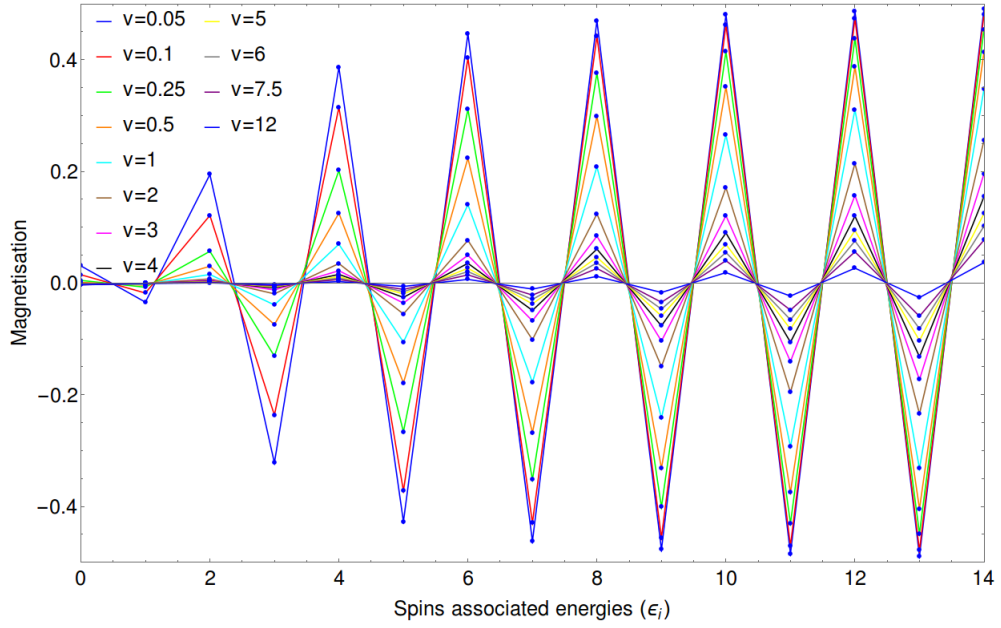
Figure 4.7: Local magnetisation in the steady state for the initial state: $|17; \uparrow\downarrow\uparrow\downarrow\uparrow\uparrow\downarrow\uparrow\downarrow\uparrow\uparrow\downarrow\uparrow\downarrow\uparrow\rangle$ for a variety of coupling constants $V$. The total number of excitations is $M = 25$ and the bosonic frequency is set to $\omega = 0.5$, near an edge of the energy band.

In Fig.4.8 four graphics of local magnetisation are shown, graphic (c) is the reference one we recall to help the comparisons. For the three others we start from an initial spin configuration less entropic than in the reference graphic. As a result, we see that in each case $V_{sup}$ is higher than in the reference state ($V_{sup} = 10$), because some local magnetisation do not cancel for $V = 10$ in (a), (b) and (d). The bosonic frequency being fixed in the middle of the energy band for each plot, we study here the impact of the initial spin configuration on the steady state. The main differences between the reference initial state and the one in (a) are the total magnetisation of the system, which are respectively 0.5 and −7.5 and the neighbouring environment of each spin. In the reference state each neighbouring spin is alternated whereas all the spins are pointing in the same direction in the other case. The total magnetisation of the fully plane polarised state is zero, so one argument to explain why $V_{sup}$ is smaller in the reference than in all the cases presented in this subsection is that the initial state of reference is simply closer in total magnetisation to a steady state fully plane polarised. Moreover, we can extend the analysis made for (a) to (b) and (d) as well and affirm that $V_{sup}$ is clearly a function of the initial configuration of the spins. This impact of the initial spin configuration enables us to introduce the notion of the memory of the initial configuration. The more an initial spin configuration prevent the system from reaching a superradiant-like state, the more the memory of the initial state is strong. Thus, we can say that a state highly entropic in its spin sector will have a weak memory of its initial configuration and so will lower $V_{sup}$.

We now explain what is locally the effect of an alternation of spins. We can observe that this divergence from the reference steady state is happening mostly when the spins in their initial

Figure 4.8: Local magnetisation in steady states for various initial states and for a variety of coupling constants $V$. The total number of excitations is $M = 25$ and the bosonic frequency is set to $\omega = 6.95$.

configuration are not alternated, by looking at the spin of index 1 and 13 in the graphic (d), and also when the energy $\epsilon_i$ of the spins is far from $\omega$ (as explained in the previous section). The initial spin configuration of graphic (d) has been chosen to have the least recognisable patterns as possible, that is why we can observe many local different spin configurations. In graphic (d), comparing the ensemble of spins with indexes 3,4 and 5 to the one of spins with indexes 9,10 and 11 confirms that an initial alternated spin configuration favours a steady state plane polarised. Therefore, we understand that even locally the configuration of spins in the initial state has an impact. Indeed, for a spin having its neighbours oriented in the same direction prevent it from reaching a plane polarisation. So we can say that there is a memory of the initial state, even locally, and that its effect competes with the coupling so starting far from the a strict alternation of spins, which is the most favourable initial state, involves $V_{sup} > 10$.

The graphic Fig.4.9, showing the bosonic occupation in terms of $V$, illustrates the effect of the alternation of spins on the global system. The curves representing the evolution of the bosonic occupation of states containing entropic spin configuration in their initial states (green and black ones) reach their final values, corresponding to a cancelling total magnetisation among the z axis, for $V \approx 8$ whereas the two other curves are still decreasing for $V = 15$. This behaviour confirm that an entropic initial state in the spin sector is favouring a fully plane polarised steady state. Another aspect Fig.4.9 is confirming is that having more excitations helps the
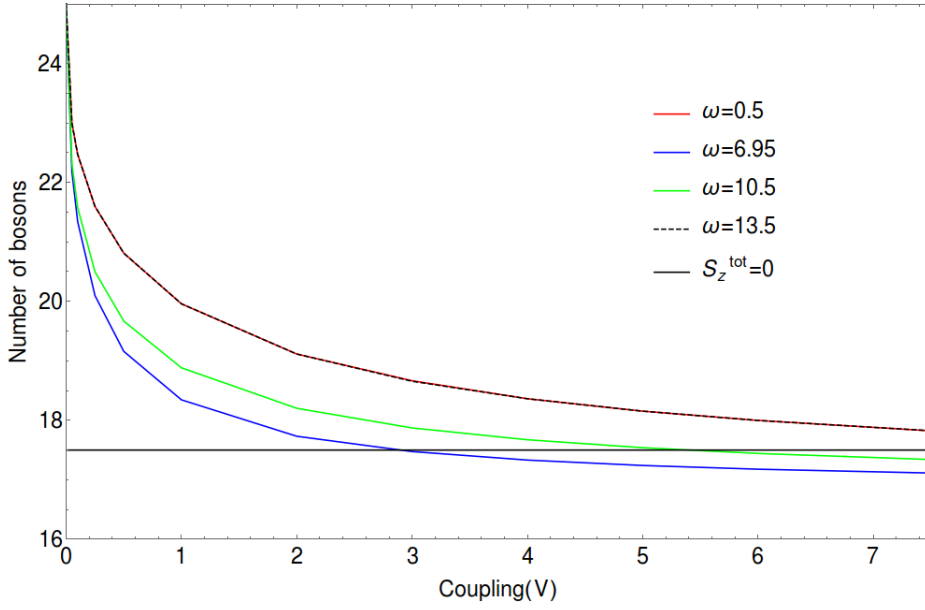
Figure 4.9: Bosonic occupation in the steady state for various initial states: $|25;\downarrow\downarrow\downarrow\downarrow\downarrow\downarrow\downarrow\downarrow\downarrow\downarrow\downarrow\downarrow\downarrow\downarrow\uparrow\rangle$, $|23;\downarrow\downarrow\downarrow\downarrow\downarrow\downarrow\downarrow\downarrow\downarrow\downarrow\downarrow\downarrow\downarrow\uparrow\uparrow\rangle$ and $|16;\uparrow\downarrow\uparrow\uparrow\downarrow\uparrow\downarrow\downarrow\uparrow\uparrow\uparrow\uparrow\uparrow\downarrow\downarrow\rangle$ as a function of $V$. The total number of excitations is $M = 25$ and the bosonic frequency is set to $\omega = 6.95$.

redistribution of the excitations. It is visible when looking at the curves corresponding with initial state containing more bosonic excitations (blue and red ones), their slopes is more important than the ones of green and black curves. Nonetheless, in that scenario, having more initial bosonic excitations implies having an initial spin configuration with few spin alternations which prevent the system from reaching a superradiant-like steady state. As a conclusion, the memory of an initial spin configuration closer to a fully planed polarised one is more efficient than having a lot of bosons in the cases presented in this subsection.

The next subsection deals with what happens to the system when a spin flip occurs near the resonance.

### 4.2.4 Spin flip at the resonance

In this subsection, we discuss the outcome of a spin alternation occurring at the resonance by comparing two plots (Fig.4.10) with the same initial state in terms of spin configuration. All the spins are pointing down except the two last ones pointing up in both cases (as for the second graphic of the last subsection), the only difference being the frequency of bosonic mode.

In Fig.4.10, we present two plots of the local magnetisation. For plot (b), both an alternation in the spin orientation in the initial state and the resonance occur in the same area. We

(a) $\omega = 0.5$

(b) $\omega = 13.5$

Figure 4.10: Local magnetisation in steady-states for two initial states for a variety of coupling constants $V$ : $|23; \downarrow\downarrow\downarrow\downarrow\downarrow\downarrow\downarrow\downarrow\downarrow\downarrow\downarrow\downarrow\uparrow\uparrow\rangle$ in both case but for two different bosonic frequencies. The total number of excitations is $M = 25$.

observe in (a) that the resonance and the spin flip occur far enough so that the two different effects do not affect each other. For this graphic, all the visible phenomena have already been explained in the previous subsections, either the resonance far from $\omega = 6.95$ and the initial spin configuration prevent the system from reaching the fully plane polarised state for $V = 7.5$ ($V_{sup} > 7.5$). The memory of the initial state we introduced in last subsection has two main consequences: an initial alternated spin configuration lower $V_{sup}$ and for weak $V$ the spins have a local magnetisation near their initial one (except near $\omega$). In (b) we observe that the resonance almost kills the effect of the memory of the initial state in its vicinity, near $\omega = 13.5$, it is hard to guess the initial state of the spins of indexes 13 and 14. The system has almost lost the information about its initial spin configuration because redistributions of the excitations is very effective there. However, in plot (b), it is visible that the memory of the initial state is not entirely killed at the resonance.

### 4.2.5 Excitation number M

Having already discussed that a large number of bosonic excitations might enhance the capability of the system to reach a fully plane-polarised state for the spins for a small coupling, we present here different plots of the local magnetisation for different values of $M$.

Fig.4.11 shows four different plots of the local magnetisation: (a) and (b) have a fully up initial polarisation and differ by $M$ wherehas (c) and (d) have a fully down initial polarisation and differ by $M$. We will compare (a) and (b) then (c) and (d) to confirm our assumption on the impact of having a lot of bosonic excitations available. Knowing that without the introduction of the bosonic bath, the initial configuration fully up and fully down are equivalent, we will as well compare (a) and (c) then (b) and (d) to see if this equivalence holds with the presence of the bosonic bath.

The behaviour of the system confirms the initial guess: the more total excitations $M$ there are,

(a) Initial state: $|0; \uparrow\uparrow\uparrow\uparrow\uparrow\uparrow\uparrow\uparrow\uparrow\uparrow\uparrow\uparrow\uparrow\uparrow\uparrow\rangle$

(b) Initial state: $|85; \uparrow\uparrow\uparrow\uparrow\uparrow\uparrow\uparrow\uparrow\uparrow\uparrow\uparrow\uparrow\uparrow\uparrow\uparrow\rangle$

(c) Initial state: $|15; \downarrow\downarrow\downarrow\downarrow\downarrow\downarrow\downarrow\downarrow\downarrow\downarrow\downarrow\downarrow\downarrow\downarrow\downarrow\rangle$

(d) Initial state: $|100; \downarrow\downarrow\downarrow\downarrow\downarrow\downarrow\downarrow\downarrow\downarrow\downarrow\downarrow\downarrow\downarrow\downarrow\downarrow\rangle$
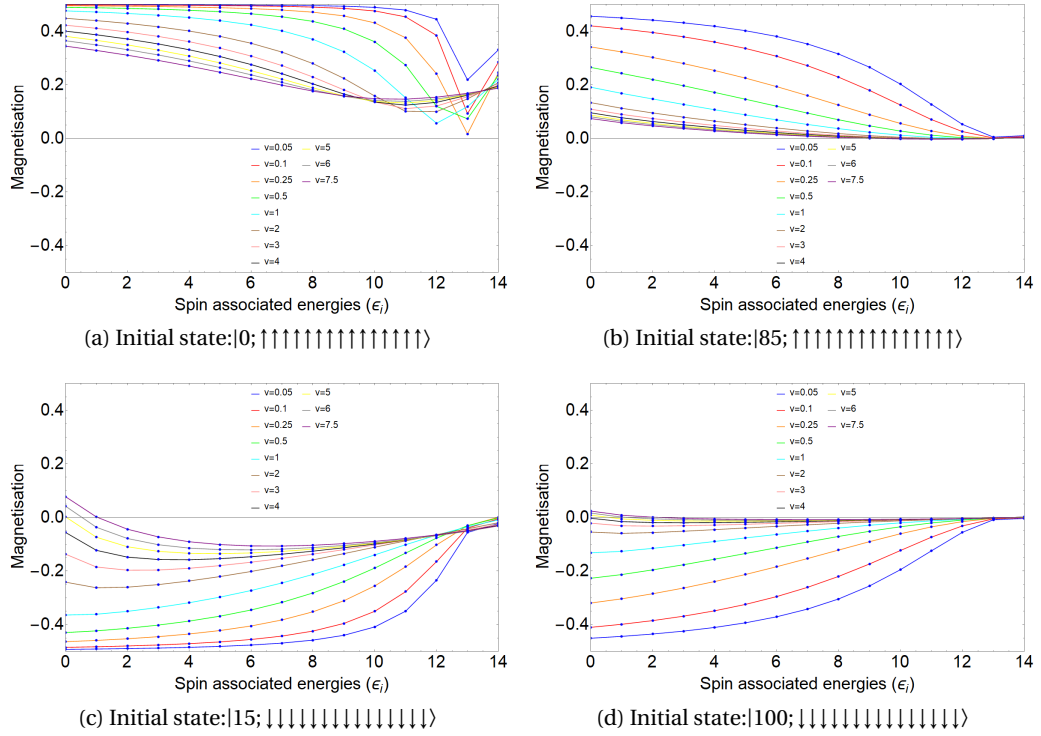
Figure 4.11: Local magnetisation in steady-states for various initial states and for a variety of coupling constants $V$. The total number of excitations is $M = 15$ for (a) and (c) and $M = 100$ for (b) and (d) and the bosonic frequency are set to $\omega = 13.5$ (because the effects are more visible than when we take $\omega = 6.95$).

the more $V_{sup}$ is small. This can be seen with the couples of plot (a) and (b) or (c) and (d), the magnetisation of the spins is closer to be zero for (b) and (d) than for (a) and (d) for all the spins and for any coupling. Thus, the previous conclusion can be rephrased in: you reach a given magnetisation state within a smaller $V$ when you have more bosonic excitations. That also explains why the two curves at $V = 7.5$ are different, it is because having an important number of bosonic excitations "accelerates" the effect of the coupling. This analysis enables to understand the interest of being able to modify the total number of excitations easily in our numerics because we have different steady states in terms of magnetisation just by changing $M$ [58]. In plot (a), because the initial spin configuration is fully-up polarised, there is absolutely no boson a $t = 0$ in the system. This explains why the redistribution of the energies seems to be really inefficient for the spins of indexes 12, 13 and 14, even being near the resonance. The absence of bosons leading to an inefficient redistribution process, it corroborates the fact that having a lot of them enhances it. Having explained in subsection 4.2.3 that there is a memory of the initial polarisation of the spins at weak coupling, by promoting a fully plane polarised steady state the bosonic excitations favour a loss of memory of the initial spin configuration.

We now, use the couples of plots (a) and (c) then (b) and (d), to state if there is a difference or not in having an initial fully up or fully down polarised. For a spin-$\frac{1}{2}$ only realisation, going

from fully up to fully down is equivalent to change the axis of quantification which induces no differences. The comparison between the couples previously mentioned, i.e. between a fully up polarised initial state and a fully down one, at fixed number of excitations, shows it is not possible to obtain (a) from (c) or (b) from (d) only by changing the axis of quantification. In both cases, the local magnetisation is positive for the spins of indexes 0 and 1 from a certain coupling $V$. More precisely, in (a), the local magnetisation stays positive for every coupling and every spin presented, in (b) the local magnetisation stays positive (or very close to zero) as well and in (c) and (d) the local magnetisation of spins of indexes 0 and 1 becomes positive for respectively $V = 7.5$ and $V = 6$. It clearly indicates that the system possesses a preferred direction of magnetisation that is not existing in the absence of bosonic bath. Thus adding a bosonic bath even with zero bosonic excitations at $t = 0$, as in plot (a) of Fig.4.11, changes with certainty the dynamics and the steady states of our systems. It is not surprising because adding an empty bosonic bath enables the excited spins to transfer their excitations to bosonic bath (if the coupling is not zero). This difference was introduced in subsection 2.2.1 where it was explained why $|M;\uparrow\uparrow \ldots \uparrow\rangle$ is not a proper vacuum (i.e. being eigenstate of $S^2(u)$) state whereas $|0;\downarrow\downarrow \ldots \downarrow\rangle$ is. Having such a deep distinction in the definition of their associated pseudovacuum is the reason why we are witnessing a preferred polarisation direction in Fig.4.11. This preferred polarisation direction explains the visible overshoot at strong coupling for initial down polarised spin configurations and the reluctance of the up polarised spins to go to a zero polarisation. Eventually, having bosons in interaction with the collection of spins-$\frac{1}{2}$ has several different impacts: it favours the redistribution of the excitations and by promoting the up polarisation, it causes an overshoot over the zero magnetisation for the spins originally down and slows down the progression to a zero magnetisation for the spins originally up.

The four curves of Fig.4.12 represent the available bosonic occupation (normalised by the number of spins) in terms of $V$ of the four cases whose local magnetisation has been previously studied in this subsection. In fact, the finite number of spins N means that, for M>N a minimal number of bosons M-N will always be present since the system can only accommodate N spin excitations. While for $M = N = 15$, we plot $b^\dagger b / N$, for $M = 100$ we first remove $M - N$ from the occupation and plot the fraction of available bosons $b^\dagger b - (M - N)/N$ which are present in the steady state. The global behaviour of the system in those cases, studied here through the evolution of the number of bosons, confirms what we just have explained. The black line representing a zero total magnetisation is approached for weaker $V$ when the initial spin configuration is down polarised because the up polarisation is a favoured direction. Indeed for $M = 15$, the polarisation population of bosons is varying more when the initial state is up polarised (red curve) than down polarised (blue curve), i.e. the bosons are giving with more efficiency their excitations to the spins to flip them than when they are accepting excitations from the spins when they flip down. Comparing the curves corresponding to $M = 15$ (blue and red) with the ones corresponding to $M = 100$ (green and black) confirms that having more bosonic excitations enhances the global redistribution of the excitations in the system because in Fig.4.12 we see that the green and the black curve reach for a weaker coupling $V$ the state of
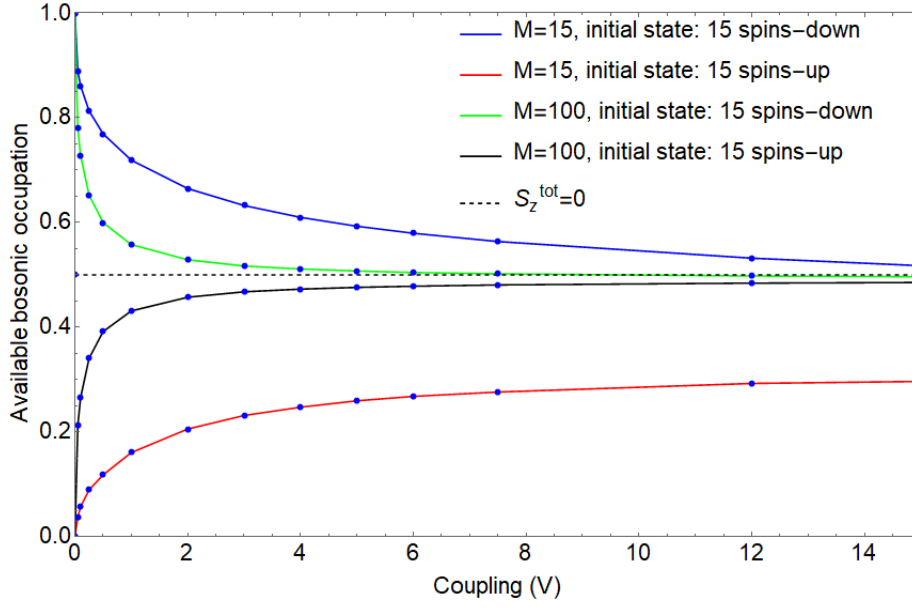
Figure 4.12: Available bosonic occupation (divided by the number of spins) in the steady-state for various initial states:$|0;\uparrow\uparrow\uparrow\uparrow\uparrow\uparrow\uparrow\uparrow\uparrow\uparrow\uparrow\uparrow\uparrow\uparrow\uparrow\rangle$, $|85;\uparrow\uparrow\uparrow\uparrow\uparrow\uparrow\uparrow\uparrow\uparrow\uparrow\uparrow\uparrow\uparrow\uparrow\uparrow\rangle$, $|15;\downarrow\downarrow\downarrow\downarrow\downarrow\downarrow\downarrow\downarrow\downarrow\downarrow\downarrow\downarrow\downarrow\downarrow\downarrow\rangle$ and $|100;\downarrow\downarrow\downarrow\downarrow\downarrow\downarrow\downarrow\downarrow\downarrow\downarrow\downarrow\downarrow\downarrow\downarrow\downarrow\rangle$ as a function of $V$. The bosonic frequency is set to $\omega = 13.5$.

zero total magnetisation. It corroborates the fact that $V_{sup}$ is smaller for systems containing an important number of bosonic excitations.

Eventually, in all the subsections, we showed that comparing $V$ to a time was consistent to describe every effect that occurs in our system in our attempt to describe its behaviour without using an analytic description. Indeed all the conjectures made through the graphic analysis of the reference state have been confirmed.

Finally, the many conjectures have been done in subsection 4.2.1 have all been confirmed in the other subsections: having an initial state highly entropic in the spin sector, a bosonic frequency in the middle of the energy band and an important number of available bosonic excitations favours the capability of the system to reach a fully plane polarised (superradiant-like) steady state for a weak coupling $V$. It supports our vision of the evolution as a function of the coupling of the steady states, i.e. the system tries to relax to a superradiant-like steady state but the local conserved charges prevent this scenario from happening for weak coupling. Eventually, can say that all along this section, the pseudo dynamics in $V$ for the steady states we derived was a satisfying picture that enabled us to understand the asymptotic physics of the systems we are considering.

In the next subsection we complete our study by following individually the evolution of few spins.

### 4.2.6   The complexity of the evolution of one spin

Through a plot of the local magnetisation of four spins as a function of the coupling $V$, we aim to show that access precisely to the evolution of each spin as a function of $V$ would be a difficult task.
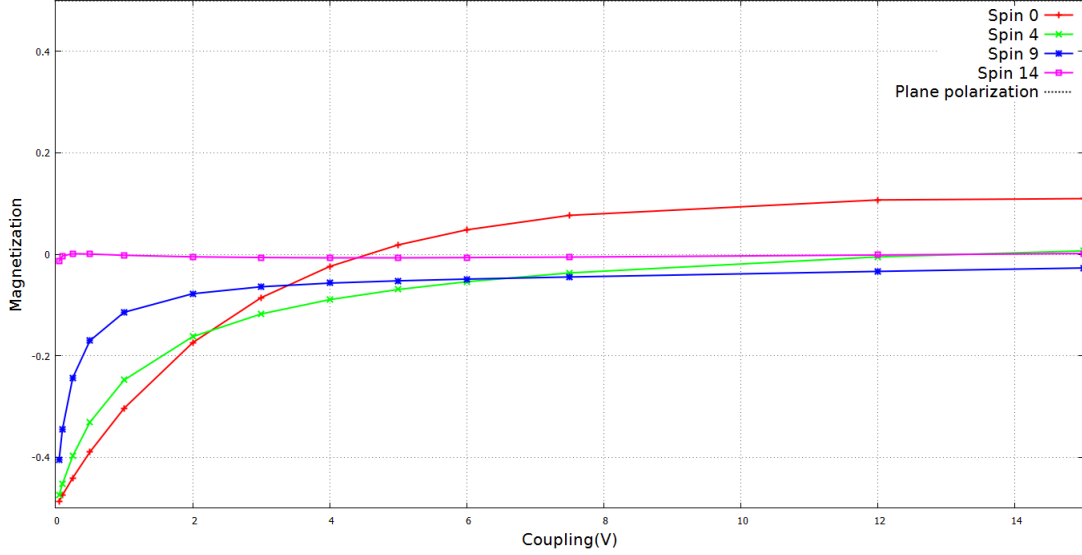


Figure 4.13: Local magnetisation of four spins, associated with $\epsilon_0, \epsilon_4, \epsilon_9$ and $\epsilon_{14}$ when $V$ goes from 0 to 15 with $M = 25$ and $\omega = 13.5$.

Fig.4.13 shows the evolution as a function of $V$ of the four spins, with associated energies $\epsilon_0$, $\epsilon_4$, $\epsilon_9$ and $\epsilon_{14}$, from the following initial state $|25; \downarrow\downarrow\downarrow\downarrow\downarrow\downarrow\downarrow\downarrow\downarrow\downarrow\downarrow\downarrow\downarrow\downarrow\downarrow\rangle$ with the bosonic frequency set at $\omega = 13.5$. In other words, because $V_{sup} > 15$ in such a case, these the magnetisation of these four spins should not be zero together. At first glance, we see that the behaviour of the magnetisation is really different regarding $\epsilon$, at $V = 15$ their magnetisation is not the same and they do not reach this value with the same way of evolving. We can also notice that as we said before, the spin whose associated $\epsilon_i$ is the nearest of $\omega$ reaches its final value for a weaker coupling than other spins. Moreover, even isolated none of these curves shows a power law or an exponential decay so we could not capture their behaviour by trying to fit them to well-known functions. However, we discovered by trying to fit these curves that there exist mainly two regimes in the evolution of the magnetisation, one for weak values of the coupling and one for strong values. We will study with more details these two regimes through the real time dynamics in next chapter.

## 4.3   Comparison between the diagonal ensemble and the Generalised Gibbs Ensemble

Our previous study in the DE was done numerically and was, de facto, quantitative. Another ensemble that can be used to carry out efficient quantitative calculations for quantum integrable models is the Generalised Gibbs Ensemble (GGE). It has the same philosophy as the Gibbs canonical ensemble but it is taking into account other conserved quantities than the energy of the system to describe the steady states of integrable models. In this section, the GGE is introduced in a first part. We explained how is define the density matrix of such an ensemble and how we numerically compute the large time expectation values of observables of interest. The second part of this section compares results obtained in the DE and in the GGE in specific cases.

### 4.3.1   Obtaining the Lagrange multipliers of the density matrix

Since it has been introduced by Rigol et al [51], the GGE has been studied a lot being able to predict the mean value of observables at large time for integrable models. It is supposed to be able to describe the steady state, after equilibration, of isolated quantum integrable systems. Even if the systems we are considering are composed of a collection of spins-$\frac{1}{2}$ interacting with a bath of bosons, the global system is isolated, it does not interact with an external environment and so the total number of excitations is conserved. Moreover, in our case the proximity between the expressions, of the scalar products in the spin-$\frac{1}{2}$ realisation (1.39) and in the spins-$\frac{1}{2}$ boson realisation (4.2) for instance, confirms that even if our spins-$\frac{1}{2}$ collection is interacting with a bath of bosons, our systems are isolated and a description by the GGE could still be considered. It is a statistical representation where we can write, as in the canonical ensemble, a density matrix dependent of the initial conditions. Thus, the mean value of a given observable $\hat{O}$ in the GGE is simply given by:

$$\langle \hat{O} \rangle_{GGE} = \text{Tr} \left[ \rho_{GGE} \hat{O} \right], \tag{4.7}$$

with

$$\rho_{GGE} = \frac{1}{Z_{GGE}} e^{-\sum_k \beta_k R_k}, \quad Z_{GGE} = \text{Tr} \left[ e^{-\sum_k \beta_k R_k} \right]. \tag{4.8}$$

The density matrix $\rho_{GGE}$ is normalised by the partition function $Z_{GGE}$, the $R_k$ are the conserved quantities of our model defined in (2.35) and the $\beta_k$ are the Lagrange multipliers we fix, as in the canonical ensemble with the temperature, by looking at the initial values of every conserved quantity of the model:

$$\langle \psi_0 | R_j | \psi_0 \rangle = \text{Tr}\left[\rho_{GGE} \hat{R}_j\right] = \frac{1}{Z_{GGE}} e^{-\sum_k \beta_k R_k} R_j. \tag{4.9}$$

Despite the fact that an unitary quantum evolution can not lead to a statistical relaxation, it is normal that the GGE does not describe the global system behaviour. But, we can wonder if this statistical ensemble could describe the local observables in the steady state of a given integrable model.

The purpose of this section is to oppose results obtained in the DE as in 4.2 to results obtained in the GGE. We want to know if the dynamics at very large time of the models ruled by the XXX Generalised Gaudin Algebra can be predicted by the use of the GGE. The question is worthy to ask because in certain integrable cases it has been shown that the GGE as it is defined in (4.8) does not give correct results, see [84, 85], (for the Heisenberg XXZ anisotropic spin-$\frac{1}{2}$ chain).

The first step to be able to carry out the quantitative study of the Gaudin models in the GGE, is to compute numerically the Lagrange multipliers appearing in (4.8). We find them numerically by solving the following set of equations, whose variables are the $\beta_k$:

$$F_j = \sum_{\dim \mathscr{H}} \left[ \frac{e^{-\sum_k^N \beta_k r_k^h} r_j^h}{\sum_{\dim \mathscr{H}} \left[ e^{-\sum_k^N \beta_k r_k^{h'}} \right]} \right] - \langle \psi_0 | R_j | \psi_0 \rangle = 0, \tag{4.10}$$

which directly comes from (4.9). In (4.10), the sum over the dimension of the Hilbert space ($\sum_{\dim \mathscr{H}}$) goes over the elements with the index $h$ (or $h'$ for the sum present in the denominator). Because the coefficients $F_j$ depend of sums running on all the Hilbert and because these sums will need to be recalculated at each loop of our algorithm, solving these equations is actually a heavy numerical task. Once again to solve this set of equations we are using a multi-linear Newton's algorithm as the one used in chapter 3. Therefore, we need to define the Jacobian matrix $J_F$ of $F$ whose elements are given by:

$$
\begin{aligned}
\frac{\partial F_j}{\partial \beta_i} &= \frac{\partial}{\partial \beta_i}\left(\mathrm{Tr}\left[\rho_{GGE} R_j\right] - \langle \psi_0 | R_j | \psi_0 \rangle\right) \\
&= \sum_{\dim \mathcal{H}} \frac{r_j^h\left((-r_i^h)e^{-\Sigma_k^N \beta_k r_k^h}\sum_{\dim \mathcal{H}} e^{-\Sigma_k^N \beta_k r_k^{h'}} + e^{-\Sigma_k^N \beta_k r_k^h}\sum_{\dim \mathcal{H}} r_i^{h'} e^{-\Sigma_k^N \beta_k r_k^{h'}}\right)}{Z_{GGE}^2}.
\end{aligned}
$$

$$(4.11)$$

In the expression of the matrix elements of the Jacobian matrix we have to deal with double sums over the dimension over the Hilbert space which add one order of magnitude in the number of operation needed numerically. Fortunately, the expression of the $r_j^h$ (2.39) belongs to the numerically efficient expressions, depending on the $\Lambda_i$, we derived. Knowing every matrix element of $J_F$, the Newton's algorithm will converge to our set of $\beta_i$ denoted $\vec{\beta}_l$ (with the index $l$ denoting the $l^{th}$ loop of the Newton's algorithm), solutions of (4.10), using the following update:

$$
(\vec{\beta}_{l+1} - \vec{\beta}_l) J_F(\vec{\beta}_l) = F(\vec{\beta}_l).
$$

$$(4.12)$$

The Jacobian matrix requiring also a lot of numerical resources has also to be recalculated at each loop. As a consequence, in this case the Newton's algorithm is not efficient to use numerically by containing many times the sum over the dimension of the Hilbert space. As one will see in next chapter, the computation using the GGE is more laborious than our computation to find the real time dynamics of a given system. This study using the GGE is more a curiosity on the validity of the description than a presentation of a practical numerical method to access the steady states of quantum integrable models.

### 4.3.2   Local magnetisation in the GGE and in the DE

In this subsection we present plots of the local magnetisation for small systems, one of $N = 7$ spins-$\frac{1}{2}$ and $M = 13$ total excitations and one of $N = 7$ spins-$\frac{1}{2}$ and $M = 113$ total excitations working in both ensembles. The method to obtain the large time expectation values of the local magnetisation in the DE is the same as the one used in the section 4.2 and the method used to obtain these expectations values in the GGE has been detailed previously in subsection 4.3.1. A comparison of the expectation values of the local magnetisation obtained in those two ensembles is carried out to see if there is differences, in the steady state, for local observables. The comparison is done graphically by trying to superpose curves representing the local

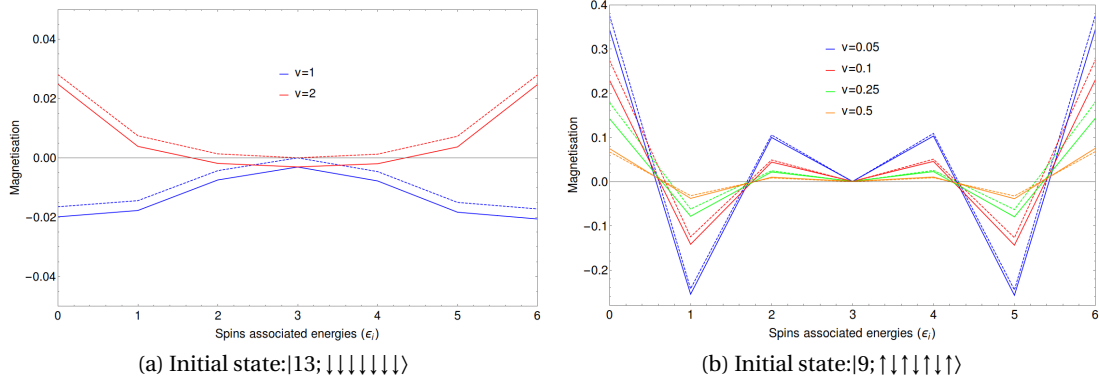magnetisation obtained using the GGE to curves obtained using the DE.



(a) Initial state:$|13; \downarrow\downarrow\downarrow\downarrow\downarrow\downarrow\rangle$      (b) Initial state:$|9; \uparrow\downarrow\uparrow\downarrow\uparrow\downarrow\uparrow\rangle$

Figure 4.14: Local magnetisation in steady-states for two initial states for a variety of coupling constants $V$. The total number of excitations is fixed at $M = 13$ and the frequency of the bosonic mode is set at $\omega = 2.99$. The dashed lines represent results obtained by using the GGE whereas the full lines represent results obtained in the DE.

In Fig.4.14, we see that the curves corresponding to the local magnetisation obtained through the GGE, in (a) and (b), do not superpose to the ones we can get using the DE, so we can directly conclude that the GGE does not give satisfying results in every case. Indeed, the dashed lines do not strictly overlap the full lines in the presented plots (a) and (b). The local magnetisation was though an appropriate candidate to a potential description by the GGE. Therefore, one important conclusion we can already make is that the GGE as it is defined in the last subsection fails to perfectly describe the results one can find for the XXX Gaudin models. Nevertheless, we can study how the validity of a GGE description is affected by the parameters of our system, i.e. $\omega$, $M$ and the initial spin configuration. Thus using Fig.4.14 and Fig.4.15, we give few more details about how the parameters act on the discrepancies between the GGE and the results given by the DE.

For a coupling $V = 0$, the descriptions using the two ensembles are trivially equal because it is the definition we have chosen (4.9). Looking at Fig.4.14 (b), the gap between the curves obtained using the GGE and the ones obtained using the DE increases with the coupling between $V = 0.05$ ($V = 0$ in fact) and $V = 0.25$ and is reduces for $V = 0.5$. Indeed, the easiest way to arrive at this conclusion is to look at the spin whose associated energy is $\epsilon_0$ in (b), the gap between the dashed lines and the full lines is smaller for $V = 0.05$ and $V = 0.5$ than for $V = 0.1$ and $V = 0.25$. In a nutshell, it seems we are witnessing a range of coupling that worsens the validity between GGE and DE and then, when the coupling increases, the validity seems to be better.

In Fig.4.14, the two curves presented are almost translated, which excludes the conclusion that near the resonance of the bosonic mode $\omega = 2.99$, the validity between GGE and DE is always better than far from it. Moreover, by looking at both Fig.4.14 and Fig.4.15 and comparing 14(a) to 15(a) and 14(b) to 15(b), we can study the impact of $M$ on the validity between GGE and

(a) Initial state:$|113;\downarrow\downarrow\downarrow\downarrow\downarrow\downarrow\downarrow\rangle$  (b) Initial state:$|109;\uparrow\downarrow\uparrow\downarrow\uparrow\downarrow\uparrow\rangle$
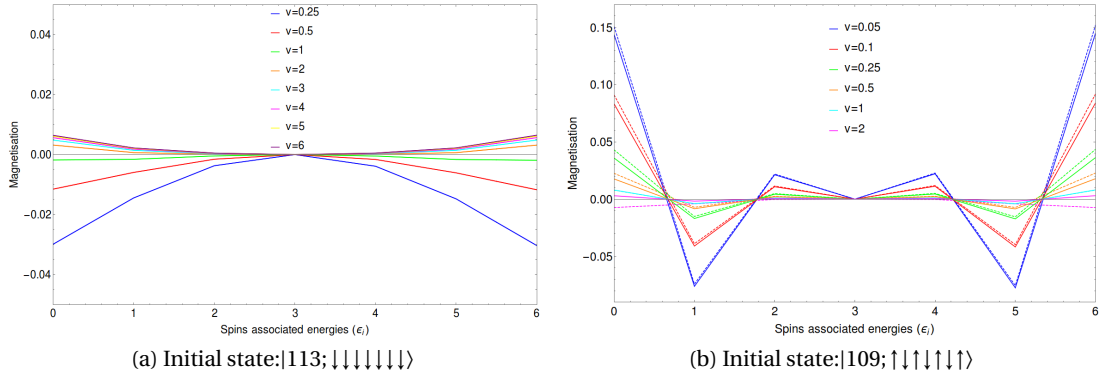
Figure 4.15: Local magnetisation in steady-states for two initial states for a variety of coupling constants $V$. The total number of excitations is fixed at $M = 113$ and the frequency of the bosonic mode is set at $\omega = 2.99$. The dashed lines represent results obtained by using the GGE whereas the full lines represent results obtained in the diagonal ensemble.

DE. We could naively expect that increasing $M$ would dampen the discrepancies between the two ensembles. The gap between the dashed lines and the full lines in Fig.4.15 (a) is really tenuous which, with respect Fig.4.14 (a) may confirm our expectation. Yet, comparing plot (b) in Fig.4.15 and Fig.4.14 contradicts the previous assumption because we can observe in Fig.4.15 (b) that the gap at $V = 2$ is clearly greater than the one for $V = 0.5$ in Fig.4.14 (b). For the initially completely down polarised we have considered, increasing the number of bosonic is improving the agreement between the two ensemble whereas it is not what we are observing for state with a highly entropic initial spin configuration. Therefore we can say, that the bosonic excitations propensity to improvement the validity is dependent on the initial spin configuration.

The graphical comparison carried out in this section shows that we can not use the GGE as it is defined to predict the steady states of our rational Gaudin models. It is not necessarily surprising because we could have expected that the definition of the GGE presented in this section contains an insufficient set of conserved quantities to be able to describe the behaviour of observables in the steady state as it is the case for some other isolated quantum systems. In [86], it is shown that for Majorana free fermions treated in Quantum Field Theory, the GGE needs that non local laws of conservations are taken into account in the definition of the density matrix of the GGE. In addition, it was also shown in [84, 85] that the GGE was not able to describe the Heisenberg XXZ spin-$\frac{1}{2}$ chain which is integrable by comparing to results obtained by a quench-action method. Once again, the problem lies in the locality of the conserved charges. Adding quasi-local conserved charges seems to have enabled to describe an adapted GGE to the problem of the Heisenberg chain [87].

The conserved charges we are considering (2.35) contain a local term $(\epsilon_i - \omega) S_i^z$ and non-local terms $\sum_{j\neq i}^{N} \frac{2V^2}{\epsilon_i - \epsilon_j} \vec{S}_i \cdot \vec{S}_j$. By assuming the GGE, as we defined it, correctly fixes the value of our conserved charges in the numerical treatment we are using, we would get the right values

for the local magnetisation only when the mean value of the non-local terms would cancel (meaning the spins would be orientated randomly). However in 4.2, provided the coupling is of the order of $V_{sup}$ or above, in the steady state we can observe a fully plane polarisation of the spins along the z axis (what we have called superradiant-like state) which is clearly opposed to have spins orientated randomly. That is why the numerical discrepancies we have between the GGE and the DE are not surprising in our case even if the systems we are working with are integrable and isolated.

## 4.4 Conclusions

In this chapter, we have explicitly studied the steady states of a class of quantum integrable models: The rational (XXX) Richardson-Gaudin models. The objectives were numerous, the mathematical work has a numerical interest, we made use of it to obtain plots of the local magnetisation and the bosonic occupation of the XXX Gaudin models and finally we derived a global vision of the behaviour of these models relying on these plots.

First of all, we wanted to highlight the rewriting of the form factors using our new variables, the $\Lambda(\epsilon_i)$, that enabled us to work very efficiently in the DE. Then, we explained repeatedly the asymptotic properties of our spins collection through a dynamical vision with the coupling $V$ as evolving parameter. This repetition aimed to convince the reader the consistency of this vision. The constant comparison with one particular Hamiltonian among our whole class, the TC Hamiltonian, chosen because it describes the phenomenon of resonance with the bosonic frequency (which is visible on our plots), helped the interpretation of the results. We want to insist on TC interpretation in this conclusion, even though all the content of this thesis is valid for any combination of conserved quantities. To summarise briefly what had been said in the section 4.2 about the numerical results, for any of their initial configuration, the spins tend to relax to a superradiant-like (fully plane polarised) steady state provided the coupling with the bosonic bath is strong enough, we called the coupling necessary to reach that steady state $V_{sup}$. For a highly entropic initial spin configuration, a frequency of the bosonic mode $\omega$ in the middle of the energy band and a great number bosonic excitation, $V_{sup}$ is minimal. However when the coupling is smaller than $V_{sup}$, the relaxation towards a plane polarisation for all the spins is interrupted. The very existence of $V_{sup}$, a critical coupling leading to a fully plane polarised steady state, is in total accordance with the results of [43], where it is shown that the superradiance phase is reached in the TC model above a critical value of the coupling $g_c$.

Finally, numerical computations considering smaller systems showed that the Generalised Gibbs Ensemble, as it was defined in this chapter, is not suitable in many cases to describe the steady states of the rational Gaudin models. It can be understood by looking at the expression of the conserved quantities we are considering, they contain non-local interaction. We observed an agreement between the predictions of the GGE and the results obtained in the DE only for a fully down-polarised spin configuration coupled to an important number of bosonic excitations.

The question of the formulation of the conserved quantities only in terms of particle number operators of the GGE is asked in [88],[89] because integrability allows the existence of stable particles. Thus expressing the GGE in terms of particle content would ensure that we are working with right conserved quantities. In the case of Gaudin models there would be an interest of finding $N$ adapted conserved quantities among the infinity we dispose.

# 5 Real Time Dynamics

From chapter 4, we know that regardless the Hamiltonian ruling the dynamics, a given initial state always leads to the same steady state. The purpose of this section is to study, through data corresponding to small systems sizes, how the Hamiltonian determines the way we reach this steady state. The fact we are considering small systems sizes is not altering deeply the physics, it is just increasing the influence of the finite size effects. Therefore, the numerical data taken into account in this chapter is enough to draw conclusions on the dynamics of rational Gaudin models but only constitutes preliminary calculations that call for another study at bigger system sizes. As in chapter 4, we are able to extract a lot of information with a simple graphic analysis by comparing different plots. While in chapter 4 no particular choice of Hamiltonian was required, we need for the work done in this chapter to chose a Hamiltonian to rule the time dynamics. In order to study this intermediate regime, we compare the evolution of different systems ruled by two different Hamiltonians. This chapter will also answer important questions: Does the the local magnetisation of the system reach a final value ? Or, do we still observe strong oscillations at infinite time ? Does the system really relax ?

This chapter is divided in two main parts. The first one introduces the Hamiltonians we work with and how we can obtain the real time dynamics of our systems. Finally, the second part follows the same construction as section 4.2, i.e. for each subsection the influence of a parameter is discussed. The study of the dynamics we present in this chapter relies on a comparison between the influence of two Hamiltonians (belonging to class of Gaudin Hamiltonians): the Tavis-Cummings Hamiltonian and a "central spin" one. The two dynamics corresponding to these two Hamiltonians will be different and this is not surprising because the excitations redistribution processes are very different. In the TC Hamiltonian case, all the spins are exchanging excitations only with the bosonic bath and this exchange is very efficient at the resonance whereas, in the case corresponding to the "central spin" Hamiltonian, only one spin is exchanging its excitation with the bosonic bath and this same spin is also coupled to the remaining spins. In a nutshell, in the TC case the bosonic bath acts as a medium for the spins to exchange excitations together while in the "central spin" case one particular spin act as a medium for the spins to exchange excitations with the bosonic bath.

## 5.1 Two different Hamiltonians

The expression (4.1) of the mean value of an observable $\hat{O}$ at a given time $t$ was introduced in the section 4.1. In this chapter, it is the real time dynamics we are interested in and we are directly using this expression of the mean value without any approximation. Firstly, we are not reduced to the DE any more which means we have to incorporate, on top of the $2^N$ the scalar products $\langle \psi_0 | n \rangle$, the $2^{2N}$ matrix elements $\langle n | \hat{O} | m \rangle$ which drastically increases the numerical resources required for our computations. Additionally, due to the presence of oscillating terms $e^{i(E_n - E_m)t}$, we have to explicitly use the eigenvalues of the Hamiltonian which governs the dynamics of a considered system.

We remember here that to belong to the class of Hamiltonians for which the results presented in this thesis apply, a Hamiltonian needs to be of the form $H = \sum_i^N \alpha_i R_i + \beta \hat{M}$ ( with the $\alpha_i$ and $\beta$ arbitrary naturals coefficients, the $R_i$ given by (2.35), $N$ the number of spins and $\hat{M}$ defined in (2.2.3)). We have extended the definition of $H$ given in 1.4 to the spin-$\frac{1}{2}$-boson case by adding $\beta \hat{M}$ to it, $\hat{M}$ being also a conserved quantity (our ensemble collection of spins and bosonic bath being an isolated system). Having in mind that we want to obtain very different dynamics leading to the same steady states, we chose to numerically study $H_0 = R_0$, a collection of spins coupled to a bosonic bath through the spin of index 0 and $H_{TC} = \sum_i^N R_i + \omega \hat{M}$ as in section 5.2. Explicitly our Hamiltonians are equal to:

$$H_0 = (\epsilon_0 - \omega) S_0^z + V\left(b^\dagger S_0^- + b S_0^+\right) + \sum_{j \neq 0}^N \frac{2V^2}{\epsilon_0 - \epsilon_j} \vec{S}_0 \cdot \vec{S}_j, \tag{5.1}$$

and

$$
\begin{aligned}
H_{TC} &= \sum_{i=1}^N \left( (\epsilon_i - \omega) S_i^z + V\left(b^\dagger S_i^- + b S_i^+\right) + \sum_{j \neq i}^N \frac{2V^2}{\epsilon_i - \epsilon_j} \vec{S}_i \cdot \vec{S}_j \right) + \omega \left( b^\dagger b + \sum_{i=1}^N S_i^z \right) \\
&= \omega b^\dagger b + \sum_{i=1}^N \epsilon_i S_i^z + V \sum_{i=1}^N (b^\dagger S_i^- + S_i^+ b) + \sum_{i=1}^N \sum_{j \neq i}^N \frac{2V^2}{\epsilon_i - \epsilon_j} \vec{S}_i \cdot \vec{S}_j \\
&= \omega b^\dagger b + \sum_{i=1}^N \epsilon_i S_i^z + V \sum_{i=1}^N (b^\dagger S_i^- + S_i^+ b),
\end{aligned}
\tag{5.2}
$$

where $\sum_{i=1}^N \sum_{j \neq i}^N \frac{2V^2}{\epsilon_i - \epsilon_j} \vec{S}_i \cdot \vec{S}_j$ cancels when computing the full sum due to the antisymmetry of its denominator. One noticeable difference between these two is that in the Tavis-Cummings

case all the spins exhibit a similar overall behaviour a part from their distance from the resonance whereas in the $H_0$ case the spin coupled to bosons should show a radically different dynamics from the remaining spins.

In the next section, we present the numerical results we obtained through plots of the real time dynamics of the local magnetisation and bosonic occupation for a small system size. Having to compute the double sum over of the dimension of the Hilbert space present in (4.1), considering a small system size enabled the numerics to be handled relatively quickly without having access to clusters of calculations.

## 5.2  Numerical Results

One should keep in mind that, regardless of the of the Hamiltonian, a given initial state will always lead to the same steady state. Therefore, even if the plots we present will differ at finite time $t$, since we are considering two different Hamiltonians, for infinite time the mean values, of the local magnetisation and of the bosonic occupation, we are presenting become equal.

### 5.2.1  Global difference between the two dynamics

First quantity we will look at, bosonic occupation, will describe the global behaviour of a given system. In the last section, we introduced the idea that looking at the local value of the magnetisation of a system can not offer many information on the global behaviour of the system when the dynamics is ruled by $H_0$. Indeed, the behaviour of a spin will be different whether we are considering the one coupled to the bosonic bath or not. Thus, to be able to compare the global dynamics of a system under $H_0$ or $H_{TC}$, we are studying the relaxation of a purely bosonic state through the evolution of the expectation value of the bosonic occupation. Up to subsection 5.2.6, we will only consider fully down polarised initial spin configuration reducing the problem to a bosonic bath emptying its excitations into a collection of spins down.

Fig.5.1 presents two plots of the time evolution of the bosonic occupation, one ruled by $H_{TC}$ (a) and one by $H_0$. The different curves of (a) reach the values they will keep in their steady states within the range of time presented whereas in (b) the curves have not reached their asymptotic values within the same range of time (except for $V = 2$). Most of our analysis relies on the extraction of an approximate characteristic time for which a given observable expectation value has reached its asymptotic value (due to the remaining finite-size oscillations). For instance, in the case of the red curve of Fig.5.1 (a), the characteristic time would be approximately $\tau = 10$ meaning that the number of bosons will simply fluctuate around its asymptotic value for a time larger than $\tau$.

First of all, an important results of Fig.5.1 is that the expectations values of the bosonic occupation do reach a true steady state (we highly expect it to be true for the magnetisation),
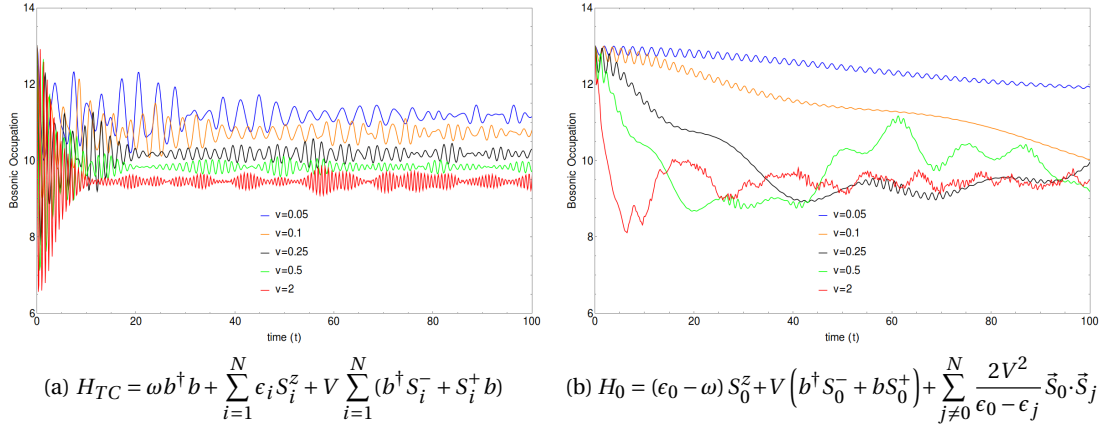
(a) $H_{TC} = \omega b^\dagger b + \sum_{i=1}^{N} \epsilon_i S_i^z + V \sum_{i=1}^{N} (b^\dagger S_i^- + S_i^+ b)$ 　　(b) $H_0 = (\epsilon_0 - \omega) S_0^z + V \left( b^\dagger S_0^- + b S_0^+ \right) + \sum_{j \neq 0}^{N} \frac{2V^2}{\epsilon_0 - \epsilon_j} \vec{S}_0 \cdot \vec{S}_j$

Figure 5.1: Evolution of the bosonic occupation as a function of the time for a variety of coupling constants $V$ governed by two different Hamiltonians. The initial state is $|13; \downarrow\downarrow\downarrow\downarrow\downarrow\downarrow\rangle$ and the bosonic mode is set at $\omega = 2.99$ in both cases.

after a relaxation of the system during a characteristic time. We observe that in the case of $H_{TC}$ the expectation values reach their coupling dependent asymptotic values within a characteristic time $\tau$ going from $\tau \approx 40$ (for $V = 0.05$) to $\tau \approx 10$ (for $V = 2$). Thus, the relaxation of the bosons is faster when the coupling with the collection of spins increases, in other words the more the bosons are coupled to the spins the faster they redistribute their excitations. The same phenomenon is seen in (b) for $H_0$, however at weak coupling the relaxation is slower than $H_{TC}$. The plots (a) and (b) are presented for the same time span, we can see without any doubt that in the case of $H_0$, the characteristic times are larger than for $H_{TC}$, up to $V = 2$, where the characteristic time seems to be of the same order in (a) and (b). We give a physical explanation to this behaviour in $H_0$: when the bosonic bath gives an excitation to the only spin coupled to it, it has to wait the reorganisation of the spins among themselves to be able to give another excitation to the coupled spin (the spin flip from up to down to give its excitation to the spins), this is a very long-lasting process at weak coupling whereas at strong coupling this bottleneck in the exchanges has disappeared, the coupled spin is always available to receive an excitation.

In the Tavis-Cummings case, the bosonic bath can exchange its excitations with all the spins enabling the systems to reach his asymptotic global configuration for the bosonic excitations efficiently even at weak coupling . Having in mind this global difference between two systems ruled by $H_{TC}$ or $H_0$, we will now use the numerical data about local magnetisation to complete the analysis we have just made by studying the local dynamics of a system.

### 5.2.2 Resonance with the bosonic mode

In 4.2.2, we learned that the more the associated energy $\epsilon_i$ of a spin is close to the frequency of the bosonic mode $\omega$, the more this spin has a near zero magnetisation along the z axis in

the steady state. For a time bigger than $\tau$, we will recover this behaviour, nevertheless in this subsection we wonder if the being close to the bosonic resonance influences the dynamics of a system as well. To answer this interrogation, we plot for $H_{TC}$ the local magnetisation time dynamics of four spins, one of them, in (b), is near the resonance and another one, in (d), is at the edge of the energy band.



Figure 5.2: Evolution of the local magnetisation of four different spins as a function of the time for a variety of coupling constants $V$ governed by $H_{TC}$. The initial state is $|13; \downarrow\downarrow\downarrow\downarrow\downarrow\downarrow\downarrow\rangle$ and the bosonic mode is set at $\omega = 2.99$ in every case.

To begin with, we can notice on the plots (a) and (c) of Fig.5.2 that the dynamics of the spins is symmetric with respect to $\omega$. Indeed, absolute values of the difference between the associated energies of $S_1$ and $S_5$, read $\epsilon_1 = 1$ and $\epsilon_5 = 5$, and $\omega$ are (almost) equal and the long time averages at all time of the local magnetisations in both plot (a) and (c) are identical. Additionally, by looking at the four plots, we have, as expected, long-time averages of the local magnetisation around zero for weaker $V$ when the associated energy of the spin of interest is closer to $\omega$.

Finally, by looking at all the curves for $V = 1$, we can observe that the characteristic time $\tau$ is not very different, it is easy to see in (a), (c) and (d) by looking at the cyan curve that $\tau \approx 20$, we also find $\tau \approx 20$ for the black curve in (b). Thus, in every case and for all the values of the coupling, their is no striking effect of the resonance on the characteristic time, it only affects the value of the local magnetisation in the steady state towards which the spins will relax.

### 5.2.3 A spin coupled to the bosonic bath

We now compare the dynamics of the spin of index 0 (we will write $S_0$), the only one coupled to the bosons in the "central spin" case. This spin is therefore coupled to the bosonic bath in both the Tavis-Cummings and the "central spin" cases .



$$\text{(a) } H_{TC} = \omega b^\dagger b + \sum_{i=1}^{N} \epsilon_i S_i^z + V \sum_{i=1}^{N} (b^\dagger S_i^- + S_i^+ b) \qquad \text{(b) } H_0 = (\epsilon_0 - \omega) S_0^z + V\left(b^\dagger S_0^- + b S_0^+\right) + \sum_{j\neq 0}^{N} \frac{2V^2}{\epsilon_0 - \epsilon_j} \vec{S}_0 \cdot \vec{S}_j$$
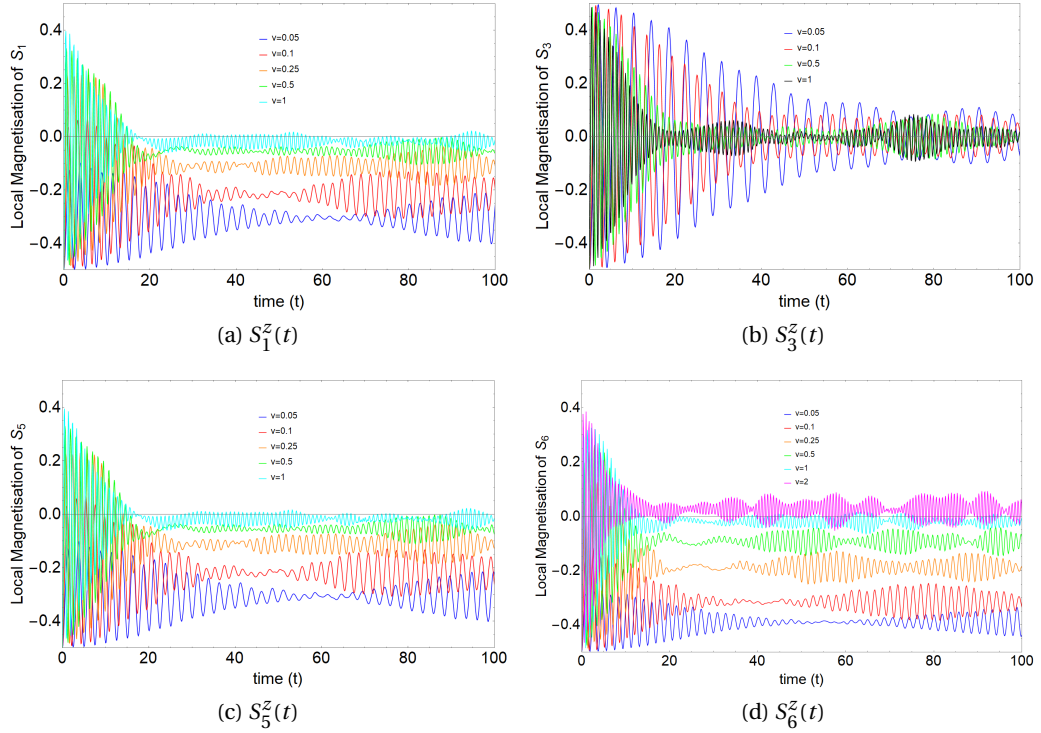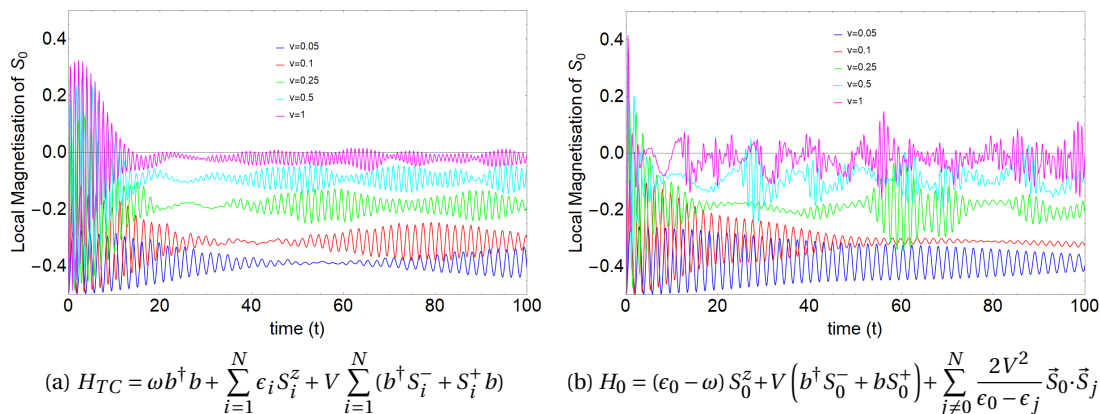
Figure 5.3: Evolution of the local magnetisation $S_0^z$ as a function of the time for a variety of coupling constants $V$ governed either by $H_{TC}$ or $H_0$. The initial state is $|13; \downarrow\downarrow\downarrow\downarrow\downarrow\downarrow\rangle$ and the bosonic mode is set at $\omega = 2.99$ in every case.

At first glance, we can observe a lot of differences between the two plots of Fig.5.3 which leads us to think that the choice of Hamiltonian has a substantial impact even when considering a spin coupled to the bosonic bath in both cases. Nevertheless we start by giving a similarity in the behaviour of the local magnetisation shown in the plots (a) and (b). By comparing the amplitudes of the oscillations around the asymptotic values of the local magnetisation for every couplings $V$, we can observe that these amplitudes are close for both Hamiltonians (except for $V = 1$). However, the striking difference in the dynamics presented in (a) and (b) is the evolution of the characteristic time $\tau$ with the coupling $V$. For $V = 0.05$ and $0.1$, $\tau_{TC}$ (the characteristic time in the Tavis-Cummings case) is smaller than $\tau_0$ (the characteristic time in the "central spin" case). Then for $V = 0.25$, the difference between $\tau_{TC}$ and $\tau_0$ becomes tenuous to finally find $\tau_{TC} > \tau_0$ for $V = 1$. This phenomenon can be explained by looking at the expressions of $H_{TC}$ and $H_0$. When governed by $H_{TC}$, the system has to reorganise itself to reach his steady state only through the interaction spin-boson $V\sum_{i=1}^{N}(b^\dagger S_i^- + S_i^+ b)$ whereas in the "central spin" case the system relies on two terms, $V\left(b^\dagger S_0^- + b S_0^+\right)$ and $\sum_{j\neq 0}^{N} \frac{2V^2}{\epsilon_0 - \epsilon_j} \vec{S}_0 \cdot \vec{S}_j$. A possible interpretation is that for $V < 1$, a system, whose dynamics is ruled by $H_{TC}$, is more efficient to distribute its excitations to each spin trough the bosonic bath than a system, whose dynamics is ruled by $H_0$, trough the only spin coupled to the bosonic bath due to the presence of $V^2$ in $\sum_{j\neq 0}^{N} \frac{2V^2}{\epsilon_0 - \epsilon_j} \vec{S}_0 \cdot \vec{S}_j$. Then for $V > 1$ this "central spin" system would be more efficient to organise its excitations among the collection of spins-$\frac{1}{2}$ trough this hyperfine interactions between the spins, still due to the presence of $V^2$ rather than $V$. Looking, at the plots describing the dynamics of $S_0$ illustrates a new mechanism of relaxation at strong

coupling.

Having talked about the differences between a spin coupled to the bosonic bath in the Tavis-Cummings case and in the "central spin" case, we describe, in the next subsection, the differences between a spin which is not coupled to the bosonic bath in the "central spin" while being coupled to the bosonic bath in the Tavis-Cummings case (as every spin).

### 5.2.4 A spin non-coupled to the bosonic bath

In this subsection, we deal with the case of a spin which is not coupled to the bosons in the "central spin" case. Once again we study the time dynamics of the local magnetisation of the considered spin, $S_1$ this time. On the one hand, in the Tavis-Cummings case this spin is coupled to the bosons and the only difference between $S_1$ and $S_0$ is that $\epsilon_1$ is closer to $\omega$ than $\epsilon_0$. We should therefore observe a difference of asymptotic mean value for the local magnetisation between Fig.5.3 (a) and Fig.5.4 (a) as explained in subsection 5.2.2, but not in characteristic time. On the other hand, for the "central spin" case the spin whose associated energy is $\epsilon_1 = 1$ is not coupled to the bosonic bath anymore, it is only coupled to the spin whose associated energy is $\epsilon_0 = 0$. Thus, we expect the dynamics of this spin to be very different in these two cases regarding which Hamiltonian we are considering.

To compare the plots (a) and (b) (we advise the reader to be careful of the different time range that exists between (a) and (b)) of Fig.5.4, we will focus on the oscillations. The purpose of plots (c) and (d) is to study and understand what what happens to our system for the greatest values of the coupling $V$. In (b), for every curve (so for every value of the coupling $V$), the oscillations are slowed down, with respect to the ones in (a), the period of relaxation much greater than in the plot (a).

The fact that the amplitudes of the oscillations are bigger only highlights the fact that the local magnetisation fluctuates more in the "central spin" around its mean value than in the Tavis-Cummings case. We have yet to take into account what is happening for $V > 1$ as explained in subsection 5.2.3, that is why we will now use the information given by the plots (c) and (d). We notice that for the two chosen values for the couplings, $V = 5, 10$, we have this time $\tau_0 < \tau_{TC}$ and the amplitudes of the oscillations are closer. Eventually, we have learned that the effect of the reorganisation is more effective, when considering $H_0$ rather than $H_{TC}$, when the coupling $V$ is above a certain value even for a spin which is not coupled to the bosonic bath. In $H_0$, a spin which is not coupled to the bosonic mode feels almost no environment at weak coupling since it is exclusively weakly coupled to a single spin. That is why we observe very slow oscillations for $V = 0.05$ and $V = 0.1$ (blue and red curves) in plot (b). However, when the coupling increases, $S_0$ becomes a better medium between the other spins (not directly coupled to the boson such as $S_1$) and the bosonic mode. At stronger couplings these spins feel more and more their environment to the point where, at strong enough couplings, the difference between $S_1$'s characteristic time for $H_0$ and $H_{TC}$ vanishes.

(a) $H_{TC} = \omega b^\dagger b + \sum_{i=1}^{N} \epsilon_i S_i^z + V \sum_{i=1}^{N} (b^\dagger S_i^- + S_i^+ b)$

(b) $H_0 = (\epsilon_0 - \omega) S_0^z + V \left( b^\dagger S_0^- + b S_0^+ \right) + \sum_{j \neq 0}^{N} \frac{2V^2}{\epsilon_0 - \epsilon_j} \vec{S}_0 \cdot \vec{S}_j$

(c) $H_{TC}$, short time dynamics at strong couplings

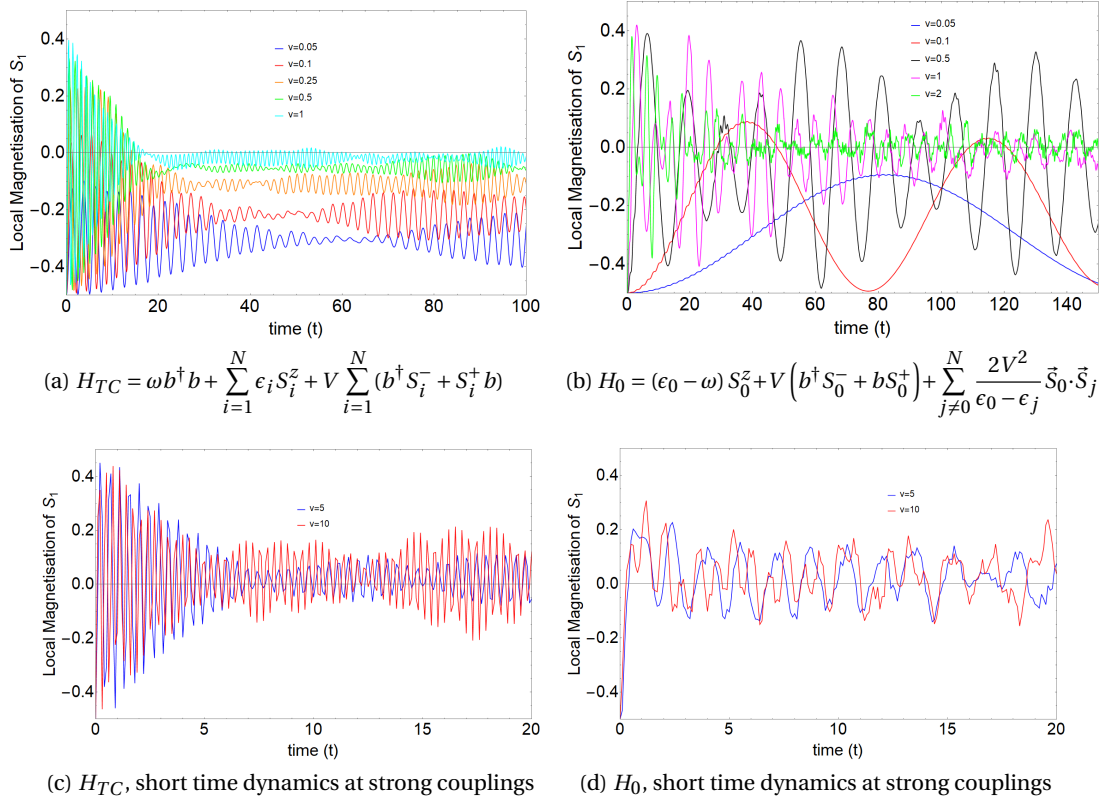(d) $H_0$, short time dynamics at strong couplings

Figure 5.4: Evolution of the local magnetisation $S_1^z$ as a function of the time for a variety of coupling constants $V$ governed either $H_{TC}$ or $H_0$. The initial state is $|13;\downarrow\downarrow\downarrow\downarrow\downarrow\downarrow\rangle$ and the bosonic mode is set at $\omega = 2.99$ in every case.

Having talked about the differences between the dynamics of the local magnetisation ruled by $H_{TC}$ or $H_0$ for a spin coupled to the bosonic bath and for one non-coupled, we can now continue by comparing the dynamics between these two kind of spin but both in a "central spin" case. To achieve that purpose we will use Fig.5.3 (b) and Fig.5.4 (b) and (d), i.e. we will study the differences between $S_0$ and $S_1$. An interesting point to mention here is that, for $V < 1$, the period of the oscillations is different in the coupled case and in the non-coupled one. Indeed, in the case of a spin coupled to the bosonic bath, the mean value of the local magnetisation oscillates at a similar rate as in the TC case, which means it oscillates faster than for a spin non-coupled. When reaching, $V = 1$, the period of the oscillations becomes the same whether the spin is coupled or not to the bosonic bath. We can conclude that for a dynamics governed by $H_0$ there are two different regimes. When $V \left( b^\dagger S_0^- + b S_0^+ \right)$ is the dominant term in the Hamiltonian, the exchanges of excitations between the unique spin coupled to the bosons and the bosonic bath is the dominant effect which can be seen graphically by regular oscillations of the local magnetisation similar to the ones observed in the TC case. Whereas, when $\sum_{j \neq 0}^{N} \frac{2V^2}{\epsilon_0 - \epsilon_j} \vec{S}_0 \cdot \vec{S}_j$ is the dominant term, the exchanges of excitations is more present among the collection of spins and the oscillations show more brutal kinks, it is not surprising

because we have now two processes considered in the "central spin" case.

### 5.2.5 Excitation number M

In this subsection, the impact of the number of total excitations $M$ is studied thanks a comparison between the two plots presented in Fig.5.5. These two plots of the local magnetisation of $S_0$ describe two systems only differing by $M$, i.e. the initial number of bosons, which enables us to strictly observe the influence of $M$ on the dynamics of these systems.
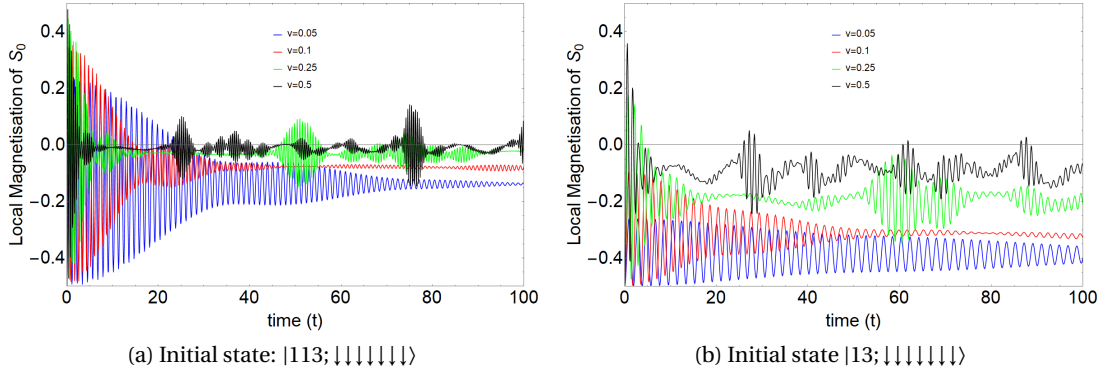


(a) Initial state: $|113; \downarrow\downarrow\downarrow\downarrow\downarrow\downarrow\rangle$   (b) Initial state $|13; \downarrow\downarrow\downarrow\downarrow\downarrow\downarrow\rangle$

Figure 5.5: Evolution of the local magnetisation $S_0^z$ as a function of the time for a variety of coupling constants $V$ governed by $H_0$ for two initial states with a different number of excitations. The frequency of bosonic mode is set at $\omega = 2.99$ in every case.

Previously in subsection 5.2.2, to study the influence of $\omega$ on the dynamics, we had to isolate the impact of the resonance, between the associated energy of a spin $\epsilon_i$ and $\omega$, on the steady state of the local magnetisation detailed in section 4.2, to understand its effect on the relaxation.

To study the impact of $M$ on the dynamics, we have to separate as well its impact on the asymptotic values of the local magnetisation. Previously, in section 4.2, we learned that in the steady state, the more a system possesses excitations the more the expectation value of the local magnetisation will be near zero. By removing this difference between the two plots (a) and (b), we understand that $M$ also influences the characteristic time $\tau$. Indeed, for every different value of the coupling $V$, $\tau$ is different. For instance in (a), the characteristic time goes from $\tau \approx 5$, for $V = 0.5$, to $\tau \approx 50$, for $V = 0.25$, and in (b) $\tau$ goes from $\tau \approx 10$, for $V = 0.5$, to $\tau \approx 80$, for $V = 0.25$. More precisely, the characteristic time is always smaller in the case where $M = 113$ than in the case where $M = 13$. But for a difference of an order of magnitude of bosonic excitation, $M = 113$ and $M = 13$, we recover only a slight difference for the characteristic time, the impact on $\tau$ of having a great number of bosonic excitations is much less substantial as being coupled or not to the bosons. We can nonetheless conclude that having a great number of excitations accelerates the relaxation towards the steady states described in section 4.2 even if this effect is weak. We can make the following interpretation: a

great number of excitations facilitates the capability for the collection of spins to adjust its final configuration having a lot of excitations available in the bosonic bath. The fact that the oscillations are faster in (a) than in (b) indicates that there are more exchanges of excitations when there is more bosonic excitations available which enhances the redistribution.

### 5.2.6   Initial state

Having talked mainly of the bosonic relaxation in this chapter, its global and local effects, we now focus our comments on the initial configuration of the spins.

The influence of the spin configuration, in the initial state, is discussed through two couples of plots, one with $H_0$ as Hamiltonian (Fig.5.6 (a) and (b)) and one with $H_{TC}$ as Hamiltonian (5.6 (c) and (d)). For each of those couples, the only difference is the spin configuration in the initial state.
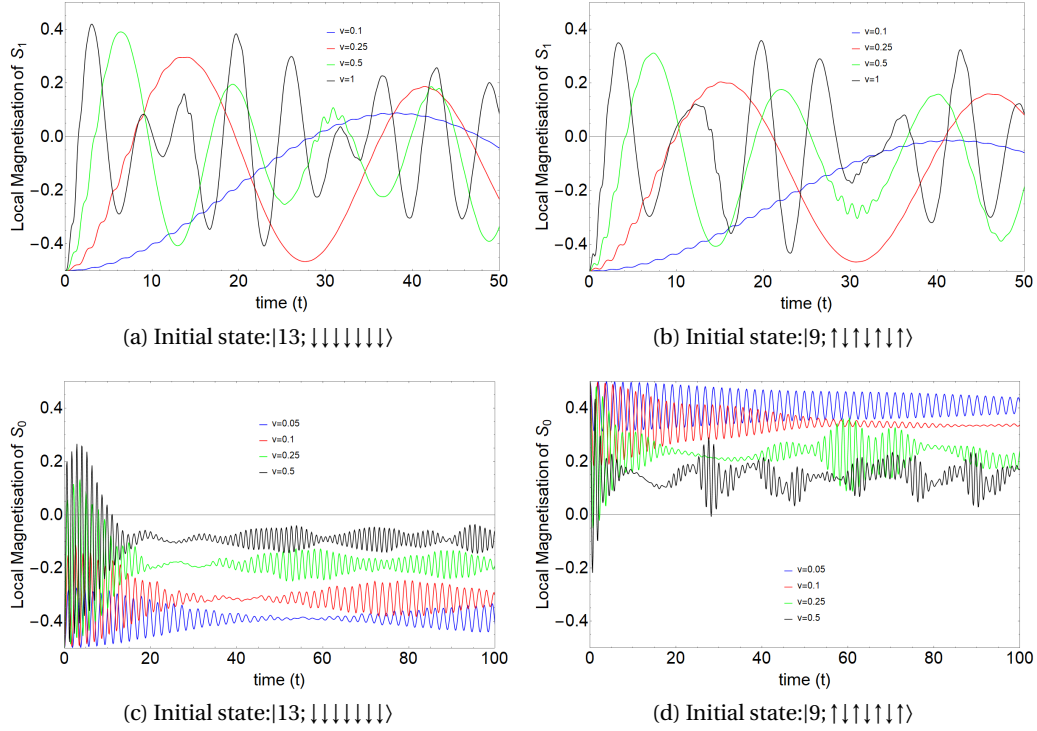


Figure 5.6: Evolution of the local magnetisation $S_1^z$ governed by $H_0$ ((a) and (b)) and $S_0^z$ governed by $H_{TC}$ ((c) and (d)) as a function of the time for a variety of coupling constants $V$. The bosonic mode is set at $\omega = 2.99$ in every case

For the plots obtained in the "central spin" case, we can notice that the period of the oscillations is slightly longer when the initial spin configuration is alternated. But this very tenuous difference in the period of the oscillations (even at strong coupling) can be explained by the weak difference of initial bosonic excitations, (a) $M = 13$ and (b) $M = 9$. So $\tau$ is smaller when

the initial spin configuration is fully down polarised, because it is the configuration containing the most initial bosonic excitations.

When the dynamics is governed by $H_{TC}$, we observe the same phenomenon, it is really visible when considering the curves for $V = 0.05$ and $V = 0.1$. Indeed, $\tau$ is clearly bigger for the red curve and the blue curve when the initial state is $|9;\uparrow\downarrow\uparrow\downarrow\uparrow\downarrow\uparrow\rangle$. Then for $V = 0.25$ and $V = 0.5$, $\tau$ becomes clearly smaller for the green curve and the black curve when the initial state is $|9;\uparrow\downarrow\uparrow\downarrow\uparrow\downarrow\uparrow\rangle$, it seems that for coupling $V > 0.1$ (which is still a relatively weak coupling) having an initial state highly entropic in the spin sector accelerates more the redistribution process than having a lot of bosonic initial excitations.

It corroborates, the fact that an initial state with spins alternation helps the system to reach efficiently its steady state. By combining these results to the ones of section 4.2, we can say that having an initial state with spins all pointing in the same direction prevent the system from reaching a superradiant-like steady state and the characteristic time to reach its steady state is also important (except for extremely weak values of the coupling).

## 5.3   Conclusion

The aim of this chapter was to complete the work presented in the chapter 4 about the dynamics of systems containing a collection of $N$ of spins-$\frac{1}{2}$ coupled to a bosonic bath and, thus, to conclude the numerical part of this thesis (chapters 3, 4 and 5). This part started in chapter 3 where it was explained how to numerically obtain the $\Lambda_i$, the variables used in the expression of the mean value of an observable of interest at a time $t$. The purpose of the chapters 4 and 5 is to make use of the numerical data, the $\Lambda_i$, to describe the whole behaviour of a given system with efficient numerical calculations. The principle is to choose an initial configuration for the spins, the numbers of bosons being complementary to the spin excitations, and let it evolve until its steady state. It was shown in chapter 4 that for every Hamiltonian, the steady state of a given initial configuration is a frozen stage of a relaxation towards a superradiant-like state. It was as well shown that only an ideal combination of the parameters of the considered system in the initial state can lead to a superradiant-like steady state. The purpose of this section was to show the dynamics of a given system from the initial time up to the asymptotic states previously cited.

The first and important conclusion we can make after the study of the real time dynamics is that the systems we are considering do relax and reach their steady state. In the section 5.2, the influence of the same parameters as the ones used in 4.2 on the dynamics was studied to differentiate the ones that influence the steady state, the relaxation time or both. Thus, we learned that considering a spin whose associated energy is near or far $\omega$ does not have a strong effect on the relaxation time even if it does on the value of the magnetisation towards this spin relaxes. The total number of excitations $M$ has a weak effect on the relaxation time, it is visible only at extremely small coupling, in that case the greater $M$ is, the quicker the system reaches its steady state. And finally, within the initial spin configuration, having spin alternations

reduces the time the system needs to reach its steady state, except at extremely weak coupling, and it favours the capability of the system to relax towards a superradiant-like steady state. Additionally, the dynamics is different regarding the Hamiltonian we are considering. The effect of the choice of Hamiltonian on the dynamics lays in the competition between the term describing the exchanges of excitations between the bosonic bath and the collection of spins and the hyperfine couplings between the spins. They are both modulated by the intensity of the coupling $V$. Indeed, the term of interaction spin-boson is of first order in $V$ whereas the term spin-spin is of second order in $V$. The results of having terms of different orders in $V$ within the Hamiltonian is that the dynamics is different regarding the value of the coupling, smaller of bigger than one, i.e. there are two regimes regarding the strength of the coupling. These two different regimes are visible through the period of the oscillations around the long-time average in the plot of the section 5.2. To study this difference in the dynamics due to the Hamiltonians, we have chosen two different ones, one with no terms of spin-spin interaction, $H_{TC}$ and one "central spin" Hamiltonian $H_0$. While in the TC case, the systems are reaching their steady state in less time than in the "central spin" case for small values of $V$, for $V > 1$ it is this time the systems associated to $H_{TC}$ that take more time to attain their steady states. This difference can be explained by the absence of second order terms in $V$ in $H_{TC}$.

Eventually, we can say that we have been able to carry out a complete study of observables, bosonic occupation and local magnetisations, relying on the determinant expressions depending on the $\Lambda_i$ we set up in the chapter 2. This shows the applicability of the results presented in the theoretical part. However, the last numerical calculations which are presented were made for small system sizes. We would need more computational power to be able present results for systems containing as many spins-$\frac{1}{2}$ as in chapter 4. Nevertheless, the size of the systems considered in the sections 4.3 and 5.2 enables to evaluate the validity of GGE to describe our asymptotic mean values or to understand the real time dynamics of our systems. However, in the case of the real time dynamics, we can spot the effect of considering small system sizes in the amplitudes of the oscillations of the mean value of our observables. These oscillations should dampen for numerical calculations on bigger systems.

# Conclusion

In this conclusion, we remind the reader that this thesis is a consistent progression from very general theoretical results to useful numerical applications.

Indeed, this work starts with an introduction on the mathematical context: the Generalised Gaudin Algebra (GGA). Following the introduction of the latter algebra, a result applicable to any realisations of the GGA is presented: the change of variables that enables to derive the quadratic Bethe equations. From this generality, the field of work is narrowed down to a specific realisation describing spin-$\frac{1}{2}$ only. The explicit expression of the quadratic Bethe equations and determinant expressions for scalar products and observables of interest are then given. Aiming to apply numerically these results to the Tavis-Cummings Hamiltonian, we have to extend these expressions to a spin-$\frac{1}{2}$-boson realisation by overcoming a lack of a proper pseudovacuum. Besides, we extend our work to a realisation containing one spin of arbitrary norm interacting with many spins-$\frac{1}{2}$. The Tavis-Cummings Hamiltonian belonging to the class of Hamiltonians of the spin-$\frac{1}{2}$-boson realisation, we apply the previously detailed machinery to find its eigenstates.

The purpose of this work being to achieve efficient numerics, we detail the algorithm used to solve the quadratic equations. Logically, following the numerical aspect of our work, comes numerical results. In a first time, because it is really efficient numerically speaking and valid for any Hamiltonian, we present the asymptotic behaviour of the systems considered which try to relax towards a fully plane polarised spin configuration, it can be interpreted as a superradiant-like steady state. Additionally, we show that the traditional definition of the GGE does not describe the asymptotic behaviour of the XXX Gaudin models through graphic examples. Concluding this thesis, we present results for the real time dynamics, driven by the Tavis-Cummings Hamiltonian and a "central spin" Hamiltonian of XXX Gaudin models, showing that the considered systems relax to their steady states. The relaxation towards the steady state is very different regarding which Hamiltonian governs it. Even with the same conserved quantities a variety of different behaviours exists and it is only dependent on how we combine these conserved quantities to build the Hamiltonian ruling the dynamics. This is a strong asset of our method, be it the $\Lambda_i$, the scalar products, the form factors, it is the same calculations for every Hamiltonian except for the eigenvalues which require a minor time to be computed numerically. Eventually, not only do the results of real time dynamics conclude the thesis, they also conclude our approach which consisted in finding efficient numerical

tools allowing the study of interesting physical phenomena such as the superradiance.

All along our progression, some paths for new research projects, both theoretical and numerical, have been opened.

For the theoretical part, our method to tackle the problem of a missing pseudovacuum and enforcing the application of the QISM must still be reproducible in other cases with other realisations of the GGA. A possible research avenue is to find determinant expressions for several spins of arbitrary norm interacting together, we have them for simple cases but a general proof still requires some efforts.

Another project of interest would be to link works for the XXX spin chain to ours. In [90, 91], the method of Separation of Variables is used to derived determinant representation for scalar products and in [92], the derivation of the determinant expressions relies on the Off-diagonal Bethe Ansatz.

For the numerical part, with small numerical power we achieved to carry out demanding computations running double sums over the dimension of the Hilbert space. Consequently, the size of the systems considered should be increased, which only requires longer calculations, to dampen the finite-size effects.

# A Appendix

## A.1    Yang-Baxter equation from Jacobi identity

In this Appendix, we show that to fulfil the Jacobi identity and then form a Lie Algebra the operators $S^x(u), S^y(u), S^z(u)$ have to satisfy the classical Yang-Baxter equation, also called Gaudin equation in that case.

Starting from the Jacobi identity we have:

$$
\left[S^x(w), \left[S^x(u), S^y(v)\right]\right] + \left[S^y(v), \left[S^x(w), S^x(u)\right]\right] + \left[S^x(u), \left[S^y(v), S^x(w)\right]\right] = 0
$$

$$
\Rightarrow \quad \left[S^x(w), \left(Y(u,v)S^z(u) - X(u,v)S^z(v)\right)\right] + \left[S^y(v), 0\right] + \left[S^x(u), \left(X(w,v)S^z(v) - Y(w,v)S^z(w)\right)\right] = 0
$$

$$
\Rightarrow \quad -Y(u,v)\left[S^z(u), S^x(w)\right] + X(u,v)\left[S^z(v), S^x(w)\right] - X(w,v)\left[S^z(v), S^x(u)\right] + Y(w,v)\left[S^z(w), S^x(u)\right] = 0
$$

$$
\Rightarrow \quad -Y(u,v)X(u,w)S^y(u) + Y(u,v)Z(u,w)S^y(w) + X(u,v)X(v,w)S^y(v) - X(u,v)Z(v,w)S^y(w)
$$

$$
\quad -X(w,v)X(v,u)S^y(v) + X(w,v)Z(v,u)S^y(u) + Y(w,v)X(w,u)S^y(w) - Y(w,v)Z(w,u)S^y(u) = 0
$$

$$
\Rightarrow \quad S^y(u)\left[-Y(u,v)X(u,w) + X(w,v)Z(v,u) - Y(w,v)Z(w,u)\right] + S^y(v)\left[X(u,v)X(v,w) - X(w,v)X(v,u)\right]
$$

$$
\quad +S^y(w)\left[Y(u,v)Z(u,w) - X(u,v)Z(v,w) + Y(w,v)X(w,u)\right] = 0. \tag{A.1}
$$

The functions $X, Y, Z$ being antisymmetric, $X(u,v)X(v,w) - X(w,v)X(v,u)$=0, we have now:

$$
\left[S^x(w), \left[S^x(u), S^y(v)\right]\right] + \left[S^y(v), \left[S^x(w), S^x(u)\right]\right] + \left[S^x(u), \left[S^y(v), S^x(w)\right]\right] = 0
$$

$$
\Rightarrow \quad \begin{cases} X(u,v)Z(v,w) - Y(u,v)Z(u,w) - Y(w,v)X(w,u) = 0 \\ X(w,v)Z(v,u) - Y(u,v)X(u,w) - Y(w,v)Z(w,u) = 0 \end{cases} . \tag{A.2}
$$

Again we use the fact that $X, Y, Z$ are antisymmetric to rewrite the last implication:

$$\left[S^x(w),\left[S^x(u),S^y(v)\right]\right] + \left[S^y(v),\left[S^x(w),S^x(u)\right]\right] + \left[S^x(u),\left[S^y(v),S^x(w)\right]\right] = 0$$

$$\Rightarrow \quad \begin{cases} X(u,v)Z(v,w) + Y(v,u)Z(u,w) + Y(v,w)X(w,u) = 0 \\ X(w,v)Z(v,u) + Y(v,u)X(u,w) + Y(v,w)Z(w,u) = 0 \end{cases}, \tag{A.3}$$

which is twice the classical Yang-Baxter equation. Therefore, we have shown that if we want our operators $S^x(u), S^y(u), S^z(u)$ to form a Lie Algebra and thus satisfy the Jacobi identity, they have to satisfy the Yang-Baxter equation:

$$X(u,v)Z(v,w) + Y(v,u)Z(u,w) + Y(v,w)X(w,u) = 0. \tag{A.4}$$

## A.2 Deriving the XXX Bethe equations

In this Appendix it is shown in details how to derive the Bethe equations from the XXX commutations rules:

$$\begin{aligned} S^2(u)\,|\lambda_1\dots\lambda_M\rangle &= S^2(u)\prod_{i=1}^{M}S^+(\lambda_i)\,|0\rangle \\ &= \left(\prod_{i=1}^{M}S^+(\lambda_i)\right)S^2(u)\,|0\rangle + \left[S^2(u),\left(\prod_{i=1}^{M}S^+(\lambda_i)\right)\right]|0\rangle \\ &= \ell(u)\,|\lambda_1\dots\lambda_M\rangle + \sum_{p=1}^{M}\prod_{i=1}^{p-1}S^+(\lambda_i)\left[S^2(u),S^+(\lambda_p)\right]\prod_{i=p+1}^{M}S^+(\lambda_i)\,|0\rangle \end{aligned} \tag{A.5}$$

with $\ell(u)$ the eigenvalue of $S^2(u)$.

From the XXX commutations relations we have access to:

$$
\begin{aligned}
\left[S^2(u), S^+(\lambda_i)\right] &= X(u, \lambda_i)\left(S^+(u)S^z(\lambda_i) + S^z(\lambda_i)S^+(u)\right. \\
&\qquad \left. -S^+(\lambda_i)S^z(u) - S^z(\lambda_i)S^+(u)\right) \\
&= X(u, \lambda_i)\left(S^+(u)S^z(\lambda_i) + \left[S^z(\lambda_i), S^+(u)\right]\right. \\
&\qquad \left. -S^+(\lambda_i)S^z(u) + \left[S^z(u), S^+(\lambda_i)\right]\right)
\end{aligned}
\tag{A.6}
$$

By using the expression $\left[S^z(u), S^\pm(v)\right] = \pm X(u, v)\left(S^\pm(u) - S^\pm(v)\right)$ we obtain:

$$
\left[S^2(u), S^+(\lambda_i)\right] = X(u, \lambda_i)\left(2S^+(u)S^z(\lambda_i) - 2S^+(\lambda_i)S^z(u)\right)
\tag{A.7}
$$

Then (A.5) becomes:

$$
\begin{aligned}
S^2(u)|\lambda_1 \ldots \lambda_M\rangle &= \ell(u)|\lambda_1 \ldots \lambda_M\rangle + 2\sum_{p=1}^{M} X(u, \lambda_p)\left(\prod_{i=1}^{p-1} S^+(\lambda_i)S^+(u)S^z(\lambda_p)\prod_{i=p+1}^{M} S^+(\lambda_i)\right. \\
&\qquad \left. -\prod_{i=1}^{p-1} S^+(\lambda_i)S^+(\lambda_p)S^z(u)\prod_{i=p+1}^{M} S^+(\lambda_i)\right)|0\rangle.
\end{aligned}
\tag{A.8}
$$

For clarity, we will separate this expression to continue the calculations:

$$
\begin{aligned}
\prod_{i=1}^{p-1} S^+(\lambda_i) S^+(u) S^z(\lambda_p) \prod_{i=p+1}^{M} S^+(\lambda_i) \quad = \quad & \prod_{i=1 \neq \lambda_p}^{M} S^+(\lambda_i) S^+(u) S^z(\lambda_p) \\
& + \sum_{q=p+i}^{M} \prod_{p+1}^{q-1} S^+(\lambda_i) \left[ S^z(\lambda_p), S^+(\lambda_q) \right] \prod_{i=q+1}^{M} S^+(\lambda_i) \\
= \quad & \prod_{i=1 \neq \lambda_p}^{M} S^+(\lambda_i) S^+(u) S^z(\lambda_p) \\
& + \prod_{i=1}^{p-1} S^+(\lambda_i) S^+(u) \sum_{q=p+i}^{M} \frac{1}{\lambda_p - \lambda_q} \prod_{i=p+1}^{q-1} S^+(\lambda_i) S^+(\lambda_p) \prod_{i=q+1}^{M} S^+(\lambda_i) \\
& - \prod_{i=1}^{p-1} S^+(\lambda_i) S^+(u) \sum_{q=p+i}^{M} \frac{1}{\lambda_p - \lambda_q} \prod_{i=p+1}^{q-1} S^+(\lambda_i) S^+(\lambda_q) \prod_{i=q+1}^{M} S^+(\lambda_i).
\end{aligned}
$$

$$(A.9)$$

Now $\prod_{i=1}^{p-1} S^+(\lambda_i) S^+(u) S^z(\lambda_p) \prod_{i=p+1}^{M} S^+(\lambda_i)$ is expressed only in terms of $S^+(.)$, it just need to be reorganised:

$$
\begin{aligned}
\prod_{i=1}^{p-1} S^+(\lambda_i) S^+(u) S^z(\lambda_p) \prod_{i=p+1}^{M} S^+(\lambda_i) \;=\;& \prod_{i=1\neq\lambda_p}^{M} S^+(\lambda_i) S^+(u) S^z(\lambda_p) \\
& + \sum_{q=p+i}^{M} \frac{1}{\lambda_p - \lambda_q} \prod_{i=1}^{p-1} S^+(\lambda_i) S^+(u) \prod_{i=p+1\neq q}^{M} S^+(\lambda_i) S^+(\lambda_p) \\
& - \sum_{q=p+i}^{M} \frac{1}{\lambda_p - \lambda_q} \prod_{i=1}^{p-1} S^+(\lambda_i) S^+(u) \prod_{i=p+1}^{M} S^+(\lambda_i) \\
=\;& \prod_{i=1\neq\lambda_p}^{M} S^+(\lambda_i) S^+(u) S^z(\lambda_p) \\
& + \sum_{q=p+i}^{M} \frac{1}{\lambda_p - \lambda_q} \prod_{i=1,\lambda_p=u}^{p} S^+(\lambda_i) \prod_{i=p+1,\lambda_q=\lambda_p}^{M} S^+(\lambda_i) \\
& - \sum_{q=p+i}^{M} \frac{1}{\lambda_p - \lambda_q} \prod_{i=1\neq p}^{M} S^+(\lambda_i) S^+(u) \\
=\;& \prod_{i=1\neq\lambda_p}^{M} S^+(\lambda_i) S^+(u) S^z(\lambda_p) \\
& + \sum_{q=p+i}^{M} \frac{1}{\lambda_p - \lambda_q} \prod_{i=1\neq q}^{M} S^+(\lambda_i) S^+(u) \\
& - \sum_{q=p+i}^{M} \frac{1}{\lambda_p - \lambda_q} \prod_{i=1\neq p}^{M} S^+(\lambda_i) S^+(u) \qquad \text{(A.10)}
\end{aligned}
$$

In a same manner we find:

$$
\begin{aligned}
\prod_{i=1}^{p-1} S^+(\lambda_i) S^+(\lambda_p) S^z(u) \prod_{i=p+1}^{M} S^+(\lambda_i) \;=\;& - \prod_{i=1\neq\lambda_p}^{M} S^+(\lambda_i) S^+(u) S^z(u) \\
& - \sum_{q=p+i}^{M} \frac{1}{u - \lambda_q} \prod_{i=1\neq q}^{M} S^+(\lambda_i) S^+(u) \\
& + \sum_{q=p+i}^{M} \frac{1}{u - \lambda_q} \prod_{i=1}^{M} S^+(\lambda_i) S^+(u) \qquad \text{(A.11)}
\end{aligned}
$$

Therefore $S^2(u)\,|\lambda_1\ldots\lambda_M\rangle$ becomes:

$$S^2(u)|\lambda_1\ldots\lambda_M\rangle = \left(\ell(u) - 2\sum_{p=1}^{M}\frac{1}{u-\lambda_p}\ell^z(u) + 2\sum_{p=1}^{M}\sum_{q=p+1}^{M}\frac{1}{(u-\lambda_p)(u-\lambda_q)}\right)|\lambda_1\ldots\lambda_M\rangle$$

$$+\left(2\sum_{p=1}^{M}\sum_{q=p+1}^{M}\frac{1}{(u-\lambda_p)(\lambda_p-\lambda_q)} - 2\sum_{p=1}^{M}\sum_{q=p+1}^{M}\frac{1}{(u-\lambda_p)(u-\lambda_q)}\right)|\lambda_1\ldots\lambda_M\rangle_{\lambda_q=u}$$

$$+\left(2\sum_{p=1}^{M}\frac{1}{u-\lambda_p}\ell^z(\lambda_p) - 2\sum_{p=1}^{M}\sum_{q=p+1}^{M}\frac{1}{(u-\lambda_p)(\lambda_p-\lambda_q)}\right)|\lambda_1\ldots\lambda_M\rangle_{\lambda_p=u}. \quad (A.12)$$

Moreover for the XXX solution, the Yang-Baxter equation becomes $\frac{1}{(u-\lambda_p)(\lambda_p-\lambda_q)} + \frac{1}{(\lambda_q-u)(u-\lambda_p)} + \frac{1}{(\lambda_p-\lambda_q)(\lambda_q-u)} = 0$ enabling us to make further simplifications:

$$S^2(u)|\lambda_1\ldots\lambda_M\rangle = \left(\ell(u) - 2\sum_{p=1}^{M}\frac{1}{u-\lambda_p}\ell^z(u) + \sum_{p=1}^{M}\sum_{q\neq p}^{M}\frac{1}{(u-\lambda_p)(u-\lambda_q)}\right)|\lambda_1\ldots\lambda_M\rangle$$

$$+\left(2\sum_{p=1}^{M}\frac{1}{u-\lambda_p}\ell^z(\lambda_p) - 2\sum_{p=1}^{M}\sum_{q\neq p}^{M}\frac{1}{(u-\lambda_p)(\lambda_p-\lambda_q)}\right)|\lambda_1\ldots\lambda_M\rangle_{\lambda_p=u}$$

$$= E(\{\lambda\},u)|\lambda_1\ldots\lambda_M\rangle + \sum_{p=1}^{M}G_p(\{\lambda\},u)|\lambda_1\ldots,\lambda_k\to u,\ldots\lambda_M\rangle, \quad (A.13)$$

Were $\lambda_k \to u$ means that the $k^{th}$ has been swapped with the parameter $u$. Thus $|\lambda_1\ldots\lambda_M\rangle$ becomes eigenstate of $S^2(u)$ provided all $G_p(\{\lambda\},u)$ cancel, that is to say when:

$$\frac{1}{u-\lambda_p}\ell^z(\lambda_p) - \sum_{q\neq p}^{M}\frac{1}{(u-\lambda_p)(\lambda_p-\lambda_q)} = 0, \quad (A.14)$$

defining the Bethe equations.

## A.3   Finding the derivatives of $\Lambda_{i;V-\delta V}$

In this appendix, we show the details of the proof by induction mentioned in the section (3.3) that is need to compute the derivatives of $\Lambda_{i;V-\delta V}$. The aim of this proof is to show the following expression:

$$B_{n;j} = \frac{-n}{v}\left(B_{n-1;j} + \frac{\partial^{n-1}\Lambda_j}{\partial v^{n-1}}\left[(\epsilon_j - \omega) + 2\Lambda_j\right]\right) + \sum_{k=1}^{n-1}\binom{n}{k}\frac{\partial^k\Lambda_j}{\partial v^k}\frac{\partial^{n-k}\Lambda_j}{\partial v^{n-k}}, \tag{A.15}$$

starting from $B_{0;j} = -\Lambda_j\Lambda_j$ and $B_{n;j} = \frac{\partial B_{n-1}}{\partial v} + \frac{1}{v}\left(-\frac{\partial^{n-1}\Lambda_j}{\partial v^{n-1}}\left[(\epsilon_j - \omega) + 2\Lambda_j\right] - B_{n-1;j}\right) + 2\frac{\partial\Lambda_j}{\partial v}\frac{\partial^{n-1}\Lambda_j}{\partial v^{n-1}}$.
First step is to verify this statement at $n = 1$.

$$
\begin{aligned}
B_{1;j} &= \frac{\partial B_{0;j}}{\partial v} + \frac{1}{v}\left(-\Lambda_j\left[(\epsilon_j - \omega) + 2\Lambda_j\right] - B_{0;j}\right) + 2\frac{\partial\Lambda_j}{\partial v}\Lambda_j \\
&= -2\frac{\partial\Lambda_j}{\partial v}\Lambda_j - \frac{1}{v}\left(\Lambda_j\left[(\epsilon_j - \omega) + 2\Lambda_j\right] + B_{0;j}\right) + 2\frac{\partial\Lambda_j}{\partial v}\Lambda_j \\
&= \frac{-1}{v}\left(\Lambda_j\left[(\epsilon_j - \omega) + 2\Lambda_j\right] + B_{0;j}\right). 
\end{aligned}
\tag{A.16}
$$

Now assuming that $B_{n;j}$ is given by the expression (A.15), we have to verify is this expression is still valid for $B_{n+1;j}$ to complete the proof.

$$
\begin{aligned}
B_{n+1;j} &= \frac{\partial B_{n;j}}{\partial v} + \frac{1}{v}\left(-\frac{\partial^n\Lambda_j}{\partial v^n}\left[(\epsilon_j - \omega) + 2\Lambda_j\right] - B_{n;j}\right) + 2\frac{\partial\Lambda_j}{\partial v}\frac{\partial^n\Lambda_j}{\partial v^n} \\
&= \frac{n}{v^2}\left(B_{n-1;j} + \frac{\partial^{n-1}\Lambda_j}{\partial v^{n-1}}\left[(\epsilon_j - \omega) + 2\Lambda_j\right]\right) \\
&\quad - \frac{n}{v}\left(\frac{\partial B_{n-1;j}}{\partial v} + \frac{\partial^n\Lambda_j}{\partial v^n}\left[(\epsilon_j - \omega) + 2\Lambda_j\right] + 2\frac{\partial\Lambda_j}{\partial v}\frac{\partial^{n-1}\Lambda_j}{\partial v^{n-1}}\right) \\
&\quad \frac{1}{v}\left(-\frac{\partial^n\Lambda_j}{\partial v^n}\left[(\epsilon_j - \omega) + 2\Lambda_j\right] - B_{n;j}\right) + 2\frac{\partial\Lambda_j}{\partial v}\frac{\partial^n\Lambda_j}{\partial v^n} \\
&\quad + \sum_k^{n-1}\binom{n}{k}\frac{\partial^{k+1}\Lambda_j}{\partial v^{k+1}}\frac{\partial^{n-k}\Lambda_j}{\partial v^{n-k}} + \sum_k^{n-1}\binom{n}{k}\frac{\partial^k\Lambda_j}{\partial v^k}\frac{\partial^{n+1-k}\Lambda_j}{\partial v^{n+1-k}}. 
\end{aligned}
\tag{A.17}
$$

For simplicity we define $A = 2\frac{\partial\Lambda_j}{\partial v}\frac{\partial^n\Lambda_j}{\partial v^n} + \sum_k^{n-1}\binom{n}{k}\frac{\partial^{k+1}\Lambda_j}{\partial v^{k+1}}\frac{\partial^{n-k}\Lambda_j}{\partial v^{n-k}} + \sum_k^{n-1}\binom{n}{k}\frac{\partial^k\Lambda_j}{\partial v^{k+1}}\frac{\partial^{n+1-k}\Lambda_j}{\partial v^{n+1-k}}$. We have now:

$$
\begin{aligned}
B_{n+1;j} &= A + \frac{-(n+1)}{v}\left(\frac{\partial^n \Lambda_j}{\partial v^n}\left[(\epsilon_j - \omega) + 2\Lambda_j\right]\right) - \frac{B_{n;j}}{v} \\
&\quad - \frac{n}{v}\left(\frac{\partial B_{n-1;j}}{\partial v} + 2\frac{\partial \Lambda_j}{\partial v}\frac{\partial^{n-1}\Lambda_j}{\partial v^{n-1}} - \frac{1}{v}\left(B_{n-1;j} + \frac{\partial^{n-1}\Lambda_j}{\partial v^{n-1}}\left[(\epsilon_j - \omega) + 2\Lambda_j\right]\right)\right) \\
&= A + \frac{-(n+1)}{v}\left(\frac{\partial^n \Lambda_j}{\partial v^n}\left[(\epsilon_j - \omega) + 2\Lambda_j\right]\right) - \frac{B_{n;j}}{v} - \frac{nB_{n;j}}{v} \\
&= A + \frac{-(n+1)}{v}\left(B_{n;j} + \frac{\partial^n \Lambda_j}{\partial v^n}\left[(\epsilon_j - \omega) + 2\Lambda_j\right]\right). \tag{A.18}
\end{aligned}
$$

We have are left to show that $A = \sum_{k=1}^{n}\binom{n+1}{k}\frac{\partial^k \Lambda_j}{\partial v^k}\frac{\partial^{n+1-k}\Lambda_j}{\partial v^{n+1-k}}$:

$$
\begin{aligned}
A &= 2\frac{\partial \Lambda_j}{\partial v}\frac{\partial^n \Lambda_j}{\partial v^n} + \sum_{k=1}^{n-1}\binom{n}{k}\frac{\partial^{k+1}\Lambda_j}{\partial v^{k+1}}\frac{\partial^{n-k}\Lambda_j}{\partial v^{n-k}} + \sum_{k=1}^{n-1}\binom{n}{k}\frac{\partial^k \Lambda_j}{\partial v^k}\frac{\partial^{n+1-k}\Lambda_j}{\partial v^{n+1-k}} \\
&= \sum_{p=1}^{n}\binom{n}{p-1}\frac{\partial^p \Lambda_j}{\partial v^p}\frac{\partial^{n-p+1}\Lambda_j}{\partial v^{n-p+1}} - \binom{n}{0}\frac{\partial \Lambda_j}{\partial v}\frac{\partial^n \Lambda_j}{\partial v^n} \\
&\quad + \sum_{k=1}^{n}\binom{n}{k}\frac{\partial^k \Lambda_j}{\partial v^k}\frac{\partial^{n+1-k}\Lambda_j}{\partial v^{n+1-k}} - \binom{n}{n}\frac{\partial \Lambda_j}{\partial v}\frac{\partial^n \Lambda_j}{\partial v^n} + 2\frac{\partial \Lambda_j}{\partial v}\frac{\partial^n \Lambda_j}{\partial v^n} \\
&= \sum_{k=1}^{n}\left(\binom{n}{k-1} + \binom{n}{k}\right)\frac{\partial^k \Lambda_j}{\partial v^k}\frac{\partial^{n+1-k}\Lambda_j}{\partial^{n+1-k}} \\
&= \sum_{k=1}^{n}\binom{n+1}{k}\frac{\partial^k \Lambda_j}{\partial^k}\frac{\partial^{n+1-k}\Lambda_j}{\partial v^{n+1-k}}. \tag{A.19}
\end{aligned}
$$

Gathering the two expressions we do have:

$$
B_{n+1;j} = \sum_{k=1}^{n}\binom{n+1}{k}\frac{\partial^k \Lambda_j}{\partial v^k}\frac{\partial^{n+1-k}\Lambda_j}{\partial v^{n+1-k}} + \frac{-(n+1)}{v}\left(B_{n;j} + \frac{\partial^n \Lambda_j}{\partial v^n}\left[(\epsilon_j - \omega) + 2\Lambda_j\right]\right). \tag{A.20}
$$

which completes the proof by induction.

# Bibliography

[1] J. Hietarinta, "Classical versus quantum integrability," *Journal of Mathematical Physics*, vol. 25, no. 6, pp. 1833–1840, 1984.

[2] J.-S. Caux and J. Mossel, "Remarks on the notion of quantum integrability," *Journal of Statistical Mechanics: Theory and Experiment*, vol. 2011, no. 02, p. P02023, 2011.

[3] J. Clemente-Gallardo and G. Marmo, "Towards a definition of quantum integrability," *International Journal of Geometric Methods in Modern Physics*, vol. 06, no. 01, pp. 129–172, 2009.

[4] L. D. Faddeev., "What is complete integrability in quantum mechanics.," in *Symposium Henri Poincaré, Brussels*, Oct 2004.

[5] S. Weigert, "The problem of quantum integrability," *Physica D: Nonlinear Phenomena*, vol. 56, no. 1, pp. 107 – 119, 1992.

[6] V. I. Arnold, *Mathematical Methods of Classical Mechanics*. .: Springer, 1978. .

[7] A. Braverman, P. Etingof, and D. Gaitsgory, "Quantum integrable systems and differential galois theory," *Transformation Groups*, vol. 2, no. 1, pp. 31–56, 1997.

[8] B. Sutherland, *Beautiful models : 70 years of exactly solved quantum many-body problems*. .: River Edge, 2004. .

[9] J. Kasprzak, M. Richard, S. Kundermann, A. Baas, P. Jeambrun, J. M. J. Keeling, F. M. Marchetti, M. H. Szymańska, R. André, J. L. Staehli, V. Savona, P. B. Littlewood, B. Deveaud, and L. S. Dang, "Bose–einstein condensation of exciton polaritons," *Nature*, vol. 443, Sep 2006.

[10] R. Balili, V. Hartwell, D. Snoke, L. Pfeiffer, and K. West, "Bose-einstein condensation of microcavity polaritons in a trap," *Science*, vol. 316, no. 5827, pp. 1007–1010, 2007.

[11] P. R. Eastham and P. B. Littlewood, "Bose condensation of cavity polaritons beyond the linear regime: The thermal equilibrium of a model microcavity," *Phys. Rev. B*, vol. 64, p. 235101, Nov 2001.

## Bibliography

[12] F. H. L. Koppens, K. C. Nowack, and L. M. K. Vandersypen, "Spin echo of a single electron spin in a quantum dot," *Phys. Rev. Lett.*, vol. 100, p. 236802, Jun 2008.

[13] J. R. Petta, A. C. Johnson, J. M. Taylor, E. A. Laird, A. Yacoby, M. D. Lukin, C. M. Marcus, M. P. Hanson, and A. C. Gossard, "Coherent manipulation of coupled electron spins in semiconductor quantum dots," *Science*, vol. 309, no. 5744, pp. 2180–2184, 2005.

[14] R. Hanson, L. P. Kouwenhoven, J. R. Petta, S. Tarucha, and L. M. K. Vandersypen, "Spins in few-electron quantum dots," *Rev. Mod. Phys.*, vol. 79, pp. 1217–1265, Oct 2007.

[15] J. Berezovsky, M. H. Mikkelsen, N. G. Stoltz, L. A. Coldren, and D. D. Awschalom, "Picosecond coherent optical manipulation of a single electron spin in a quantum dot," *Science*, vol. 320, no. 5874, pp. 349–352, 2008.

[16] K. Hennessy, A. Badolato, M. Winger, D. Gerace, M. Atatüre, S. Gulde, S. Fält, E. L. Hu, and A. Imamoglu, "Quantum nature of a strongly coupled single quantum dot–cavity system," *Nature*, vol. 445, Feb 2007.

[17] M. Pioro-Ladrière, T. Obata, T. Y., Y.-S. Shin, T. Kubo, K. Yoshida, T. Taniyama, and S. Tarucha, "Electrically driven single-electron spin resonance in a slanting zeeman field," *Nature Physics*, vol. 4, Aug 2008.

[18] Y. Wu, I. M. Piper, M. Ediger, P. Brereton, E. R. Schmidgall, P. R. Eastham, M. Hugues, M. Hopkinson, and R. T. Phillips, "Population inversion in a single ingaas quantum dot using the method of adiabatic rapid passage," *Phys. Rev. Lett.*, vol. 106, p. 067401, Feb 2011.

[19] R. H. Dicke, "Coherence in spontaneous radiation processes," *Phys. Rev.*, vol. 93, pp. 99–110, Jan 1954.

[20] K. Baumann, C. Guerlin, F. Brennecke, and T. Esslinger, "Dicke quantum phase transition with a superfluid gas in an optical cavity," *Nature*, vol. 464, Apr 2010.

[21] K. Baumann, R. Mottl, F. Brennecke, and T. Esslinger, "Exploring symmetry breaking at the dicke quantum phase transition," *Phys. Rev. Lett.*, vol. 107, p. 140402, Sep 2011.

[22] M. P. Baden, K. J. Arnold, A. L. Grimsmo, S. Parkins, and M. D. Barrett, "Realization of the dicke model using cavity-assisted raman transitions," *Phys. Rev. Lett.*, vol. 113, p. 020408, Jul 2014.

[23] A. J. Kollár, A. T. Papageorge, V. D. Vaidya, Y. Guo, J. Keeling, and B. L. Lev, "Supermode-density-wave-polariton condensation with a bose–einstein condensate in a multimode cavity," *Nature communications*, vol. 8, Feb 2017.

[24] F. Dimer, B. Estienne, A. S. Parkins, and H. J. Carmichael, "Proposed realization of the dicke-model quantum phase transition in an optical cavity qed system," *Phys. Rev. A*, vol. 75, p. 013804, Jan 2007.

[25] D. Nagy, G. Kónya, G. Szirmai, and P. Domokos, "Dicke-model phase transition in the quantum motion of a bose-einstein condensate in an optical cavity," *Phys. Rev. Lett.*, vol. 104, p. 130401, Apr 2010.

[26] J. Klinder, H. Keßler, M. R. Bakhtiari, M. Thorwart, and A. Hemmerich, "Observation of a superradiant mott insulator in the dicke-hubbard model," *Phys. Rev. Lett.*, vol. 115, p. 230403, Dec 2015.

[27] J. Keeling, M. J. Bhaseen, and B. D. Simons, "Collective dynamics of bose-einstein condensates in optical cavities," *Phys. Rev. Lett.*, vol. 105, p. 043001, Jul 2010.

[28] E. G. D. Torre, S. Diehl, M. D. Lukin, S. Sachdev, and P. Strack, "Keldysh approach for nonequilibrium phase transitions in quantum optics: Beyond the dicke model in optical cavities," *Phys. Rev. A*, vol. 87, p. 023831, Feb 2013.

[29] M. Gaudin, *La fonction d'onde de Bethe*. Masson, 1983. .

[30] C. Zhang, S. Tewari, R. M. Lutchyn, and S. Das Sarma, "$p_x + i p_y$ superfluid from s-wave interactions of fermionic cold atoms," *Phys. Rev. Lett.*, vol. 101, p. 160401, Oct 2008.

[31] A. Faribault, P. Calabrese, and J.-S. Caux, "Exact mesoscopic correlation functions of the richardson pairing model," *Phys. Rev. B*, vol. 77, p. 064503, Feb 2008.

[32] A. Faribault, P. Calabrese, and J.-S. Caux, "Quantum quenches from integrability: the fermionic pairing model," *Journal of Statistical Mechanics: Theory and Experiment*, vol. 2009, no. 03, p. P03018, 2009.

[33] A. Faribault, P. Calabrese, and J.-S. Caux, "Bethe ansatz approach to quench dynamics in the richardson model," *Journal of Mathematical Physics*, vol. 50, no. 9, p. 095212, 2009.

[34] J. von Delft and D. Ralph, "Spectroscopy of discrete energy levels in ultrasmall metallic grains," *Physics Reports*, vol. 345, no. 2–3, pp. 61 – 173, 2001.

[35] F. Braun, J. von Delft, D. C. Ralph, and M. Tinkham, "Paramagnetic breakdown of superconductivity in ultrasmall metallic grains," *Phys. Rev. Lett.*, vol. 79, pp. 921–924, Aug 1997.

[36] W. A. Coish, J. Fischer, and D. Loss, "Exponential decay in a spin bath," *Phys. Rev. B*, vol. 77, p. 125329, Mar 2008.

[37] W. A. Coish, J. Fischer, and D. Loss, "Free-induction decay and envelope modulations in a narrowed nuclear spin bath," *Phys. Rev. B*, vol. 81, p. 165315, Apr 2010.

[38] M. Bortz, S. Eggert, C. Schneider, R. Stübner, and J. Stolze, "Dynamics and decoherence in the central spin model using exact methods," *Phys. Rev. B*, vol. 82, p. 161308, Oct 2010.

[39] L. Cywiński, W. M. Witzel, and S. Das Sarma, "Electron spin dephasing due to hyperfine interactions with a nuclear spin bath," *Phys. Rev. Lett.*, vol. 102, p. 057601, Feb 2009.

## Bibliography

[40] L. Cywiński, W. M. Witzel, and S. Das Sarma, "Pure quantum dephasing of a solid-state electron spin qubit in a large nuclear spin bath coupled by long-range hyperfine-mediated interactions," *Phys. Rev. B*, vol. 79, p. 245314, Jun 2009.

[41] M. Tavis and F. W. Cummings, "Exact solution for an $n$-molecule—radiation-field hamiltonian," *Phys. Rev.*, vol. 170, pp. 379–384, Jun 1968.

[42] M. Tavis and F. W. Cummings, "Approximate solutions for an $n$-molecule-radiation-field hamiltonian," *Phys. Rev.*, vol. 188, pp. 692–695, Dec 1969.

[43] J. Larson and E. K. Irish, "Some remarks on 'superradiant' phase transitions in light-matter systems," *Journal of Physics A: Mathematical and Theoretical*, vol. 50, no. 17, p. 174002, 2017.

[44] P. Kirton and J. Keeling, "Suppressing and restoring the dicke superradiance transition by dephasing and decay," *Physical Review Letters*, 2 2017.

[45] J. Keeling, M. J. Bhaseen, and B. D. Simons, "Fermionic superradiance in a transversely pumped optical cavity," *Phys. Rev. Lett.*, vol. 112, p. 143002, Apr 2014.

[46] S. Agarwal, S. M. H. Rafsanjani, and J. H. Eberly, "Tavis-cummings model beyond the rotating wave approximation: Quasidegenerate qubits," *Phys. Rev. A*, vol. 85, p. 043815, Apr 2012.

[47] B. N. M. Korepin V E, Izergin A G, *Quantum Inverse Scattering Method and Correlation Functions*. Cambridge, 1993.

[48] S. N. A, "Calculation of scalar products of wave functions and form factors in the framework of the algebraic bethe ansatz," *Teor. Mat. Fiz.*, vol. 79, p. ., 1989.

[49] A. Faribault, O. E. Araby, C. Strater, and V. Gritsev, "Gaudin models solver based on the Bethe ansatz/ordinary differential equations correspondence," *Phys. Rev.*, vol. B83, p. 235124, 2011.

[50] O. El Araby, V. Gritsev, and A. Faribault, "Bethe ansatz and ordinary differential equation correspondence for degenerate gaudin models," *Phys. Rev. B*, vol. 85, p. 115130, Mar 2012.

[51] M. Rigol, V. Dunjko, V. Yurovsky, and M. Olshanii, "Relaxation in a completely integrable many-body quantum system: An ab initio study of the dynamics of the highly excited states of 1d lattice hard-core bosons," *Phys. Rev. Lett.*, vol. 98, p. 050405, Feb 2007.

[52] G. Ortiz, R. Somma, J. Dukelsky, and S. Rombouts, "Exactly-solvable models derived from a generalized gaudin algebra," *Nuclear Physics B*, vol. 707, no. 3, pp. 421 – 457, 2005.

[53] A. Faribault and D. Schuricht, "Integrability-based analysis of the hyperfine-interaction-induced decoherence in quantum dots," *Phys. Rev. Lett.*, vol. 110, p. 040405, Jan 2013.

[54] A. Faribault and D. Schuricht, "Spin decoherence due to a randomly fluctuating spin bath," *Phys. Rev. B*, vol. 88, p. 085323, Aug 2013.

[55] O. El Araby, V. Gritsev, and A. Faribault, "Bethe ansatz and ordinary differential equation correspondence for degenerate gaudin models," *Phys. Rev. B*, vol. 85, p. 115130, Mar 2012.

[56] J. Links, H.-Q. Zhou, R. H. McKenzie, and M. D. Gould, "Algebraic bethe ansatz method for the exact calculation of energy spectra and form factors: applications to models of bose–einstein condensates and metallic nanograins," *Journal of Physics A: Mathematical and General*, vol. 36, no. 19, p. R63, 2003.

[57] A. Faribault, H. Tschirhart, and N. Muller, "Determinant representation of the domain-wall boundary condition partition function of a richardson–gaudin model containing one arbitrary spin," *Journal of Physics A: Mathematical and Theoretical*, vol. 49, no. 18, p. 185202, 2016.

[58] H. Tschirhart and A. Faribault, "Algebraic Bethe ansatze and eigenvalue-based determinants for Dicke-Jaynes-Cummings-Gaudin quantum integrable models," *Journal of Physics A: Mathematical and Theoretical*, vol. 47, no. 40, 2014.

[59] J. Dukelsky, G. G. Dussel, C. Esebbag, and S. Pittel, "Exactly solvable models for atom-molecule hamiltonians," *Phys. Rev. Lett.*, vol. 93, p. 050403, Jul 2004.

[60] E. K. Sklyanin, "Separation of variables in the gaudin model," *Journal of Soviet Mathematics*, vol. 47, no. 2, pp. 2473–2488, 1989.

[61] L. Amico, H. Frahm, A. Osterloh, and T. Wirth, "Separation of variables for integrable spin–boson models," *Nuclear Physics B*, vol. 839, no. 3, pp. 604 – 626, 2010.

[62] A. G. Izergin, D. A. Coker, and V. E. Korepin, "Determinant formula for the six-vertex model," *Journal of Physics A: Mathematical and General*, vol. 25, no. 16, p. 4315, 1992.

[63] V. E. Korepin, "Calculation of norms of bethe wave functions," *Communications in Mathematical Physics*, vol. 86, no. 3, pp. 391–418, 1982.

[64] A. Faribault and H. Tschirhart, "Common framework and quadratic bethe equations for rational gaudin magnets in arbitrarily oriented magnetic fields," Apr 2017.

[65] S. Belliard, N. Crampé, and E. Ragoucy, "Algebraic bethe ansatz for open xxx model with triangular boundary matrices," *Letters in Mathematical Physics*, vol. 103, no. 5, pp. 493–506, 2013.

[66] P. W. Claeys, S. De Baerdemacker, and D. Van Neck, "Read-green resonances in a topological superconductor coupled to a bath," *Phys. Rev. B*, vol. 93, p. 220503, Jun 2016.

[67] P. W. Claeys, S. D. Baerdemacker, M. V. Raemdonck, and D. V. Neck, "The dicke model as the contraction limit of a pseudo-deformed richardson-gaudin model," *Journal of Physics: Conference Series*, vol. 597, no. 1, p. 012025, 2015.

## Bibliography

[68] P. W. Claeys, S. De Baerdemacker, M. Van Raemdonck, and D. Van Neck, "Eigenvalue-based method and form-factor determinant representations for integrable xxz richardson-gaudin models," *Phys. Rev. B*, vol. 91, p. 155102, Apr 2015.

[69] P. W. Claeys, S. D. Baerdemacker, M. V. Raemdonck, and D. V. Neck, "Eigenvalue-based determinants for scalar products and form factors in richardson–gaudin integrable models coupled to a bosonic mode," *Journal of Physics A: Mathematical and Theoretical*, vol. 48, no. 42, p. 425201, 2015.

[70] S. Belliard and N. Crampe, "Heisenberg xxx model with general boundaries: Eigenvectors from algebraic bethe ansatz," *SIGMA*, vol. 9, Nov 2013.

[71] N. Crampe, E. Ragoucy, V. Rittenberg, and M. Vanicat, "Integrable dissipative exclusion process: Correlation functions and physical properties," *Phys. Rev. E*, vol. 94, p. 032102, Sep 2016.

[72] N. Crampé, "Algebraic bethe ansatz for the totally asymmetric simple exclusion process with boundaries," *Journal of Physics A: Mathematical and Theoretical*, vol. 48, no. 8, p. 08FT01, 2015.

[73] J. Avan, S. Belliard, N. Grosjean, and R. Pimenta, "Modified algebraic bethe ansatz for {XXZ} chain on the segment – {III} – proof," *Nuclear Physics B*, vol. 899, pp. 229 – 246, 2015.

[74] S. Belliard and R. A. Pimenta, "Slavnov and gaudin-korepin formulas for models without u(1) symmetry: the twisted xxx chain," *SIGMA*, vol. 11, Dec 2015.

[75] P. Baseilhac and K. Koizumi, "Exact spectrum of the xxz open spin chain from the q-onsager algebra representation theory," *Journal of Statistical Mechanics: Theory and Experiment*, vol. 2007, no. 09, p. P09006, 2007.

[76] H. Frahm, J. H. Grelik, A. Seel, and T. Wirth, "Functional bethe ansatz methods for the open xxx chain," *Journal of Physics A: Mathematical and Theoretical*, vol. 44, no. 1, p. 015001, 2011.

[77] R. Murgan and R. I. Nepomechie, "Bethe ansatz derived from the functional relations of the open xxz chain for new special cases," *Journal of Statistical Mechanics: Theory and Experiment*, vol. 2005, no. 05, p. P05007, 2005.

[78] W. Galleas, "Functional relations from the yang–baxter algebra: Eigenvalues of the {XXZ} model with non-diagonal twisted and open boundary conditions," *Nuclear Physics B*, vol. 790, no. 3, pp. 524 – 542, 2008.

[79] N. Crampé, E. Ragoucy, and D. Simon, "Eigenvectors of open xxz and asep models for a class of non-diagonal boundary conditions," *Journal of Statistical Mechanics: Theory and Experiment*, vol. 2010, no. 11, p. P11038, 2010.

[80] V. Alba and P. Calabrese, "The quench action approach in finite integrable spin chains," *Journal of Statistical Mechanics: Theory and Experiment*, vol. 2016, no. 4, p. 043105, 2016.

[81] U. Seifert, P. Bleicker, P. Schering, A. Faribault, and G. S. Uhrig, "Persisting correlations of a central spin coupled to large spin baths," *Phys. Rev. B*, vol. 94, p. 094308, Sep 2016.

[82] F. Buccheri, A. De Luca, and A. Scardicchio, "Structure of typical states of a disordered richardson model and many-body localization," *Phys. Rev. B*, vol. 84, p. 094203, Sep 2011.

[83] C. Sträter, *Quantum Integrability and its Application to the Dicke Model.* PhD thesis, Ludwig Maximilian University of Munich, 2011.

[84] B. Pozsgay, M. Mestyán, M. A. Werner, M. Kormos, G. Zaránd, and G. Takács, "Correlations after quantum quenches in the $xxz$ spin chain: Failure of the generalized gibbs ensemble," *Phys. Rev. Lett.*, vol. 113, p. 117203, Sep 2014.

[85] B. Wouters, J. De Nardis, M. Brockmann, D. Fioretto, M. Rigol, and J.-S. Caux, "Quenching the anisotropic heisenberg chain: Exact solution and generalized gibbs ensemble predictions," *Phys. Rev. Lett.*, vol. 113, p. 117202, Sep 2014.

[86] F. H. L. Essler, G. Mussardo, and M. Panfil, "Generalized gibbs ensembles for quantum field theories," *Phys. Rev. A*, vol. 91, p. 051602, May 2015.

[87] E. Ilievski, J. De Nardis, B. Wouters, J.-S. Caux, F. H. L. Essler, and T. Prosen, "Complete generalized gibbs ensembles in an interacting theory," *Phys. Rev. Lett.*, vol. 115, p. 157201, Oct 2015.

[88] E. Ilievski, E. Quinn, J. D. Nardis, and M. Brockmann, "String-charge duality in integrable lattice models," *Journal of Statistical Mechanics: Theory and Experiment*, vol. 2016, no. 6, p. 063101, 2016.

[89] E. Q. Enej Ilievski and J.-S. Caux, "From interacting particles to equilibrium statistical ensembles," 1 2017.

[90] N. Kitanine, J. M. Maillet, G. Niccoli, and V. Terras, "On determinant representations of scalar products and form factors in the sov approach: the xxx case," *Journal of Physics A: Mathematical and Theoretical*, vol. 49, no. 10, p. 104002, 2016.

[91] N. Kitanine, J. M. Maillet, G. Niccoli, and V. Terras, "The open xxx spin chain in the sov framework: scalar product of separate states," 2016.

[92] J. Cao, W.-L. Yang, K. Shi, and Y. Wang, "Off-diagonal bethe ansatz and exact solution of a topological spin ring," *Phys. Rev. Lett.*, vol. 111, p. 137201, Sep 2013.